OXIDATION STUDIES INVOLVING COPPER AND SILVER ELECTRODES

by

Kenneth Ian MacDonald

A THESIS

submitted in partial fulfilment of the requirements for the award of Doctor of Philosophy of Loughborough University of Technology.

September 1972

Supervision: N.A. HAMPSON

J.B. LEE

The work described in this thesis has not been submitted, in full or in part, to this or any other Institution for a higher degree.

ACKNOWLEDGEMENTS

I wish to express my thanks to my supervisors Dr. N.A. Hampson and Dr. J.B. Lee for their advice and encouragement given to me throughout the past three years.

I would also like to express my thanks to my fellow research students for their help and friendship; to Professor R.F. Phillips for providing the facilities to carry out this work; to the members of the technical staff of the Chemistry Department for their assistance; to Loughborough University of Technology for the provision of my research grant and finally to Mrs. E. Cook for typing this thesis so carefully.

SUMMARY

A study of the reactions that occur at copper and silver electrodes in alkaline solutions, at potentials between those corresponding to hydrogen and oxygen evolution reactions, has been effected. The major reactions that have been identified are:-

at a silver electrode

$$2\,Ag + 2OH^- \longrightarrow Ag_2O + H_2O + 2e \qquad (i)$$

$$Ag_2O + 2OH^- \longrightarrow 2AgO + H_2O + 2e \qquad (ii)$$

at a copper electrode

$$2Cu + 2OH^- \longrightarrow Cu_2O + H_2O + 2e \qquad (iii)$$

$$Cu + 2OH^- \longrightarrow CuO + H_2O + 2e \qquad (iv)$$

$$Cu + 2OH^- \longrightarrow Cu(OH)_2 + 2e \qquad (v)$$

Of these reactions (i), (ii), (iii) and (iv) have been shown to be controlled by solid phase processes, whereas reaction (v) is thought to be controlled by a dissolution precipitation mechanism.

The oxidation of α-amino acids at copper and silver anodes yielded the nor-nitrile as the major reaction product in every case investigated.

The reaction is thought to occur with the α-amino acid in an adsorbed state at the electrode. It is suggested that the oxidation proceeds through an imine intermediate and that the release of this intermediate into the solution produces a trace of the nor-aldehyde as the only other reaction product. These oxidations have been shown to be specific and to occur readily at these electrodes, whereas no such reactions occur if these electrodes are replaced by Pt, Au or PbO_2 electrodes.

CONTENTS

CHAPTER 1

INTRODUCTION

In recent years there has been a considerable increase in the interest in anodic oxidations of organic molecules at solid metal electrodes, stimulated partly by the prospect of a useful electrode reaction that would be applicable to the fuel cell and partly by the possibility of producing an industrially important electrode synthesis. Historically electro-organic oxidations date back over a hundred years to when such processes as the Kolbe reaction[1] were being extensively investigated. The lapse of intensive interest in such reactions was possibly due to the rather uncontrolled nature of most of the early processes in which a wide variety of products were produced.

A useful organic synthesis is usually a selective reaction, and an ability to vary this selectivity by changes in reaction conditions immediately makes such a system very attractive to the organic chemist. In principle such variability of selectivity is possible in electro-organic reactions by suitable control of parameters such as potential, current density, concentration of the reactants and selection of electrode material.

The choice of the electrode material for an electro-organic oxidation is limited to those metals that will not dissolve or form insulating oxide films under anodic potential conditions. Mercury has proved to be a very useful metal for the examination of the kinetics and mechanisms of electro-organic reductions[2]. It has not however been

used extensively for electrode oxidations since the formation of an oxide film at 0.2 V (n.h.e.) limits its usefulness. Inert electrodes such as platinum and glassy carbon have been extensively used in anodic oxidations and it is clear from this work that fission of organic molecules may occur in the region of the electrode/electrolyte double layer without adsorption or interaction of the organic molecule with the electrode surface. It is likely, however, that a greater degree of specificity of these oxidations could be obtained if the electrode material participated in the electrode reaction, instead of just acting as a source or sink of electrons for the reaction involving the organic molecule. Many metals show a readiness to form bonds with a variety of organic molecules and so it can be expected that some of these metals should show novel interactions with organic compounds leading to specificity in electro-organic oxidations. A further interesting possibility of selectivity arises from the variable valency of a metal. Since it is known that the reduction potential of a metal ion can be drastically altered by complexing with a suitable ligand we therefore have an additional variable worthy of investigation.

Silver and its compounds are known to react specifically with certain functional groups of organic molecules, this property having been applied in the separation of organic species by chromatographic methods[3] using silver compounds. It was because of these properties that the use of a silver anode was first investigated in these laboratories. The silver oxides that are formed under anodic conditions in alkaline solutions are not insulators and so the system was an obvious choice for investigation. Also the oxides of silver have proved to be useful and specific oxidising agents in isolation from the electrode system[4].

Although considerable work[5] has been carried out on the electrode system $Ag|OH^-$, there is still some doubt concerning the primary oxidation reactions that occur, and consequently an extension of the investigation into this aspect and also its usefulness in electro-organic oxidations was considered worthwhile. This present investigation was instigated in order to provide some of this data and also to compare the silver electrode with similar electrode systems in the same group, viz. copper and gold. It was hoped that this extension would enable the effect of increasing the electronegativity on the electrode specificity to be investigated. The $Cu|OH^-$ system is also interesting in its own right since the cupric ion is extensively used to oxidise aldehydes, carbohydrates and acetylenes.

CHAPTER 2

THEORETICAL CONSIDERATIONS

Electrode reactions are characterised by a charge transfer to or from ions or neutral molecules at an electrode/electrolyte interphase that can act as a controllable electron source or sink. A simplified picture of a general electrochemical reaction at any electrode will therefore contain at least three finite stages:

Mass transfer of reactants to the electrode surface

Electron or charge transfer step

Mass transfer of products away from the electrode surface.

Such a generalisation may ignore some very important factors since frequently the reacting species undergo a preliminary reaction in which they are transformed into an electroactive form. There are also subsequent reactions which may consume the initial product and produce electrochemically inactive materials or even regenerate the starting material (catalytic reaction). The possibility of the reactants or products being in an adsorbed state at the electrode surface is also ignored. The extent to which adsorption plays a part with the attendant inequalities of concentrations and electroactivities of adsorbed and solution species, strongly influences many processes. Finally, there are the specific effects of the solid electrode on the above processes which may involve the actual surface conditions that exist during the electrolysis.

A complete analysis of the mechanism of an electrode process involves a great deal more than the general description above. A thorough picture of the mechanism would include evaluation of the rates of each of the above mentioned steps, the measurement of the various electrochemical parameters that characterise the charge transfer and a study of the influence of the solution environment on these properties. In practice one must often be satisfied with a far less complete study, but by consideration of the general factors discussed above a great deal of valuable information can be gained.

This simple picture is useful in that it highlights some of the main theoretical considerations that need to be discussed. It is of prime importance to have an understanding of the nature of the electrode surface and the accompanying double layer; the mode of transport of both the reactants and the products during the reaction and also the mechanism of the charge transfer process.

2.1. The Electrode/Electrolyte Interphase

It is essential that a description of the structure of the electrode/electrolyte interphase accompanies any discussion of electrode processes, since the local concentration of the reacting species at the charged interphase will be an important factor in the rates of the electrochemical reaction.

The simplest model of the distribution of charged species at the interphase was proposed by Helmholtz[6] who regarded the interphase as a "double layer" of charges; there being a layer of charge in the electrode that was equal in magnitude

but opposite in sign to a charged layer in the electrolyte. The two thin layers of charge were parallel and the system approximating to that of a parallel plate condenser having an electrical capacity C_L. This implies that the electrical behaviour of this double layer is purely capacitative and that there is no ohmic leakage resistance component in parallel, corresponding to a discharge of ions. This requirement is an idealisation since under most practical conditions an electrode/electrolyte interphase will have a small current passing corresponding to the occurrence of some net electrode reaction. The only practical system that approaches this idealised condition is a mercury cathode between the reversible hydrogen potential and - 0.9 V (n.h.e.), such an electrode is termed "ideally polarisable".

The theory of Helmholtz was modified by Gouy[7] and Chapman[8] who developed the concept of a diffuse layer rather than a compact layer of ions in the electrolyte. This consideration was necessary since the Helmholtz model neglected the thermal distribution of ions that occurs at finite temperatures. Comparison of experimental results with values calculated from the Gouy-Chapman theory reveals discrepancies due to the fact that they had considered ions as point charges which could thus approach to within infinitely small distances of the electrode surface.

Stern[9] combined the Helmholtz theory with that of Gouy and Chapman. By considering the finite size of the ions he showed that the diffuse part of the double layer extended from the bulk of the solution up to within a finite distance of the electrode surface. Consequently the overall double layer now consists of a diffuse layer and a compact layer close to the electrode surface. Grahame[10] further improved the

theory by subdividing the compact layer into an inner and outer compact plane. The inner Helmholtz plane is governed by the plane of closest approach of solvent dipoles and specifically adsorbed ions. The outer Helmholtz plane is determined by the plane of closest approach of solvated cations.

A generally accepted model of the electrical double layer is shown in Figure 1.

Using this model of the double layer Grahame has shown that the double layer capacitance is given by:

$$\frac{1}{C_L} = \frac{1}{C_{diff.}} + \frac{1}{C_{comp}} \qquad (2.1)$$

where

C_L = total double layer capacitance

C_{diff} = capacitance of the diffuse layer

C_{comp} = capacitance of the compact layer.

As the electrolyte becomes more dilute the capacitance associated with the compact layer becomes significantly larger than the diffuse layer component. It can be seen therefore that C_L will become virtually independent of C_{diff} in dilute electrolytes. At very low concentrations a sharp minimum is noted on a C_L versus electrode potential plot. This minimum is associated with the point of zero charge on the electrode, hence forth designated the p.z.c.

FIG1 Model of the electical double layer

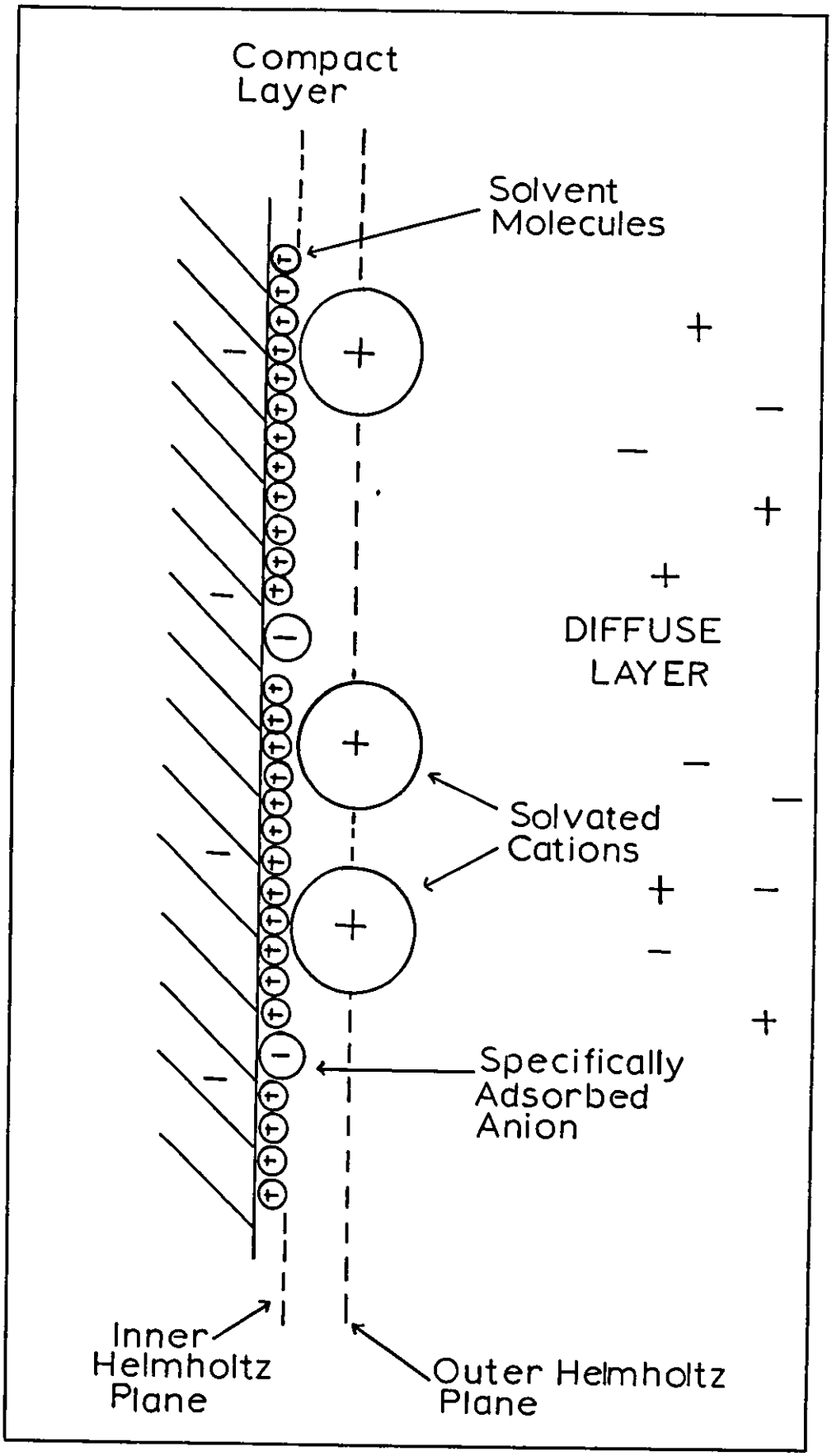

The importance of the p.z.c. has been thoroughly discussed by Frumkin[11,12], who indicated that the p.z.c. is not affected by the introduction of potential determining ions. The p.z.c. may therefore be used in the discussion of charge adsorption at a polarisable electrode in the presence of potential determining ions. The term "rational potential"; E_r, is introduced to describe the potential of an electrode with respect to the p.z.c. Thus at positive E_r values adsorption of negative ions is favoured, while at negative E_r values positive ions are attracted to the interphase. Likewise when there is little or no charge on the electrode, when the magnitude of E_r is small, adsorption of neutral molecules competes favourably with ionic adsorption.

The adsorption of neutral molecules has a profound effect on the values of the double layer capacitance. There is a substantial decrease of the capacitance in the potential region close to the p.z.c. and also two sharp capacitance maxima occur on both sides of the p.z.c. The decrease in the values of the capacitance between the two maxima is connected with the lower polarisability of the organic molecule compared to the solvent. The capacitance maxima result from the desorption of the organic molecules at potentials on either side of the p.z.c.

A study of the differential capacitance and a knowledge of the p.z.c. is thus an important preliminary to the study of reactions at an electrode/electrolyte interphase.

2.2. Mass Transport in Solution

Transport of the reactant species to and from the electrode surface will

occur by three main processes: migration, diffusion and convection.

2.2. (i) Migration

Mass transport by migration is the result of the force exerted on charged particles by an electrical field. Migration will always contribute to the total mass transport of charged species in electrode reactions. The effects of migration can normally be minimised by the presence of an excess of background or supporting electrolyte.

2.2. (ii) Diffusion

This is always an important mode of transport. Its' extent is measured by the diffusion coefficient that is dependent upon the dimensions of the diffusing species (including solvation sheaths that depend on the nature of the species and solvent) and the viscosity of the solvent.

Consider the linear diffusion of reacting species to a plane electrode in a static solution (no migration or convection) with respect to the reaction:

$$O + ne \rightleftharpoons R \qquad (2.2.)$$

Concentrations are denoted by C_o and C_R, with the superscripts 's' and 'b' to signify concentrations at the electrode surface or in the bulk of the electrolyte. If we carry out an electrolysis at a constant potential three experimental factors are noticeable, namely that the current is proportional to C_o^b and to the electrode area, and that the

current decreases with the time of electrolysis. Any derivation of the time/current relationship for linear diffusion must fit these experimental facts.

The number of moles of a substance diffusing across a given cross-sectional area (A cm^2) in a time dt is proportional to the concentration gradient of the diffusing species

$$\frac{dN}{dt} = K A \frac{\partial C_o}{\partial x} \qquad (2.3.)$$

The proportionality constant K is defined as the diffusion coefficient D_o hence:

$$\frac{dN}{dt} = D_o A \frac{\partial C_o}{\partial x} \qquad (2.4.)$$

This equation relates the diffusion rates to concentration and is known as Fick's first law. A useful modification is obtained if we consider the number of moles diffusing through unit area in unit time - the flux of material. The flux is usually defined as, q, and is given by:

$$q = \frac{dN}{A\,dt} = D_o \frac{\partial C_o}{\partial x} \qquad (2.5.)$$

If we consider the electrolysis over a period of time then C_o, and hence $\frac{\partial C_o}{dx}$ must vary and in fact C_o will decrease since O is being consumed at the

electrode. It is therefore necessary to know C_o both as a function of distance from the electrode and time. The change in C_o with time between two planes at distances x and x + dx from the electrode surface (x = o) will be the difference between the number of moles of O entering the plane at x + dx and the number leaving at plane x,

thus
$$\frac{\partial C_o}{\partial t} = \frac{q(x + dx) - q(x)}{dx} \qquad (2.6.)$$

$$\frac{\partial C_o}{\partial t} = \frac{\partial q}{\partial x} \qquad \text{as} \quad dx \rightarrow O$$

$$\therefore \quad \frac{\partial C_o}{\partial t} = D_o \frac{\partial^2 C_o}{\partial x^2} \qquad (2.7.)$$

This is Fick's second law and the fundamental equation for linear diffusion in solution.

The current flow associated with this process will be proportional to the flux at x = O.

$$i_t = n F A q(O, t) = \left(n F A D_o \frac{\partial C_o}{\partial x}\right)_{O,t} \qquad (2.8.)$$

The value of the concentration gradient at the electrode surface can be obtained from (2.7.) by applying the appropriate conditions (x = O).

$$\left(\frac{\partial C_o}{\partial x}\right)_{x=0} = \frac{C_o^b}{\pi^{\frac{1}{2}} D_o^{\frac{1}{2}} t^{\frac{1}{2}}} \qquad (2.9.)$$

Hence the instantaneous current at a plane electrode under linear diffusion control is

$$i_t = \frac{n F A D_o^{\frac{1}{2}} C_o^b}{\pi^{\frac{1}{2}} t^{\frac{1}{2}}} \qquad (2.10.)$$

This equation (2.10.) satisfies all three of the original experimental requirements.

2.2. (iii) Convection

Convective mass transport does not take place on its own but is always accompanied by diffusion. Both of these forms of mass transport occur simultaneously but one or the other may predominate, as in forced convection (stirring) when linear diffusion will only have a minor contribution if one considers the overall mass transport in the entire solution. A fuller discussion of forced convection is given in Chapter 3.

One of the first approaches to mass transfer in electrode processes was given by Nernst[13] who assumed that there was a thin stationary layer (thickness $\sim 10^{-3}$ cm) of solution in contact with the electrode. Within this layer he postulated that diffusion alone controlled the transfer of reacting species to the electrode. Outside this layer diffusion was negligible and the concentration of electroactive material was maintained at a value of C^b by convective transfer. This hyperthetical layer has become

known as the "Nernst diffusion layer". Nernst also assumed that the concentration varied linearly with distance within this layer

$$\frac{\partial C_o}{\partial x} = \frac{C_o^b - C_o^s}{\delta N} \qquad (2.11.)$$

where δN is the thickness of the Nernst diffusion layer.

Hence

$$q = \frac{D_o (C_o^b - C_o^s)}{\delta N} \qquad (2.12.)$$

and

$$i = \frac{n F A D_o (C_o^b - C_o^s)}{\delta N} \qquad (2.13.)$$

At high overpotentials, $C_o^s = 0$, the limiting current is given by 'i_L'

$$i_L = \frac{n A F C_o^b}{\delta N} \qquad (2.14.)$$

The most serious objection to the Nernst treatment lies in its purely qualitative nature. While the concept of the thickness δN is useful experimentally it does not allow any predictions as to the variation of δN with solution parameters such as viscosity, diffusion coefficients, etc.

A hydrodynamic treatment of the problem leads to the concept of a thin "diffusion boundary layer" close to the electrode surface, within which the largest

changes of concentration occur. The liquid flow velocity within this layer is not zero except at the electrode surface ($x = O$). The thickness of this layer, δ, is proportional to the physical properties of the solution, such as viscosity and velocity, as well as to the value of D_o. This means that every electroactive species has its own value of δ.

The hydrodynamic treatment leads to a physical picture not unlike the original Nernst hypothesis. A fuller discussion of this treatment is given in the experimental section where the conditions at a rotating disc electrode are considered.

2.3. Charge Transfer Process

There are two basic mechanisms for the transfer of charge across the double layer; the redox electrode and the metal-ion electrode reactions. In the redox electrode reaction the reacting species and products are in the electrolyte and the charge transfer is by electrons acting as charge carriers. It is possible, and in fact common, for there initially to be adsorption of the reacting species followed by charge transfer and then desorption of the products into the solution. This reaction may in turn be followed by proceeding solution reactions. The metal-ion electrode reaction requires that the reacting ion passes through the electrode/electrolyte double layer and is discharged at the electrode.

In this account the redox reaction (2.2.) will again be considered.

$$O + ne \underset{k_a}{\overset{k_c}{\rightleftharpoons}} R$$

At the equilibrium potential charge is simultaneously being donated and accepted by the electrode in a dynamic equilibrium. According to the generally accepted theory of Volmer and Erdez-Gruz[14] both the anodic and cathodic processes are controlled by potential dependent activation energy barriers; this concept has been discussed elsewhere[15]. The partial currents associated with these two processes are given by:

$$i_c = n F k_c C_o^s \qquad (2.15.)$$

$$i_a = n F k_a C_R^s \qquad (2.16.)$$

where C_o^s and C_R^s are the electrode surface concentrations of the oxidised and reduced species and k_c and k_a are the potential dependent rate constants. The net current, i, flowing through the system is given by

$$i = i_c - i_a$$

$$i = n F (k_c C_o^s - k_a C_R^s) \qquad (2.17.)$$

It is found that the variation of k_c and k_a with the electrode potential is exponential and these rate constants have the form:

$$k_c = k_c^o \exp\left(\frac{-\alpha n F E}{RT}\right) \qquad (2.18.)$$

$$k_a = k_a^o \exp\left(\frac{(1-\alpha)\, n\, F\, E}{RT}\right) \qquad (2.19.)$$

where E is the potential of the electrode measured against any convenient reference electrode (e.g. n.h.e.) and k_c^o and k_a^o are the values of k_c and k_a at this reference potential. We therefore obtain:

$$i = n F \left[k_c^o C_o^s \exp\left(\frac{-\alpha\, n\, F\, E}{RT}\right) - k_a^o C_R^s \exp\left(\frac{(1-\alpha)\, n\, F\, E}{RT}\right) \right] \qquad (2.20.)$$

At the reversible potential E_r, $i = O$ and hence:

$$i_c = i_a = i_o$$

$$i_o = n F k_c^o C_o^s \exp\left(\frac{-\alpha\, n\, F\, E_r}{RT}\right)$$

$$i_o = n F k_a^o C_R^s \exp\left(\frac{(1-\alpha)\, n\, F\, E_r}{RT}\right) \qquad (2.21.)$$

where i_o is the exchange current and the overpotential, η, is defined as:

$$\eta = E - E_r \qquad (2.22.)$$

Introducing (2.21.) and (2.22.) into (2.20.) gives:-

$$i = i_o \left[\exp\frac{-\alpha\, n\, F\, \eta}{RT} - \exp\frac{(1-\alpha)\, n\, F\, \eta}{RT} \right] \qquad (2.23.)$$

This expression (2.23.) has been verified using a quantum mechanical treatment by Horiuti and Polanyi[16].

For low overpotentials ($|\eta| << \frac{RT}{nF}$), the overpotential/current curve is linear and the proportionality between the overpotential and the current corresponds to an electrical resistance, the charge transfer resistance, (R_D).

$$R_D = - \left(\frac{\partial \eta}{\partial i}\right)_{i \to 0} \qquad (2.24.)$$

Differentiating (2.23.) and putting $\eta = O$ the expression is:-

$$\left(\frac{\partial i}{\partial \eta}\right)_{\eta = 0} = - \frac{n F \cdot i_o}{RT} \qquad (2.25)$$

$$\therefore \quad R_D = \frac{RT}{n F} \times \frac{1}{i_o} \qquad (2.26.)$$

Thus the exchange current density may be obtained from the charge transfer resistance at equilibrium ($\eta = O$). If we are examining the electrical characteristics of a pure charge transfer controlled reaction, when a direct current is passing, R_D is the only factor that has to be considered. If however an alternating current is passing through the same system then the double layer capacitance, C_L, must also be considered. Hence the anlogue of the system becomes a parallel combination of both R_D and C_L.

For high cathodic overpotentials the Erdey-Gruz and Volmer equation (2.23.) gives the Tafel relationship[17]

$$\eta = \frac{RT}{\alpha n F} \log i_o - \frac{RT}{\alpha n F} \log i \qquad (2.27.)$$

and for a high anodic overpotential

$$\eta = \frac{RT}{(1-\alpha) n F} \log i_o - \frac{RT}{(1-\alpha) n F} \log i \qquad (2.28.)$$

Hence the magnitude of the exchange current density may also be obtained from high overpotential measurements by extrapolation of the current/potential curves back to the equilibrium overpotential, $\eta = O$.

The dependence of the exchange current on the reactant concentration has also been established[18] and for reaction (2.2.) it can be shown that:-

$$i_o = n F K^o a_R{}^{\alpha} a_o{}^{1-\alpha} \qquad (2.29.)$$

from a combination of the Erdez-Gruz and Volmer equation with the Nernst equation that gives:-

$$\exp\left[-\frac{(\alpha n F)}{RT}(E_e - E^o)\right] = \left(\frac{a_o}{a_R}\right)^{-\alpha} \qquad (2.30.)$$

The activities a_R and a_o are usually replaced by the corresponding concentrations, since the activities are unknown.

$$i_o = n F K^o C_R^{\alpha} C_o^{1-\alpha} \qquad (2.31.)$$

Where K^o is the apparent standard rate constant.

CHAPTER 3

EXPERIMENTAL CONSIDERATIONS

3.1. Experimental Techniques

3.1. (i) Electrolytes were prepared from A.R. grade chemicals and water, bidistilled from deionized stock. The electrolytes used for the experimental work involving determination of the differential capacitance and also for experiments involving galvanostatic and linear sweep voltammetry methods were extensively purified. This purification was achieved by pumping the electrolyte through a purification limb, in the electrolytic cells, which contained specially prepared activated charcoal[19]. The charcoal used was of granular gas adsorption grade that was extracted in a soxhlet apparatus with constant boiling hydrochloric acid. The acid was changed at weekly intervals and the extraction continued until the acid remained colourless throughout a week. This procedure generally took about three months. The charcoal was then washed with water, also under reflux in a soxhlet, until the washings showed no positive test for chloride ions. The purification of the electrolytes, using this charcoal, usually took about four weeks circulation until a satisfactory level of cleanliness had been achieved.

3.1. (ii) Electrodes The analytical test electrodes were all prepared from polycrystalline metal wires that were cast from the metal under an atmosphere of

nitrogen. The metal wires were all of 99.999% purity and supplied by Johnson Mathey Company Limited. The metal wires were soldered to contact wires and inserted in glass tubes. The wires were then sealed into the glass tubes by encapsulating the wire and the glass tube in polyethylene. The reacting electrode area was exposed by cutting the polyethylene at right angles to the long axis (see Figure 2). This type of test electrode was used for all of the analytical experimental work except that involving a rotating disc electrode.

The rotating disc electrode was of the type used by Azim and Riddiford[20], where the metal wire was soldered into a steel shaft. The steel shaft and wire were then encapsulated with polyethylene and then machined into a cone configuration (see Figure 3).

The counter electrodes, for the linear sweep voltammetry and galvanostatic measurements, also the reference electrode in the latter case, were constructed in the same manner as the test electrode. The surface area of the metal wire exposed was many times greater in the case of these electrodes.

The static preparative electrodes used in the oxidations of α-amino acids were of the same basic construction as the counter electrodes described above. The rotating electrodes used in the preparative oxidations were of the cone-disc type used by Newson and Riddiford[21].

The last type of electrode that was used was in the investigation of the surface oxides, formed at copper electrodes in alkaline solutions, using a stereoscan electron microscope. The electrodes were made from copper sheet (99.9% purity) that was cut into discs to which an electrical contact was soldered.

FIG 2 Test electrode

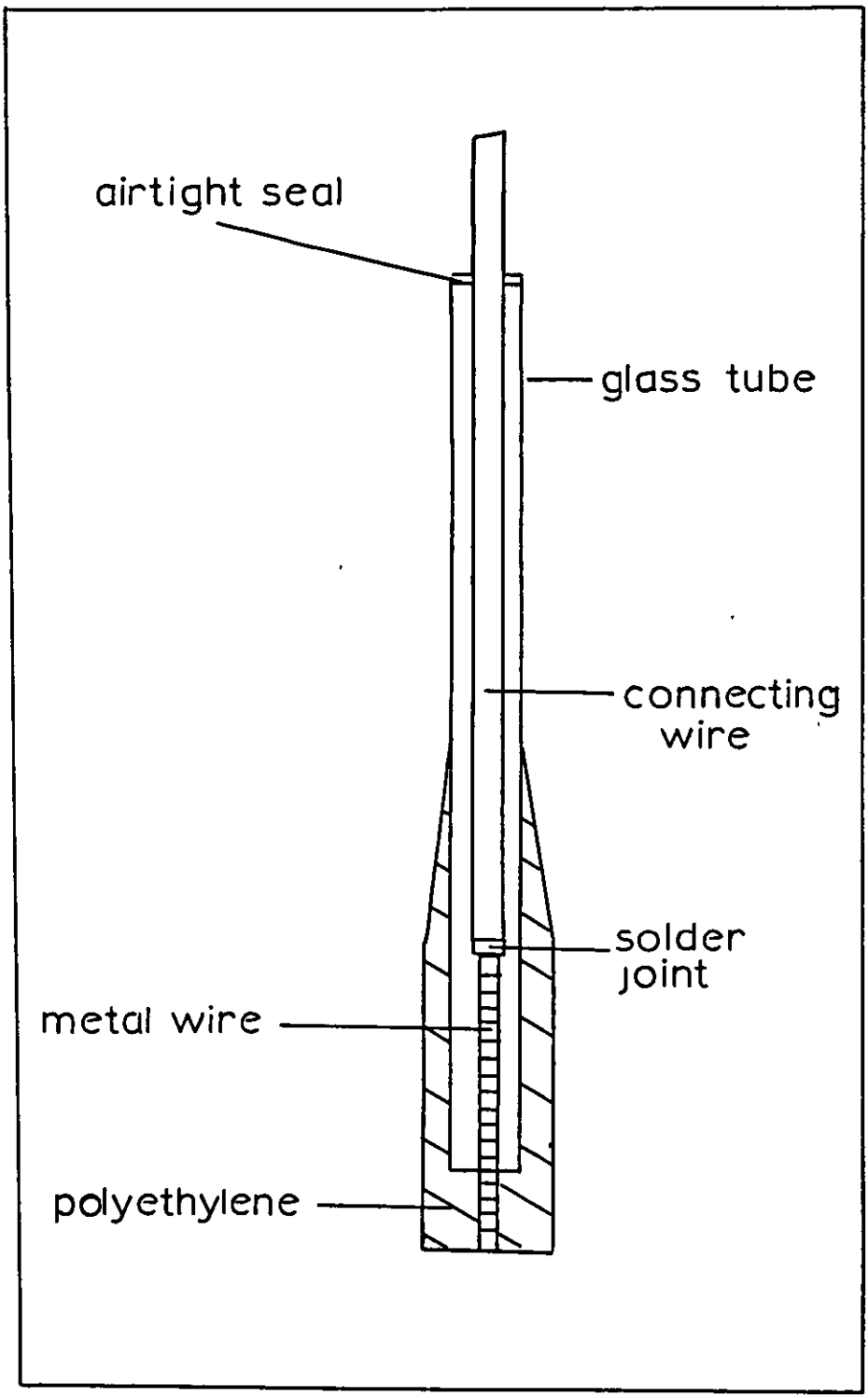

FIG 3 Rotating disc electrode

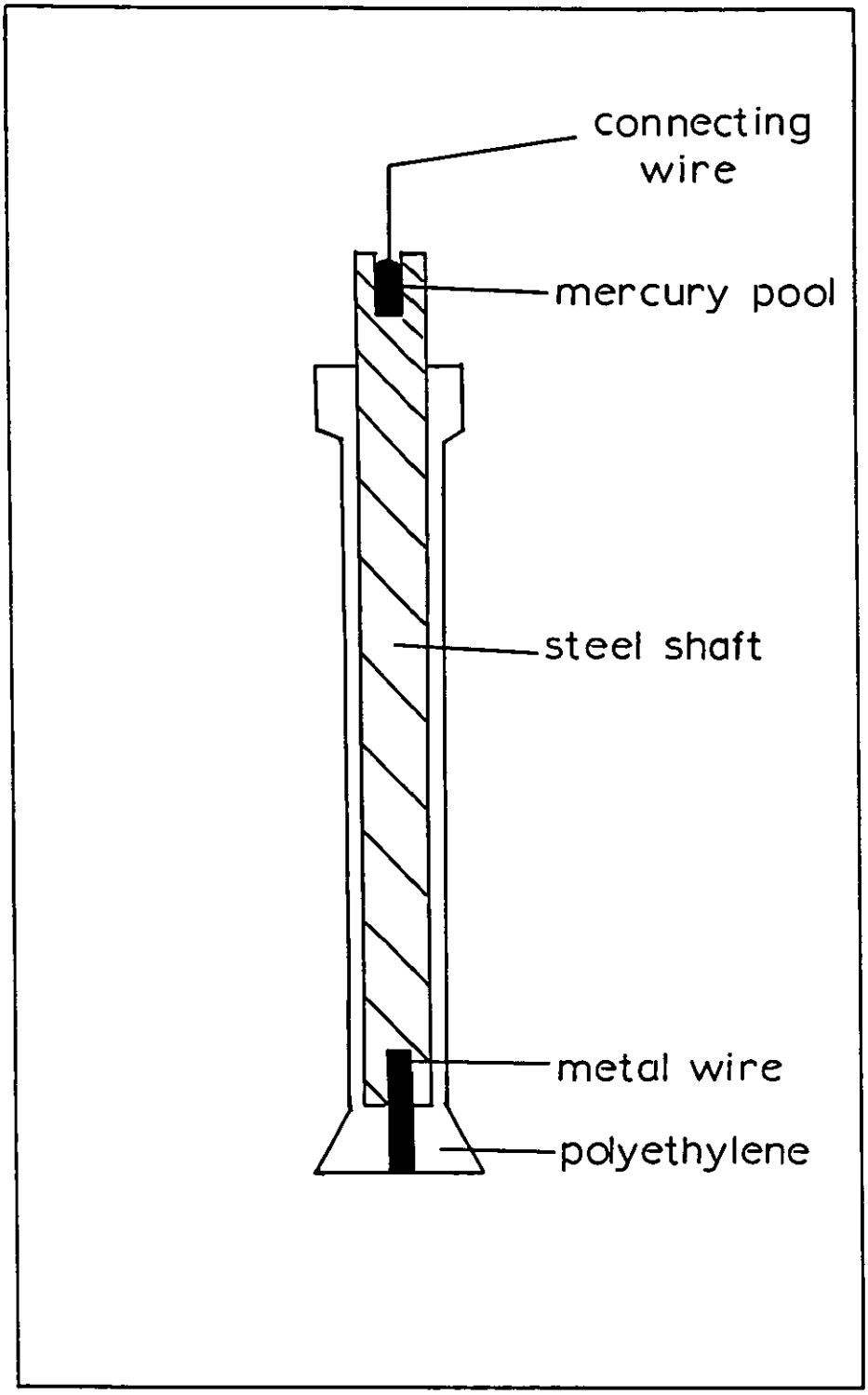

3.1. (iii) Electrolytic Cells Various designs of glass cells have been used in this study and they are shown in Figures 4 and 5. The electrolytic cells and all the glassware used in these experiments were cleaned by steeping in a 50/50 mixture of concentrated nitric and sulphuric acids for ten days. The acid was removed by numerous washings with deionized water, after which they all were allowed to stand for a day in bidistilled water, and finally washed with bidistilled water.

3.1. (iv) Organic Compounds The α-amino acids that were used in the oxidation studies were all chromographically homogeneous (B.D.H., Limited). All other organic reagents that were used were distilled from laboratory grade chemicals.

3.2. Experimental Methods

3.2. (i) Differential Capacitance Measurements A Shering bridge[22] was used to match the electrode/electrolyte interphase as a series combination of resistance and capacitance[23]. The circuit diagram for the bridge is shown in Figure 6.

A wave analyser (Hewlett Packard Type 302A) was used as the a.c. generator and tuned voltmeter for null deflection (B.F.O. mode). The generator has a frequency range of 10 Hz - 50 K.Hz in divisions of 10 Hz. A single control tunes both the oscillator and the voltmeter. The voltmeter had a narrow pass band with a meter range of 30 μV to 300 V F.S.D.

The output from the generator was applied to the bridge through an isolated 65:1 step down transformer. The amplitude of the perturbing a.c. was adjusted

FIG 4 Electrolytic cells

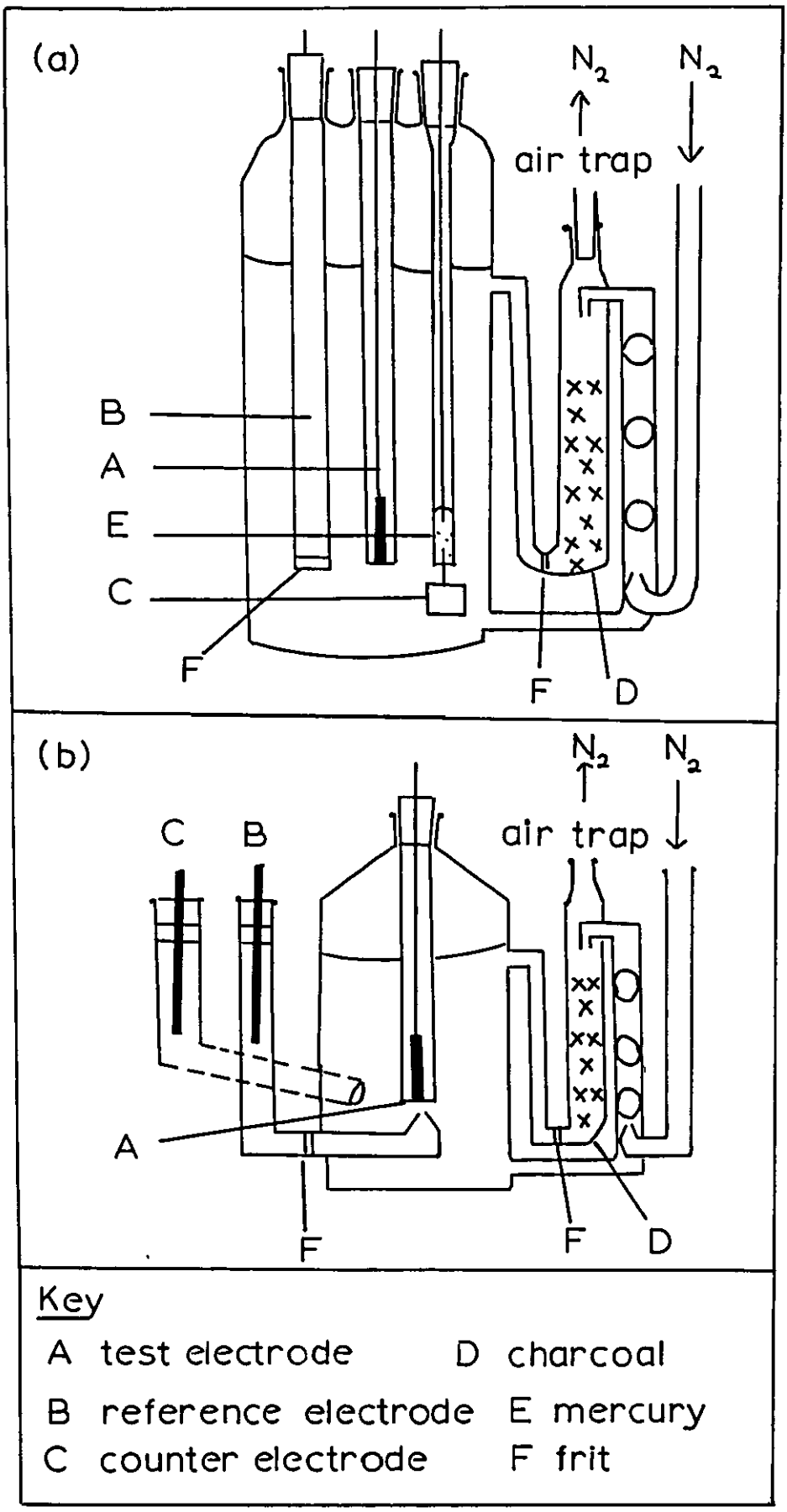

Key

A	test electrode	D	charcoal
B	reference electrode	E	mercury
C	counter electrode	F	frit

FIG 5 Electrolytic cells

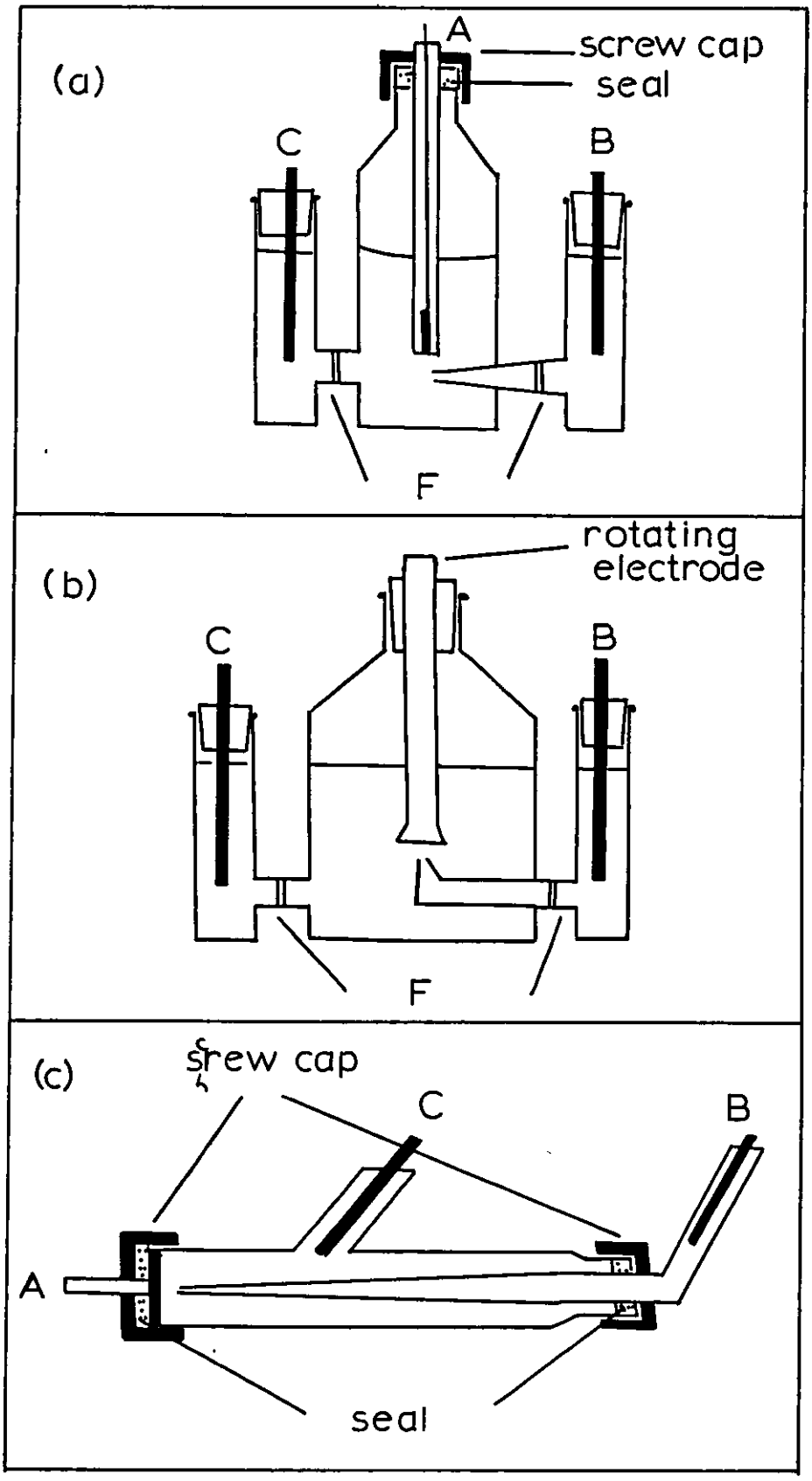

FIG 6 Schering bridge

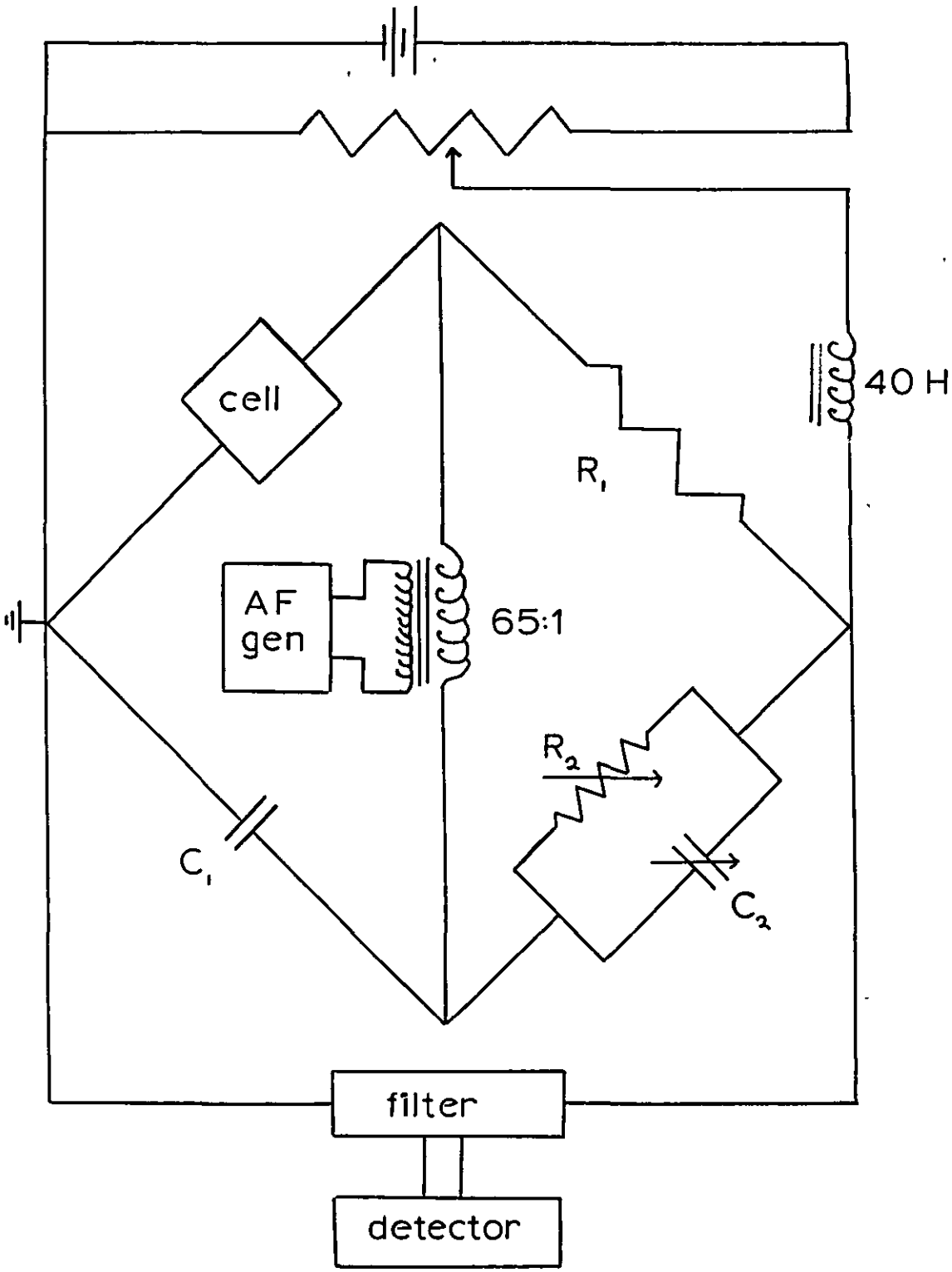

to 6.5 mV peak to peak. The bridge component variable capacitances and resistances were Muirhead 0.1% grade or Sullivan 0.1% grade. The bridge was polarised symmetrically. During all the experiments the test electrode was connected to earth in order to avoid screening difficulties. The a.c. and d.c. circuits were separated by a 40 H choke. The potentials were measured using a digital voltmeter (Solartron Type L.M.1604). The impedance of a cell analogue was measured over a range of frequencies. The discrepancy between the bridge readings and the known values is shown in Table 1.

TABLE 1

Frequency	10 Hz - 1 K Hz	1-5 K Hz	5-10 K Hz	20 K Hz
error <	1%	1%	5%	10%

The bridge could therefore be used within the frequency range 10 Hz - 10 K Hz.

3.2. (ii) Linear Sweep Voltammetry (L.S.V.) The principle of L.S.V. is to apply a potential to the electrode/electrolyte system and vary this potential linearly with time. The electrolyte is not stirred and so diffusion is the major mode of mass transport. At the commencement of an anodic sweep the rate of an electrochemical reaction is low and so negligible current flows. As the potential moves to more anodic values the rate of electron transfer at the electrode increases and this is reflected as an increased current flow. The reacting species are progressively removed

from the vicinity of the electrode and this effect causes current limitations. These limitations become progressively predominant and the faradaic current exhibits a maximum value. The magnitude of this maximum value is proportional to the concentration of the reacting species that control the current flow.

In the case of a metal electrode in alkaline solutions the current limitations may be due to either the removal of OH^- at the electrode surface at a faster rate than it can be replaced by diffusion in the electrolyte, or alternatively the access of metal or O^{-2} ions to the reaction layer is restricted. It is possible for both of these effects to occur simultaneously.

The relationship between the sweep rate, reactant concentration and the peak currents are given by the equations discussed by Delahay[24] for a reversible electrode reaction.

$$i_p = 2.72 \times 10^5 \, n A D_o^{\frac{1}{2}} C_o (S.R.)^{\frac{1}{2}} \qquad (3.1.)$$

for an irreversible electrode reaction:

$$i_p = 3.01 \times 10^5 \, n (\alpha n_a)^{\frac{1}{2}} A D_o^{\frac{1}{2}} C_o (S.R.)^{\frac{1}{2}} \qquad (3.2.)$$

At overpotentials in excess of $\sim +100$ mV the anodic electrode reaction can be considered to be sufficiently irreversible for the cathodic reaction to be neglected.

It is possible therefore, using the L.S.V. method, to distinguish between the two possible modes of diffusion control, those of solid or solution phase control.

It is also possible to obtain approximate values for the diffusion coefficients of the rate controlling species. Such values can only be approximate since there will be some doubt of the exact values of variables such as A (electrode area), C_o (the concentration of the rate controlling species) and also uncertainty about the extent of the reversibility of these processes.

Calculations of α values from E_p, the potential at which the peak current flows, is possible in theory. Delahay[24] has shown that E_p is independent of the reactant concentration but varies with the sweep rate (S.R.) in a rather complicated manner. In practice the inherent uncertainties of a study at a solid metal electrode make such calculations difficult.

The potential sweep experiments were carried out using a fast response potentiostate in conjunction with a linear sweep generator (Chemical Electronics Ltd. Type R.M.2). The current/time traces were recorded on a chart recorder (Bryans Type 2700). Potentials were accurately measured using a digital voltmeter (Solartron Type L.M.1604). A block diagram of the overall circuit is shown in Figure 7.

3.2. (iii) Measurements With A Rotating Disc Electrode The theoretical problem of controlling mass transport of reacting species from solution to the surface of a rotating disc electrode has been fully discussed by Levich[25]. The theoretical system considered comprised of a thin horizontal laminar rotating with a constant angular velocity, about an axis perpendicular to the laminar, in a fluid of infinite extent. The practical system takes the form of a disc of 1 mm to several cms in diameter rotated at a constant

FIG 7 L.S.V. circuit

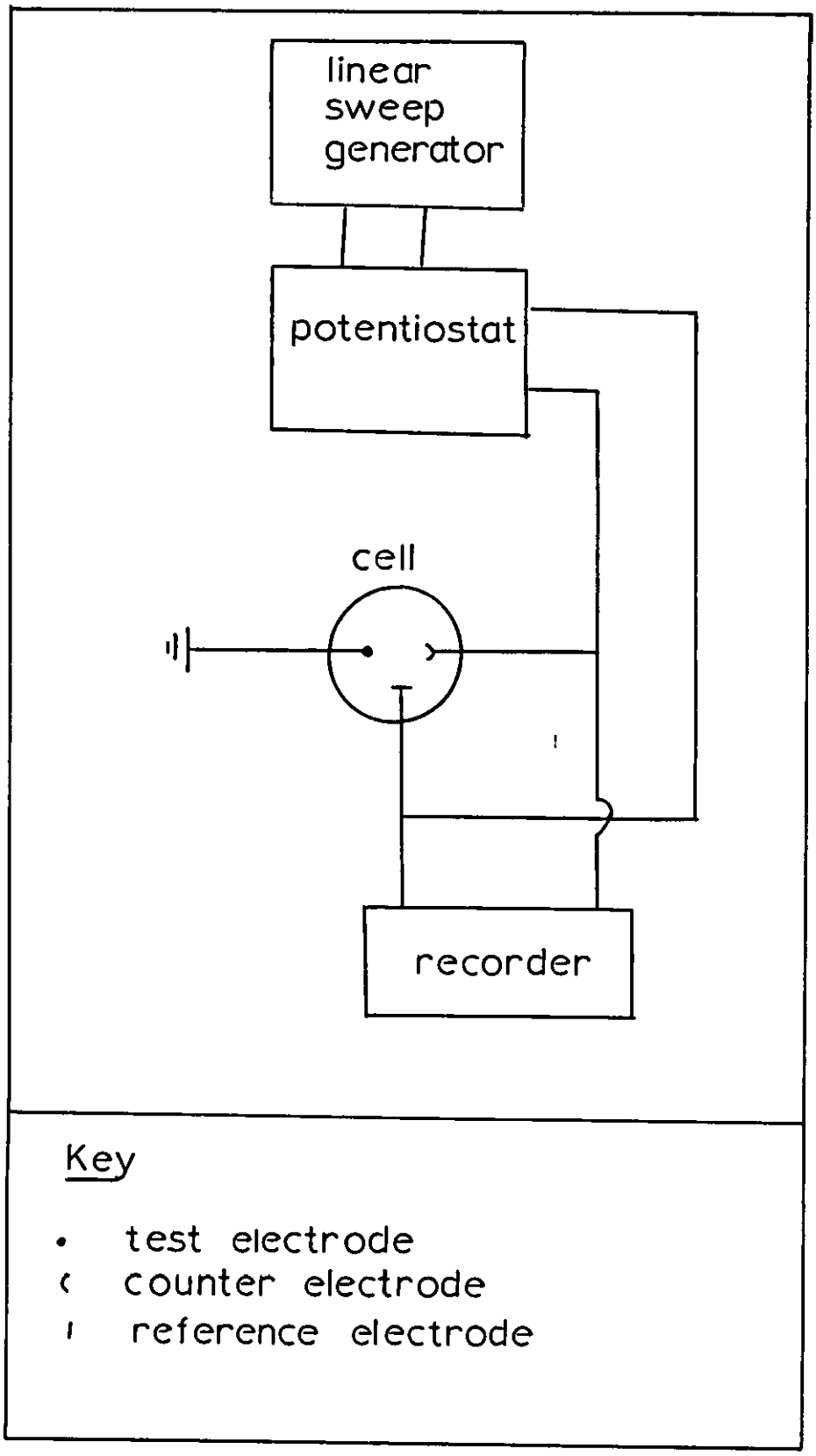

speed in a fluid contained in a laboratory scale-vessel. The physical dimensions of the vessel and the various types of disc electrodes that have been used are discussed fully and critically by Riddiford[26] and Gregory[27,28], and Jordan[29].

A practical disc will function in the same manner of an infinite laminar provided that:

a) The Reynolds number is very much greater than the value which leads to a contribution to the mass transport from natural convection.

b) The Reynolds number is less than that of the critical value for the onset of turbulence.

c) That no serious edge effects are introduced by having a disc of finite size.

d) That all bounding surfaces, other than the disc itself, are effectively at an infinite distance from the electrode.

e) The disc itself is horizontal and has a minimum eccentricity and rugosity of much less than the boundary layer thickness.

The Reynolds number, Re, is given by:-

$$Re = \frac{r^2 \omega}{\nu} \qquad (3.3.)$$

where r is the radius of the disc, ω the angular velocity and ν the viscosity of the

solution.

Since the Reynolds number is a function of the disc radius, it can be seen that for a relatively large disc the centre of the disc may be experiencing laminar flow whilst the outer edge is experiencing turbulent flow. For this reason the design of the disc electrode used was such that only the centre of the rotating disc was of the electroactive material. Providing that there is approximately a clearance of 5 cms between the edge of the disc and the nearest boundary surface, such as a cell wall, condition (d) is obeyed.

For the electrochemical case of the transport of ions in solution to the electrode surface, Levich[25] has shown that the limiting current for a reaction controlled by mass transport in solution is:

$$i_d = 0.62\, n\, F\, A\, C_o^b\, D_o^{\frac{2}{3}}\, \nu^{-1/6}\, \omega^{\frac{1}{2}} \qquad (3.4.)$$

In the case when $i < i_d$ we have a net current flowing that is made up of an anodic current equivalent to that flowing at infinite rotation speed and the backward cathodic reaction.

hence $i_{net} = i_{(\infty)} - i_{cathodic}$

$$= i_{(\infty)} - n\, F\, K_b\, C_o^s \qquad (3.5.)$$

~~inverting gives:~~ see Appendix

$$\frac{1}{i} = \frac{1}{i_{(\infty)} - n F K_b C_o^s} \qquad (3.6.)$$

~~expanding (3.6.) using the binomial expansion and substituting for~~:

$$i_{(\infty)} = \frac{n F D_o C_o^b}{\delta}$$

where

$$\delta = 1.61 D_o^{\frac{2}{3}} \nu^{1/6} \omega^{-\frac{1}{2}}$$

we obtain an expresssion:

$$\frac{1}{i} = \frac{1}{i_{(\infty)}} + \frac{K_b}{\text{constant } \omega^{\frac{1}{2}}} \qquad (3.7.)$$

Thus a plot of i^{-1} versus $\omega^{-\frac{1}{2}}$ should be linear with an intercept of $i_{(\infty)}^{-1}$.

The design of the rotating disc assembly used has been described above and is shown in Figure 3. The electrolytic cell is shown in Figure 5(b). Contact between the r.d.e. and the external circuit was made through a mercury pool contact. The external circuit consisted of a motor/generator that rotated the disc electrode, the speed of which was controlled by a velodyne amplifier (Figure 8). The rotation speed of the disc was measured using a stroboscope (Dawe Type 1200 E). The potential control was by a potentiostat (Chemical Electronics Limited Type R.M.2) and potential measurements were taken with a digital voltmeter (Solartron Type L.M.1604).

FIG 8 Velodyne circuit

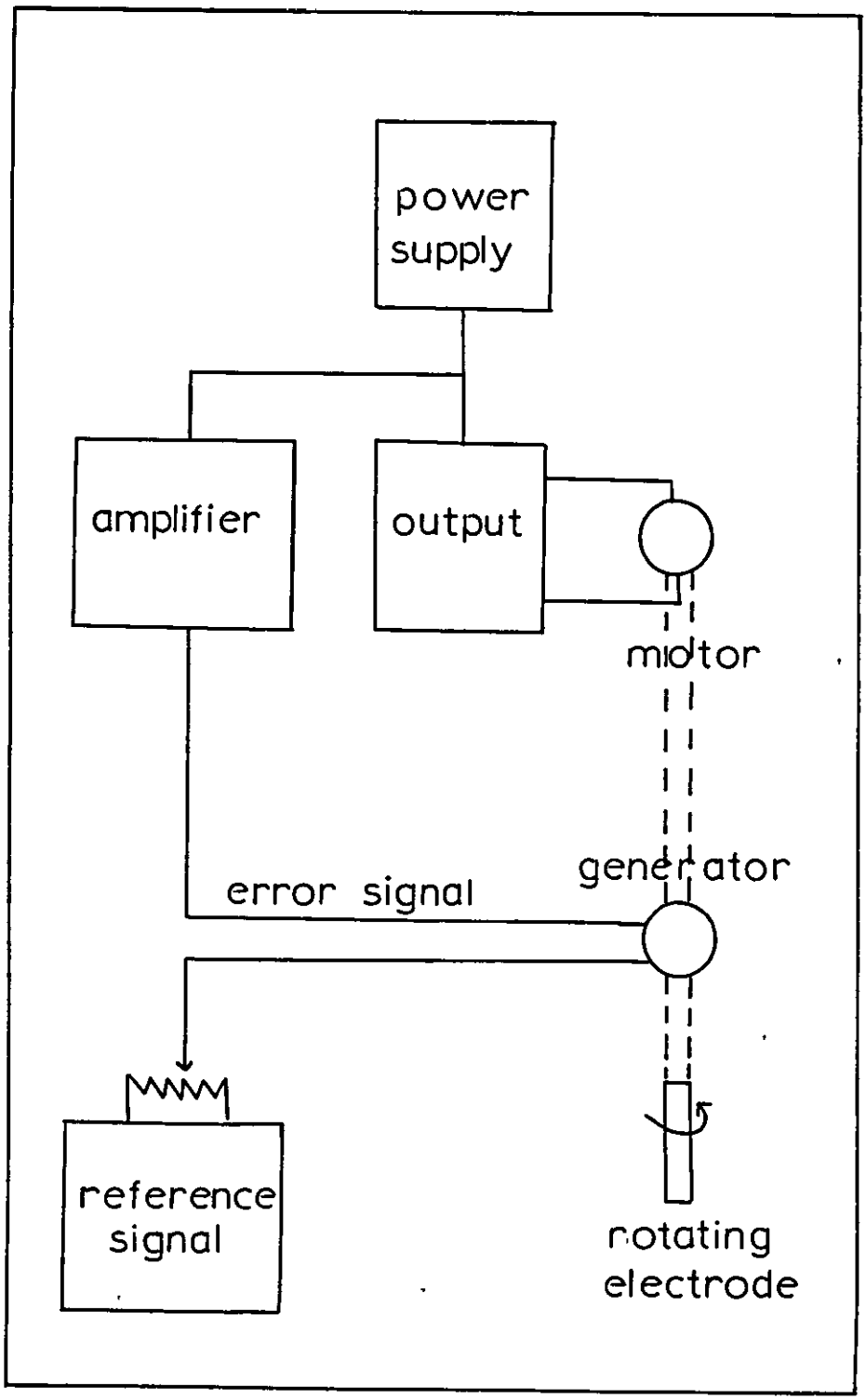

A combination of linear sweep voltammetry and a rotating disc electrode system has been used in studies of electrode reactions. This is because such a technique provides much useful information concerning electrode reactions occurring over a wide range of potentials, whilst controlling the mass transport of ionic species in the electrolyte. The information that is obtained may only be used in a qualitative manner since no mathematical treatment of electrode reactions under such experimental conditions has been reported.

3.2. (iv) Galvanostatic Measurements When a current time step-function is applied to an electrode the resultant potential-time response would be a step-function also if charge transfer were the only rate controlling process. This ideal response is not obtained and the real potential-time transient is of the type shown in Figure 9. At least three factors intrude to contribute to the nature of the real potential-time response. The resistance of the electrolyte between the tip of the luggin capillary and the test electrode results in a higher than expected potential. This appears in practise as a vertical gap in the real response trace and can be readily corrected. The capacitance of the electrode requires a finite current flow before the new potential is obtained. The slope of the potential-time trace at zero time yields the electrode capacitance[29] according to:

$$\left(\frac{\partial E}{\partial t}\right)_{t \to o} = \frac{-i}{C_L} \qquad (3.8.)$$

FIG 9 Galvanostic pulse

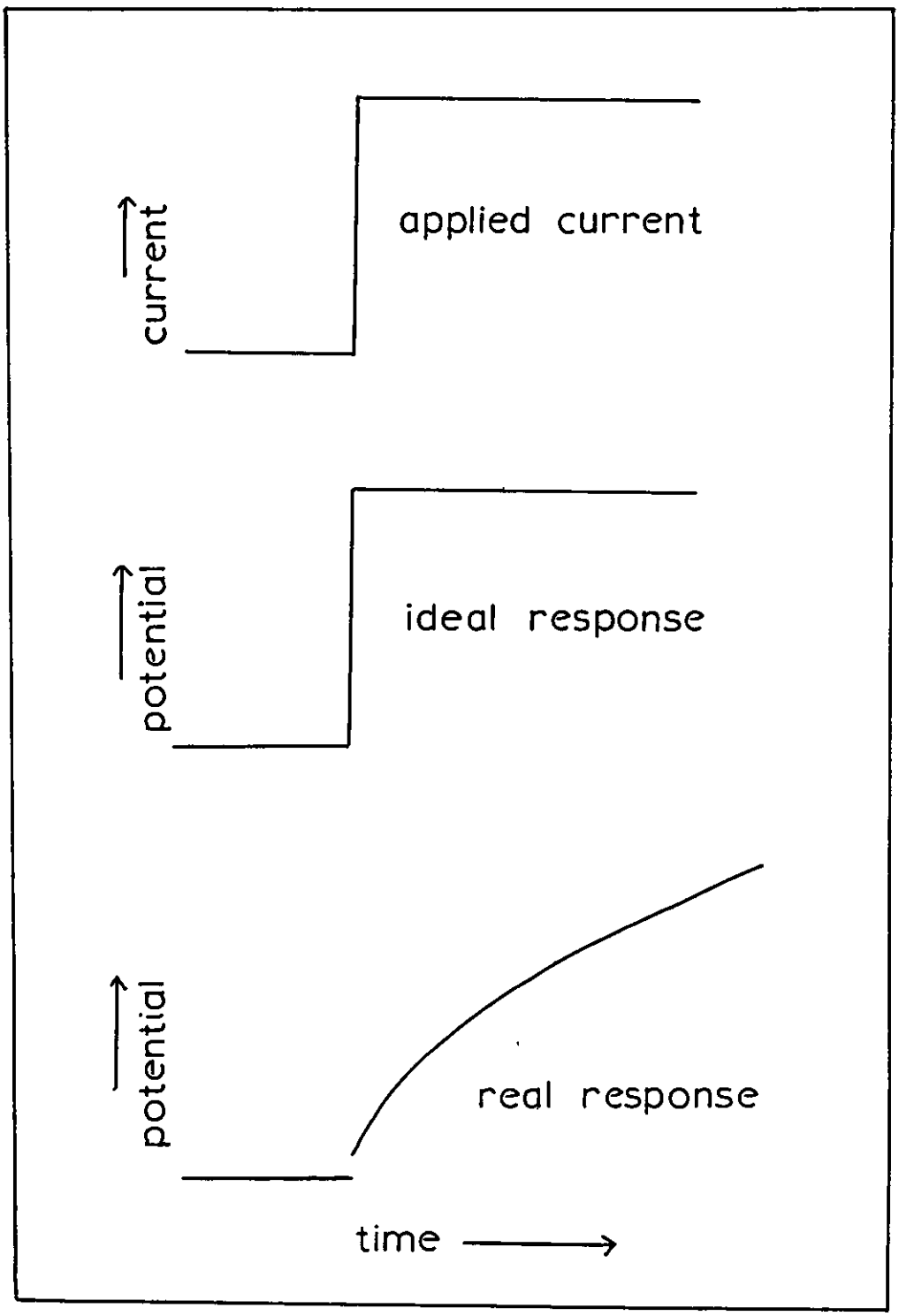

FIG 10 Galvanostic circuit

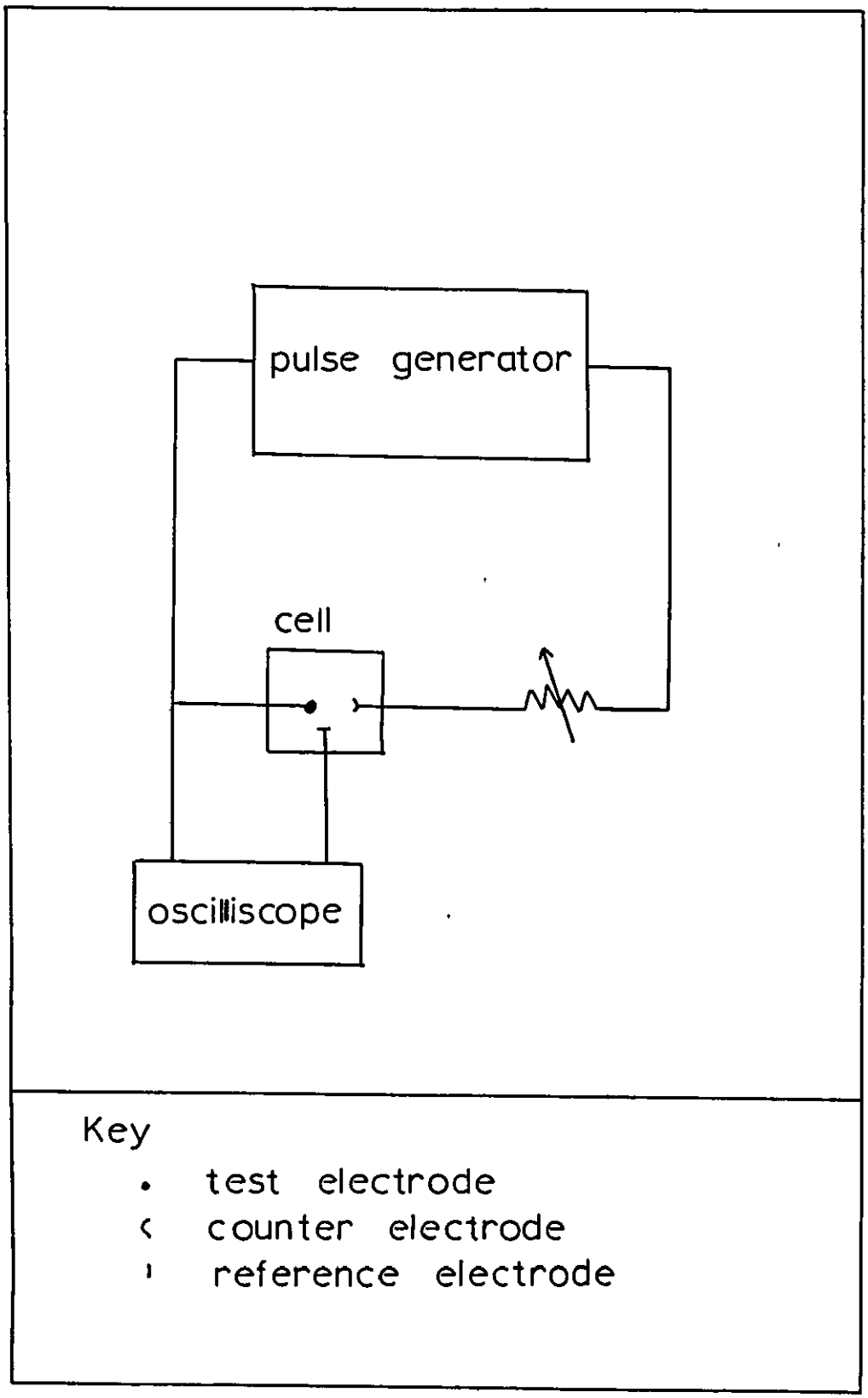

Changes in the concentration of the electroactive species at the electrode cause a further time dependent potential change. The activation overpotential, η_D, can be derived by extrapolation of the potential-time trace to zero time, where the diffusion overpotential, η_d, will be zero. When the exchange reaction is slow ($i_o < 10^{-2}$ A cm^{-2}) the extrapolation to derive η_D is relatively easy. When the exchange reaction is faster ($i_o > 10$ A cm^{-2}) the double layer charging process intrudes on the reaction making analysis of the η-t traces difficult. Gerischer and Krause[30] have developed a double pulse technique in which a short, intensive prepulse is used to charge the double layer before the application of the main pulse.

The electrical circuit used in the present experiments is shown in Figure 10. The square current pulse was obtained from a pulse generator (Lyons Type P.G.23), the output of which was of variable amplitude up to a maximum of 500 mA into 50 Ω. The range of the current amplitudes was increased by introducing resistances, in series, into the circuit. Using micro-electrodes it was found convenient to introduce a load resistance to limit the current amplitude. The current amplitude was estimated by measuring the potential developed across a standard resistance in the pulse circuit using an oscilloscope (Hewlett Packard Type 130C). The potential response of the test electrode to the current pulse was measured between the test electrode and an unpolarised reference electrode (of the same material as the test electrode) via a luggin capillary, using an oscilloscope (Hewlett Packard Type 130C). The transient produced was recorded from the oscilloscope screen with a polaroid camera (Hewlett-Packard Type 196 B).

CHAPTER 4

A REVIEW OF THE SYSTEM Ag/OH^-

A study of the differential capacitance of an electrode is an essential preliminary study in an investigation of the kinetics of electrochemical reactions at the electrode. The differential capacitance of silver has been studied in neutral[31,32] and alkaline[33] electrolytes. The values of the E_z, the potential of zero charge, have been reported in the range 0.5 V (n.h.e.) to the more probable value of -0.7 V (n.h.e.). The most recent results obtained with non-interacting electrolytes[32,34] supporting this lower value. Also a correlation of E_z with the electronic work function[35] for different metals indicates that the E_z should lie $\sim$ -0.7 V (n.h.e.). This values is by no means fully accepted since recent studies involving the adsorption of neutral organic compounds indicates that the E_z may lie at a more positive potential[36].

In spite of numerous papers published concerning the oxidation of silver electrodes in alkaline solutions there is also some uncertainty concerning the primary electrochemical oxidations involved. It is generally accepted that there are two electrochemically well defined oxides formed at silver anodes in alkaline solutions:

(a) Ag(I) oxide, Ag_2O, $E^\circ = 0.338$ V (n.h.e.)

(b) A higher oxide with the stoichiometric formula AgO, $E^\circ = 0.599$ V (n.h.e.)

Although the stoichiometry of AgO indicates that the silver is present in the Ag(II) oxidation state, magnetic susceptibility measurements[37] show that AgO is diamagnetic and crystal structure measurements[38] show that there are two distinct Ag-O distances. It appears therefore that AgO exists as the Ag(I) Ag(III) oxide.

Historically the first electrochemical investigationsinto the anodic behaviour of silver in alkaline solutions have generally been by galvanostatic and potentiostatic pulse polarisation experiments, in which the appropriate step function is applied to the electrode at equilibrium. Using such methods the two oxidation steps of the silver lattice have been identified corresponding to the reaction:

$$2\,Ag + 2OH^- \longrightarrow Ag_2O + H_2O + 2e \qquad (4.1.)$$

$$Ag_2O + 2OH^- \longrightarrow 2\,AgO + H_2O + 2e \qquad (4.2.)$$

by various workers, e.g. Pokorny and Luther[39] and Hickling[40].

The careful galvanostatic studies by Hickling revealed the two stages formation of the Ag_2O layer, double layer charging confusing the first few instants of the oxide formation. Kabanov et al[41] concluded from their measurements that these two processes were the formation of a dense Ag_2O layer (10 μ thick) followed by the formation of a more porous oxide layer. Yoshizawa and Takehara[42], who combined electromicroscopy with their galvanostatic experiments observed only the formation of a layer of spherically shaped Ag_2O centres on silver plated platinum electrodes. A similar conclusion was drawn by Wales and Burbank[43] who examined

working silver electrodes, insitu, using an x-ray diffraction technique, who stated that a thin film of Ag_2O was first formed followed by a thicker layer of AgO.

In a recent comprehensive study of anodically formed silver oxides Briggs et al[44] have concluded that there are at least three distinct layers of anodically formed oxides. The primary layer of argentous oxide consists of a random orientated deposit of small crystallites, the thickness of the layer being 50 - 100 Å. The secondary layer of relatively large (~1 000 Å) blocks of argentous oxide is formed upon this primary layer, the size and shape of these particles depending on the method of preparation. This secondary layer does not completely cover the primary and they are both subsequently covered by a tertiary layer of oxide (hemispherical centres ~ 200 Å). The conversion of the argentous oxide layer to argentic oxide destroys the orientation of the Ag_2O as the AgO centres grow. The final argentic product being randomly orientated and the centres are in the size range 0.1 - 3.0 μ. The mechanism of the formation of the Ag_2O was reported to be controlled by the diffusion/migration of Ag ions through a randomly orientated basal layer. The oxidation of Ag_2O to AgO involved the progressive nucleation of AgO centres coupled with three dimensional growth.

One perplexing feature of the anodic behaviour of Ag in OH^- is the appearance of effects that indicate that there is a faradaic reaction occurring at potentials lower than that required for the formation of argentous oxide. This effect is most readily observed during potential sweep measurements. Dirkse and DeVries[45],

who used both slow and rapid potentiodynamic scanning techniques, have shown that for anodic sweeps a minor current peak, before the massive Ag_2O formation, is observed. This subsidary peak should also be observable during the reduction of the oxidised layer, but a corresponding reduction peak is only observed if the potential scan is reversed before the massive Ag_2O formation.

One explanation of this phenomenon, that has been postulated by Dirkse, was that the peak represented the formation of AgOH. This conclusion was based on the dependence of the potential at which the peak commenced, upon the hydroxide concentration. A similar conclusion was drawn by Stonehart[46] who examined the oxidation of monatomic layers of silver on a rhodium substrate.

An alternative explanation of this reaction process was put forward by Clarke et al[47] who concluded that this reaction peak was due to the oxidation of "activated" silver lattice sites. The product of this oxidation could either be AgOH, as suggested by Dirkse, or more likely Ag_2O. This conclusion was based on the fact that the magnitude of this reaction peak was increased markedly when a reduced, completely oxidised electrode (i.e. an electrode where the normal surface Ag lattice had been transformed into that of the oxide lattice in which the Ag atoms are relatively widely spaced) was reoxidised.

A more recent investigation into this process by Giles and Harrison[48] states that this reaction peak corresponds to the faradaic dissolution of Ag as $Ag(OH)_2^-$, with diffusion of the products away into solution. These workers also found that the "shape" of the peak was a function of the electrode roughness since results at a freshly polished single crystal differed from those of a silver bead electrode.

CHAPTER 5

OXIDATION OF SILVER ELECTRODES IN ALKALINE SOLUTIONS

5.1. Experimental

5.1. (i) Stationary Electrode The test electrode was of spectroscopically pure silver and constructed in the manner described in section 3.1. (i). It was cleaned on roughened glass (lubricated with bidistilled water) and then chemically etched (15% HNO_3) before every reading. The electrode area was 4.54×10^{-2} cm^2. The counter electrode was of silver gauze, the electrode area being many times greater than that of the test electrode. The reference electrode was a saturated calomel electrode. The electrolytic cell was of the type shown in Figure 5 (a), and was filled with pure sodium hydroxide electrolyte prepared from A.R. sodium hydroxide and bidistilled water.

The electrical circuit used for the linear sweep voltammetry has been described in section 3.2. (ii).

5.1. (ii) Rotating Electrode The test electrode was again of spectroscopically pure silver and constructed in the manner described in section 3.1. (ii). (See Figure 3). The reactive electrode area was 4.54×10^{-2} cm^2. The counter electrode was of silver gauze and the reference electrode was a saturated calomel electrode. The

r.d.e. was cleaned on fine emery paper and or roughened glass (both lubricated with bidistilled water) and then chemically etched (15% HNO_3) before every reading.

The electrolytic cell was of the type shown in Figure 5 (b) and was filled with pure aqueous sodium hydroxide electrolyte.

The rotation of the r.d.e. was controlled by a velodyne amplifier in conjunction with a motor/generator as described in section 3.2. (ii).

5.2. Results

5.2. (i) Stationary Electrode A typical potentiodynamic current curve obtained for a stationary silver electrode in NaOH (1.0 mol l^{-1}) is shown in Figure 11. It can be seen from this curve that there are three "reaction peaks" *, corresponding to three electrochemical reactions that have occurred (reactions (i), (ii) and (iii)).

It was found that the peak height of the minor preliminary peak was dependent upon the length of time that the test electrode was left in contact with the electrolyte, before the linear sweep scan was commenced. A summary of this

---

*Footnote The term "reaction peak" has been used to describe the current peaks that occur on the L.S.V. traces corresponding to electrode reactions occurring in that potential region.

FIG 11 L.S.V curve for Ag|OH^-

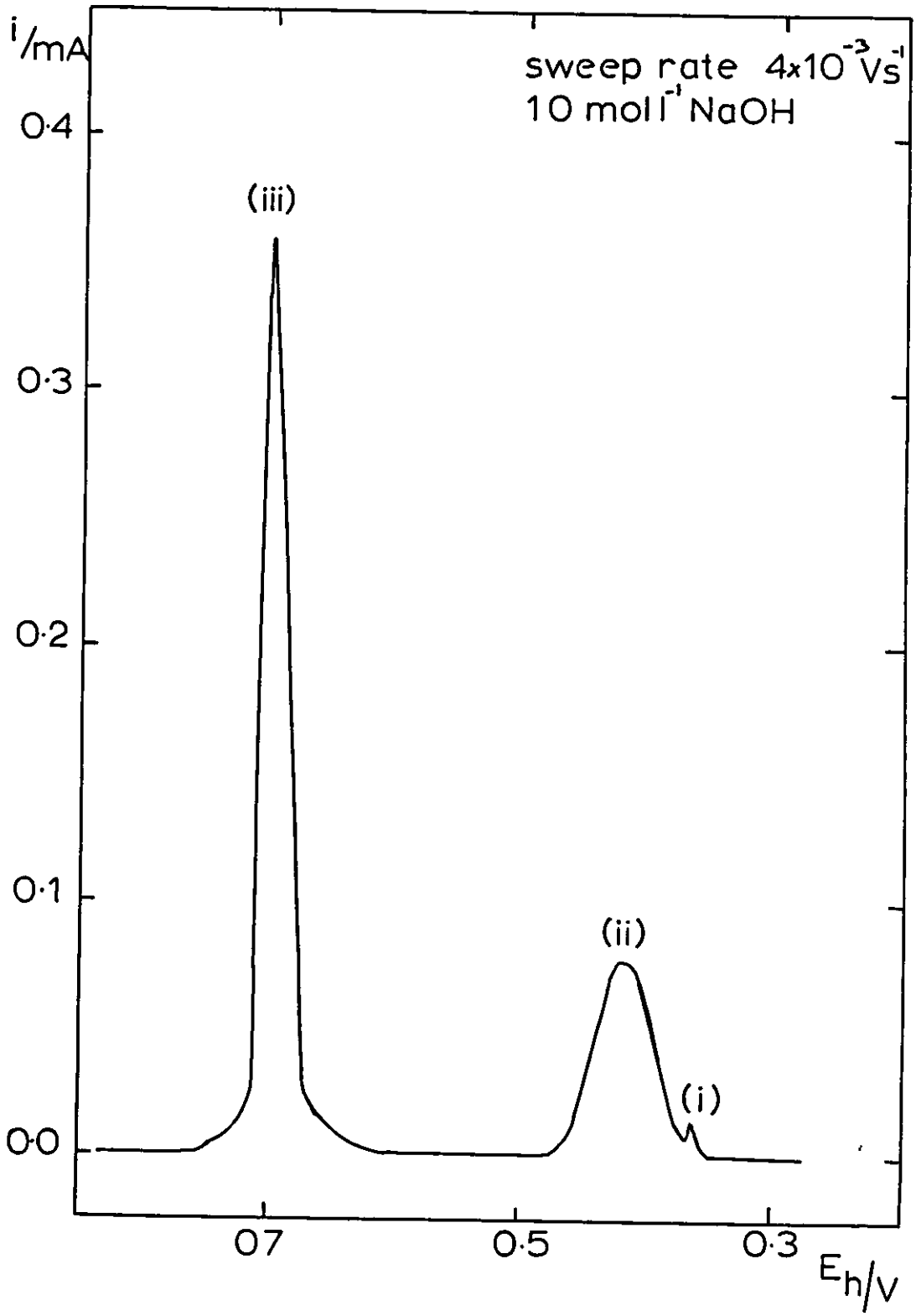

time dependence is shown in Table 2.

The height of this reaction peak was greatly enhanced when a linear sweep scan was carried out at a cycled electrode. This effect has been reported previously[47], but the time of contact required for the elimination of the preliminary peak from the potentiodynamic current curves was much longer in these present experiments. It was also observed that there was no corresponding reduction peak for this reaction peak when the direction of the potential scan was reversed after the formation of peak (ii). If however the direction of the scan was reversed before the start of peak (ii) then a corresponding reduction peak was observed.

TABLE 2.

Contact Time (min.)	Peak Height (mA)
5	0.027
10	0.025
15	0.020
45	0.020
60	0.014
18 hours	0.000

When the potential sweeping rate was changed the peak heights, i_p, of reaction peaks (ii) and (iii) varied accordingly. The variation of these peak heights with the square root of the sweeping rate ($\sqrt{S.R.}$) is shown in Figures 12 and 13, for reactions (ii) and (iii) respectively, for a range of electrolyte concentrations.

FIG 12 Dependence of i_p on $\sqrt{S.R}$

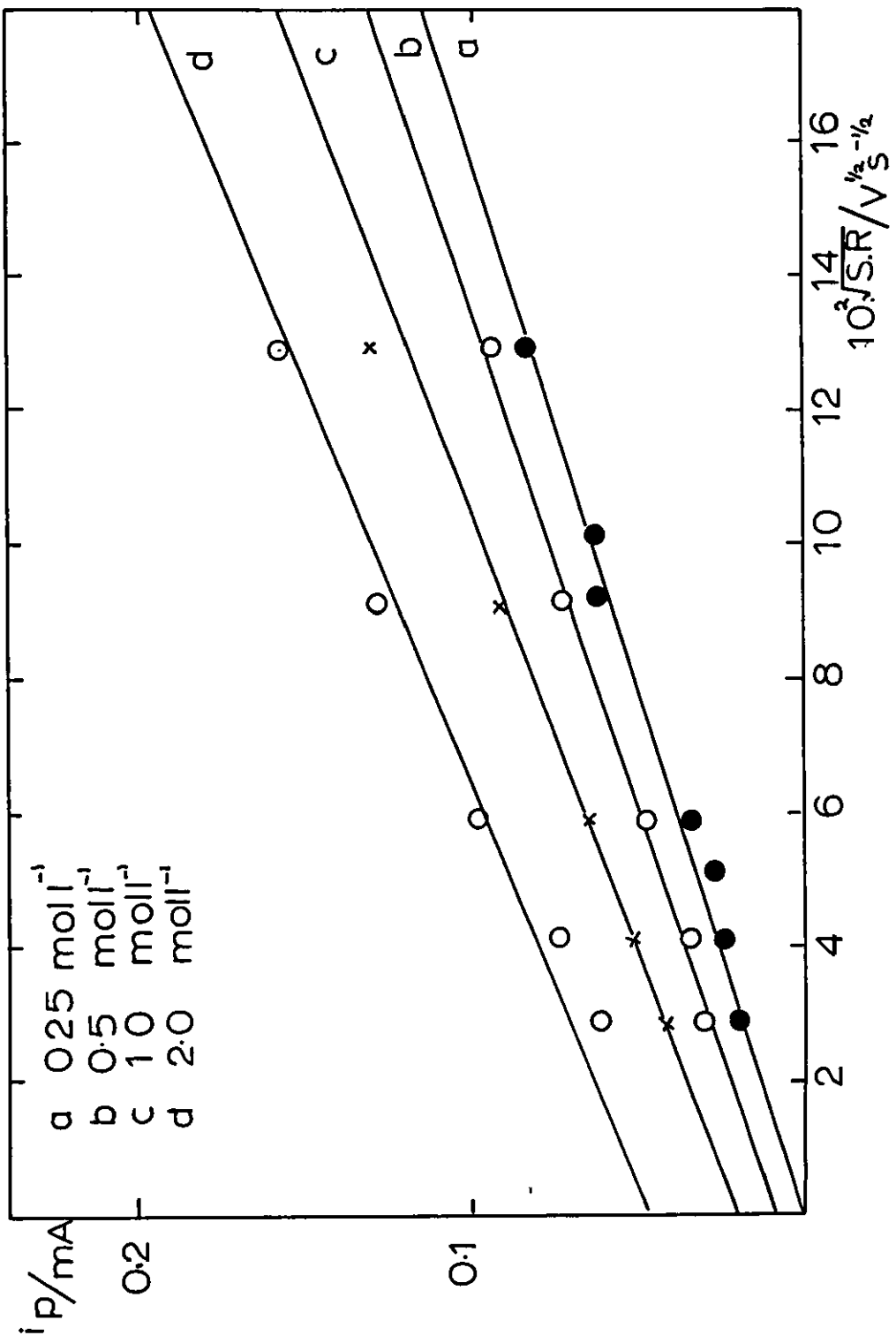

FIG 13 Dependence of i_p on $\sqrt{SR}$

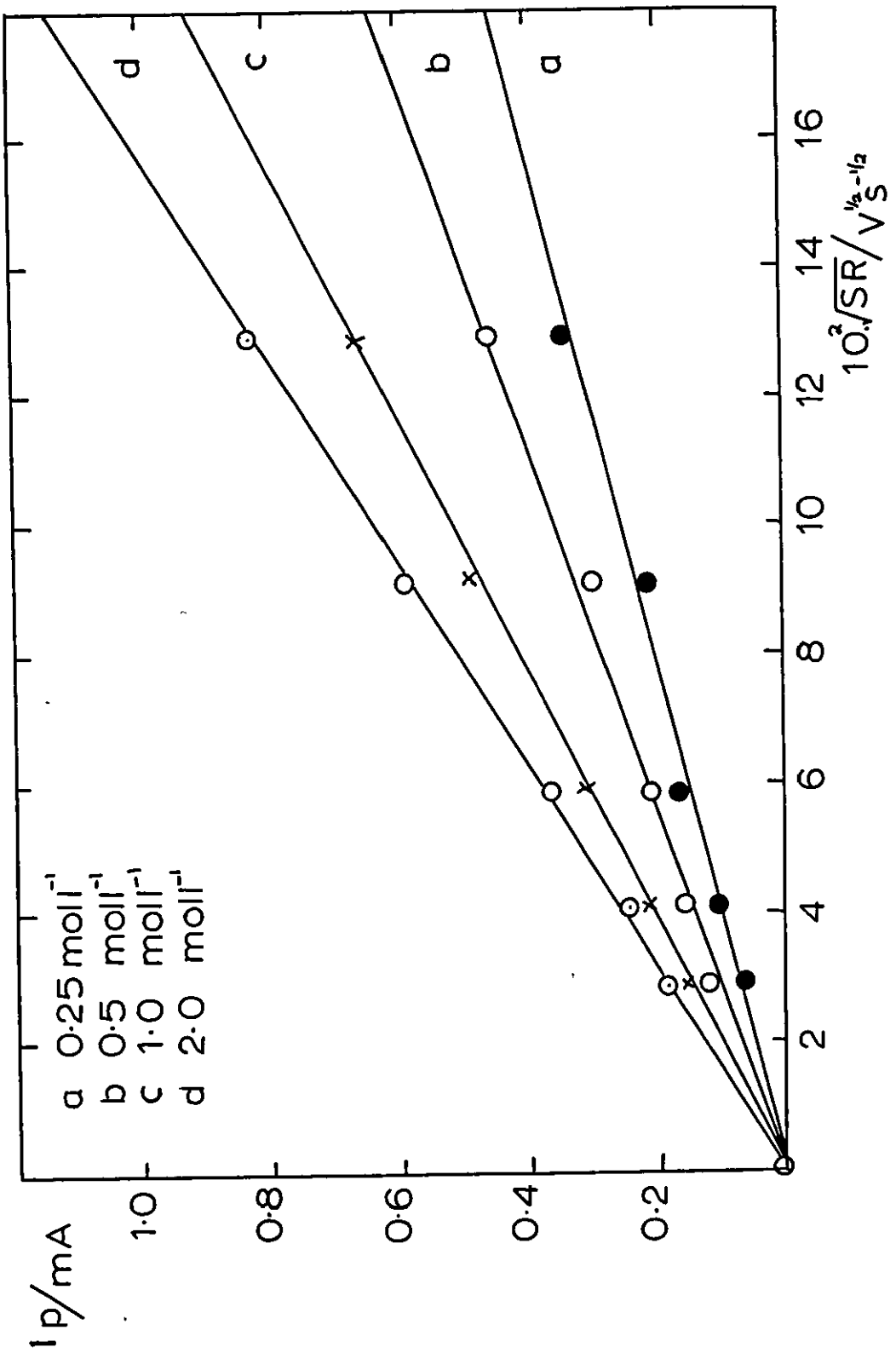

Calculations from the i_p vs $\sqrt{S.R.}$ plots using the equations derived by Delahay[24] give values of $1\text{-}4 \times 10^{-10}$ cm s^{-1} for an apparent diffusion coefficient for the rate controlling species in reaction (ii) and of 4×10^{-8} cm s^{-1} for an apparent diffusion coefficient for the rate controlling species in reaction (iii).

5.2. (ii) Rotating Electrode When a potential sweep was applied to a silver r.d.e. a potential/current curve, similar to that found with a stationary electrode, was obtained. The only significant difference was that the reaction peaks were broader for the case where the electrode was rotated. The variation of the peak heights, i_m, with changes in the rotation speed, ω, for reactions (ii) and (iii), are shown in Figure 14 where i_m^{-1} is plotted against $\omega^{-\frac{1}{2}}$. The variation of the preliminary reaction peak height with changes of the rotational speed is shown in Table 3.

TABLE 3 Dependence of peak height for reaction (i) on rotation speed

1.0 mol l^{-1} NaOH, 8.33×10^{-3} V s^{-1}, 23°C

Rotation Speed (r.p.m.)	Peak Height (m.A.)
500	0.035
650	0.038
1 000	0.032
2 000	0.032
3 000	0.031
4 000	0.036

FIG 14 Dependence of i_m^{-1} on $w^{-1/2}$

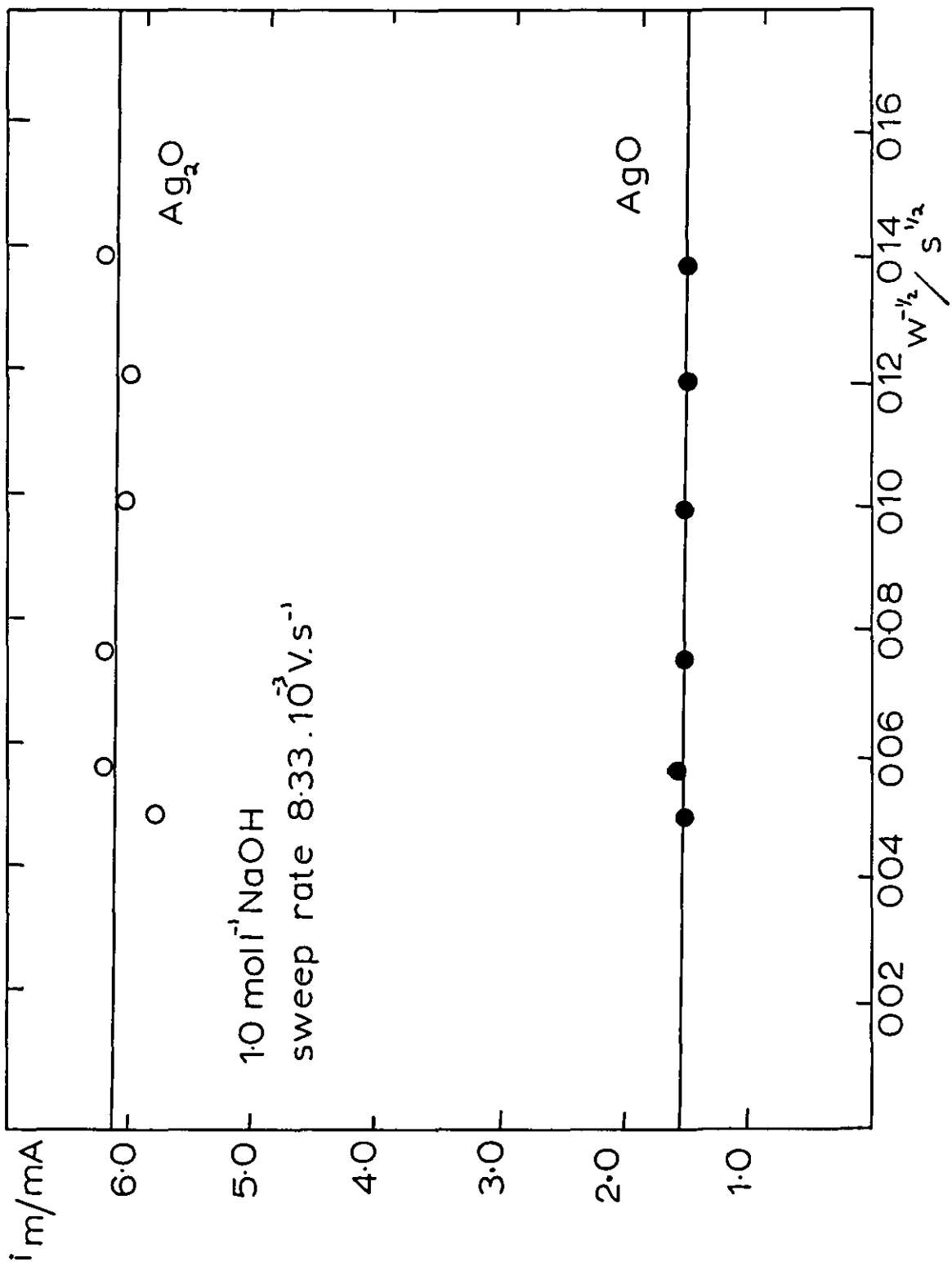

5.3. Discussion

The potentials at which the two major reaction peaks occur (reaction peaks (ii) and (iii) in Figure 3) correspond to the electrochemical formation of Ag_2O and AgO respectively at the silver electrode in sodium hydroxide electrolyte. The preliminary peak (reaction peak (i)) is readily observed in these experiments but is not present when the electrode is left in contact with the electrolyte for a period of 18 hours prior to the start of the potential sweep. This time dependence of this reaction peak height has been reported previously[47], although in the present experiments the duration of the contact time for the complete removal of the reaction peak is much longer. The enhanced height of this reaction peak when a cycled electrode is reoxidised has also been reported[47], as has the observation that a corresponding reduction peak is only observed if the direction of the potential scan is reversed before the massive formation of Ag_2O.

The variation of the peak height, corresponding to this preliminary reaction, with changing rotational speed is shown in Table 3. It is observed that there is very little variation of the peak height within the range of rotation speeds investigated. It seems likely therefore that this preliminary reaction is controlled by a solid phase process. This is in contrast to the findings of Giles and Harrison[48], who found that the reaction that occurred at potentials less positive than those required for the formation of Ag_2O was due to the diffusion controlled dissolution of silver as $Ag(OH)_2^-$. Giles and Harrison did however find that the shape of the reaction peak was a function of the electrode roughness, since variation in the shape of the peak was found between

experiments using a freshly polished single crystal and those using a silver bead electrode. This latter point appears to support a conclusion that this peak represents the oxidation of an active silver lattice, as do the reported findings in this current investigation. It is concluded therefore that the electrode process that results in this preliminary reaction peak is the oxidation of active silver lattice sites. The product of this oxidation may be AgOH, as suggested by Dirkse[45], but is more likely to be Ag_2O.

An analysis of the variation of the peak height, for reaction peak (ii), with $\sqrt{S.R.}$ is shown in Figure 13. The resulting straight line plots, of the results for the four concentrations that were investigated, are approximately parallel and their slopes independent of the electrolyte concentration. An apparent diffusion coefficient for the reacting species concerned in the rate controlling process, calculated from the equations discussed by Delahay[24], was $1\text{-}4 \times 10^{-10}$ cm s^{-1}. This value is too small for the rate controlling process to be a solution phase reaction. Since the rate of the reaction has been shown to be independent of the electrolyte concentration, it is concluded that the rate controlling process is most likely due to the diffusion of Ag^+ through a solid phase at the electrode. This is in agreement with the findings of Clarke et al[47], Croft[50], Takehara et al[51] and Kuhoz[52]. The intercepts with the i_p axis, associated with the graphs of i_p vs $\sqrt{S.R.}$, are probably due to the occurrence of a preliminary process that is not connected with this diffusion process. The magnitude of these apparent intercepts reflects the magnitude of the preliminary process.

A similar analysis of the i_p and $\sqrt{S.R.}$ data for reaction peak (iii) is shown in Figure 13. Again straight line graphs are obtained, typical of diffusion controlled reactions, but the slopes of the lines are dependent upon the concentration of the electrolyte, indicating that the diffusion control is dependent upon $[OH^-]$. The straight line plots all pass through the origin as predicted by equation (3.2.). A value of an apparent diffusion coefficient of the rate controlling species was calculated to be 2×10^{-8} cm s^{-1}. This value is again too small for the rate controlling process to be due to the diffusion of ionic species in the solution and it is suggested that the reaction is controlled by the diffusion of OH^- through a solid phase at the electrolyte/electrode interphase.

Microscopic evidence[43,44] indicates that the solid phase of AgO is deposited at the Ag_2O| electrolyte interphase. The oxidation of the Ag_2O to AgO involves the progressive nucleation of AgO centres coupled with their three-dimensional growth[53]. It is likely therefore that the rate controlling process, for the oxidation of Ag_2O to AgO, involves the transference of OH^- ions through this solid phase to the Ag_2O|AgO interphase.

These conclusions, that both the Ag/Ag_2O and Ag_2O/AgO reactions are controlled by solid phase processes, are confirmed by the results of the experiments at a rotating silver electrode in 1.0 mol l^{-1} NaOH electrolyte. The variation of the reaction peak currents, corresponding to reactions (ii) and (iii), with changing rotation speed are shown in Figure 14. The straight line graphs parallel to the $\omega^{-\frac{1}{2}}$ axis indicate that the reaction peak currents are independent of rotation

FIG 15 Oxidation of a Ag electrode

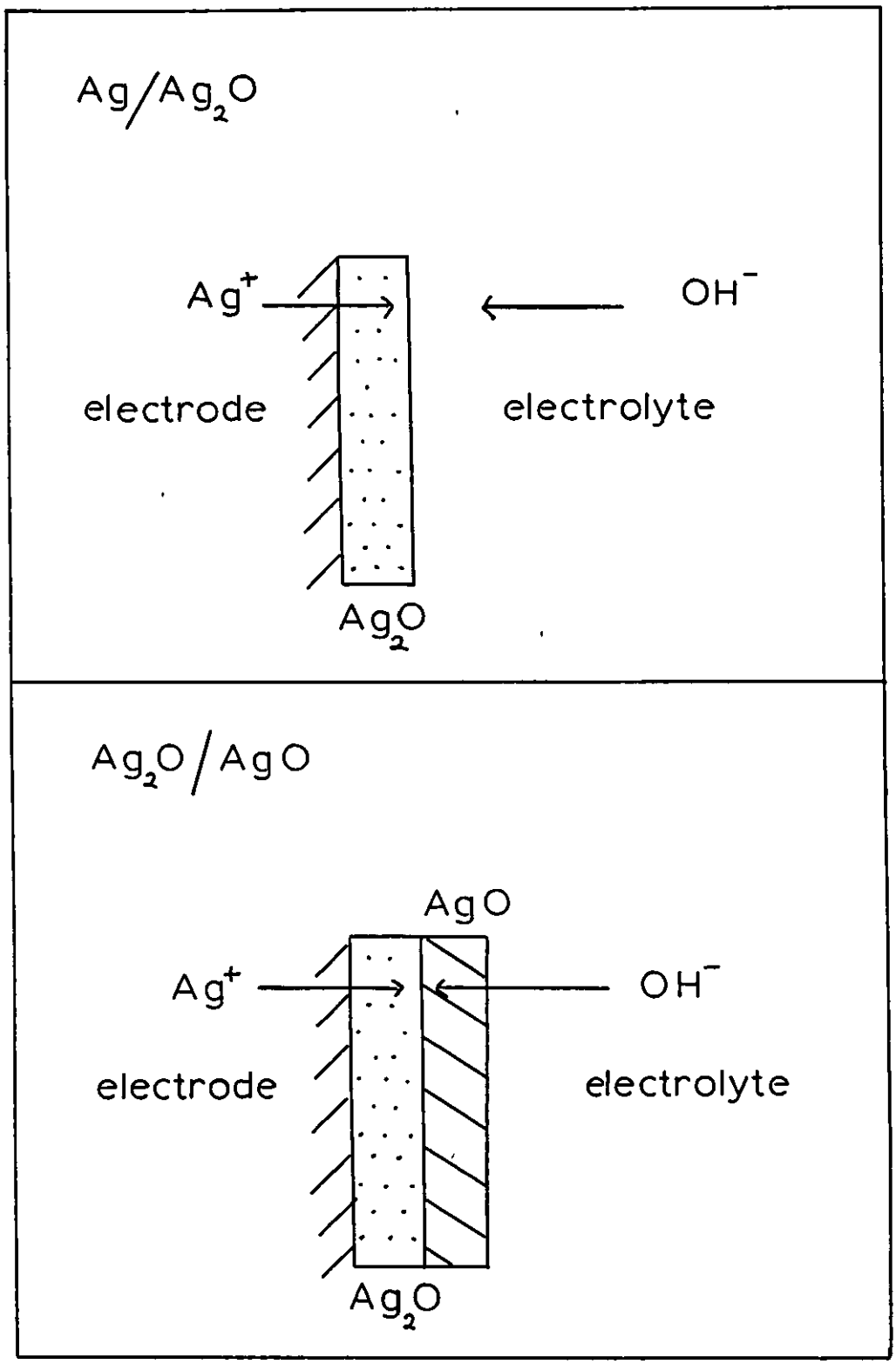

speed. Hence these reactions are not controlled by the convective transport of OH^-, or any other ionic species, through the solution and therefore the rate controlling processes could be the transference of the reactive species through a solid phase.

The overall conclusions concerning the nature of the controlling processes for the two major oxidations are summarised in Figure 15. It can be seen that the rate controlling process for the oxidation Ag/Ag_2O is depicted as the transference of Ag^+ through the oxide layer to the oxide | electrolyte interphase. The rate controlling process for the oxidation Ag_2O/AgO is depicted as the transference of OH^- through an oxide layer to the $Ag_2O|$ AgO interphase.

CHAPTER 6

THE OXIDATION OF α-AMINO ACIDS AT SILVER ANODES

6.1. Introduction

Silver in its higher valency state is a useful reagent for the oxidation of organic functional groups[54]. Chemical oxidations with silver (II) picolinate[55,56] or the oxide AgO[56,57] have shown such compounds of silver to be powerful and selective oxidants. Complementary studies of electrochemical oxidations at silver electrodes in aqueous electrolytes have shown that the system Ag | AgO | OH^- is both effective and specific in its oxidising action[58,59].

Using the electrode system Ag | AgO | OH^- various amine compounds have been oxidised at potentials greater than 0.6 V (n.h.e.). This work is summarised in a recently published review article[60]. Primary aliphatic amines are rapidly oxidised at such an electrode system with current densities of greater than 100 mA cm^{-2} and coulombic yields of greater than 90%. Primary aliphatic amines with a mono substituted α-carbon atom gave the corresponding nitrile and aldehyde, α, α-di substituted compounds gave the corresponding ketone and α, α, α-trisubstituted compounds gave the corresponding alcohol, nitro compounds and unsaturated hydrocarbons. The proposed mechanism for these oxidations involved an imine intermediate.

The rate of oxidation of secondary amines at silver anodes was found to be considerably slower than that of primary amines and current densities of ~ 1 mA cm^{-2}

were observed. If the oxidation of secondary amines of the type R'R''NH were to proceed by a pathway analogous to that of the primary amines then the initial product would have been an azo-methine (schiff base) of the type R' = NR'' or R'' = NR', wherever this was permitted by the presence of an α-hydrogen atom. The oxidations of secondary amines and the corresponding azo-methines at silver anodes yielded different products, and in no case was an azo-methine found among the products of the oxidation of secondary amines. It has been suggested that the various products of these oxidations (aldehydes, nitriles, alcohols, ketones and hydrocarbons) could arise via a mechanism involving a carbonium ion[59] or hydride transfer to surface oxygen atoms with the formation of Ag-bound imine and free alcohol[60].

The oxidative decarboxylation of α-amino acids give rise to moderate yields of the appropriate nor-aldehyde or nor-ketone when for example silver (i) oxide[61], sodium hypochlorite[62] and peroxodisulphate-silver mixtures are employed as oxidants[63]. Oxidation of α-amino acids by silver (II) picolinate gives almost quantitative yields of the nor-aldehyde, where as the action of the Ag(I) (III) oxide yields the nor-acid in most cases, although the corresponding aldehyde is produced as an intermediate[56]. The reaction of α-amino acids at silver anodes have not hitherto been investigated.

6.2. Experimental

The electrolytic cells, electrodes and electrochemical procedures for the kinetic study are those described in section 5.1. (i). The preparative studies

were carried out in the same type of electrolytic cell but the test electrode used was of silver plate and had a surface area of 5.8 cm^2. The electrolytes were based on aqueous sodium hydroxide (1 mol l^{-1} NaOH) and the α-amino acids (chromatographically homogeneous).

Preparative oxidations were run for four hours with the α-amino acid (0.125 mol l^{-1}) dissolved in the base electrolyte, at a potential of 0.75 V (n.h.e.). Organic products were extracted from the electrolyte into ether before and after acidification of the base electrolyte. Preliminary analysis of the extracts was by g.l.c. (Pye 104 chromatograph) using two of the following stationary phases: polypropyleneglycol, polyethylene glycol adipate, carbowax 15 000 M and fluorosilicone. The components of the extracts were identified by comparison with authenic standards.

The apparatus and techniques of the rotating disc experiments are those described in section 5.1. (ii), the addition of phenyl glycine (0.5 mol l^{-1})being the only change in the experimental conditions.

6.3. Results

6.3. (i) Potential Sweep Experiments A typical current/potential curve corresponding to the application of a linear potential gradient to a polished and etched silver electrode, initially at equilibrium with the electrolyte, is shown in Figure 16, curve A. The significance of the various reaction peaks has been discussed

in section 5.3. The addition of an α-amino acid to the electrolyte causes the magnitude of the two major reaction peaks to increase (see Figure 16, curve B), the increase being proportional to the concentration of the α-amino acid present (see Figure 17). It can be observed that in the absence of the α-amino acid the peaks corresponding to the formation of Ag_2O and AgO are of approximately the same peak area, indicating that the AgO is formed solely from the further oxidation of the Ag_2O layer. In the presence of the α-amino acid the increase in peak area is considerably greater for the AgO peak than that of Ag_2O. Thus this effect cannot be caused by an amino acid "assisted" thickening of the oxide layer. It is also noticeable that the reaction current falls to zero between the two major reaction peaks, whereas on increasing the potential, immediately after the formation of the AgO, an appreciable current flows.

When the potential sweep rate is changed the peak heights vary accordingly. An analysis of the variation of the reaction current with $\sqrt{S.R.}$ is shown in Figure 18.

6.3. (ii) Rotating Electrode Experiments When a potential sweep was applied to the rotating disc the potential/current curve was of the same form as that described for a stationary electrode. An analysis of the i_m^{-1} and $\omega^{-\frac{1}{2}}$ data, for the system Ag $|OH^-$, phenyl glycine, is shown in Figure 19.

6.3. (iii) Constant Potential Experiments At potentials below that required for

FIG 16 LSV curve for $Ag|OH^-$, 2-amino butyric acid

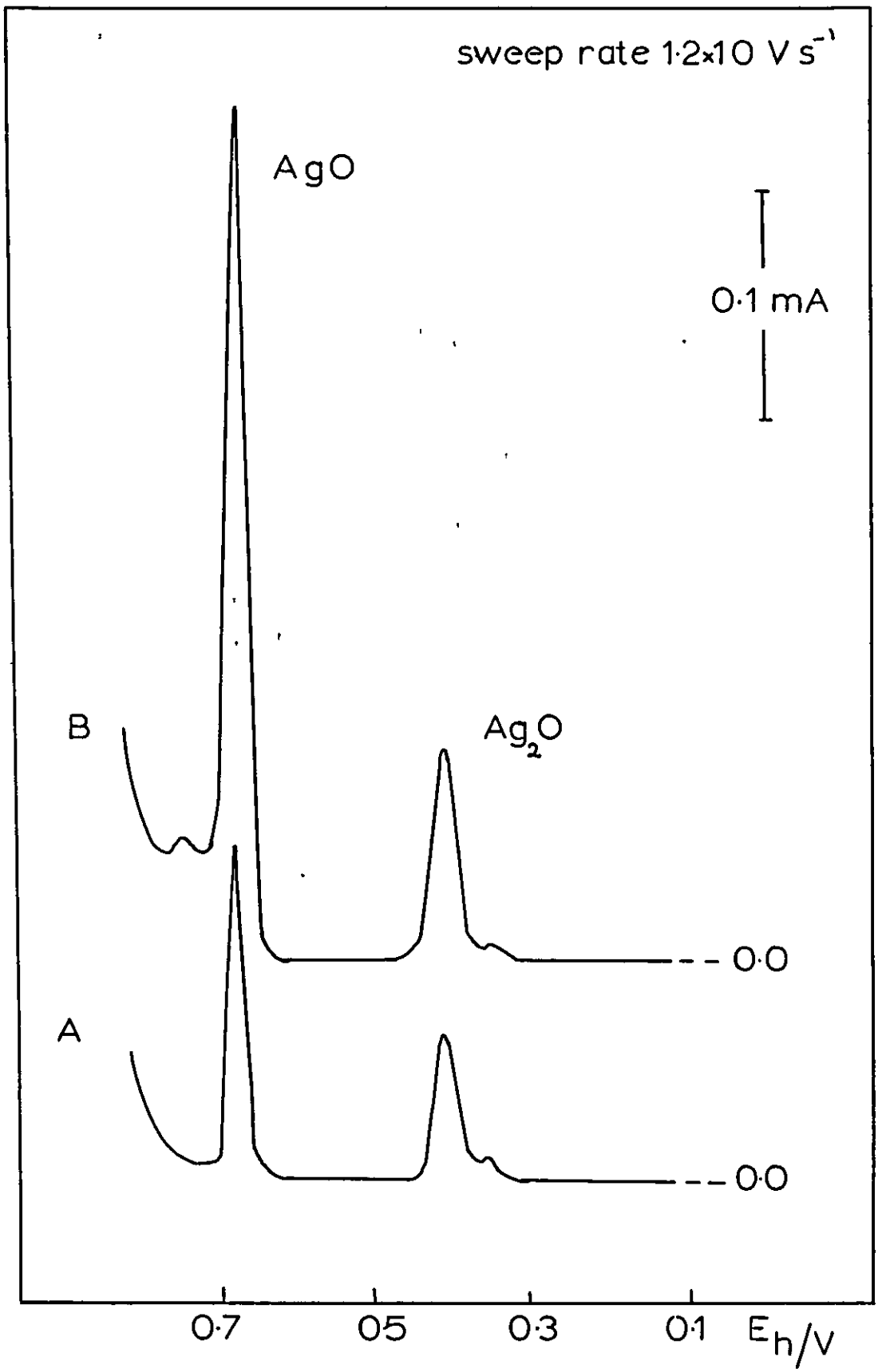

FIG 17 Dependence of i_p on [amino acid]

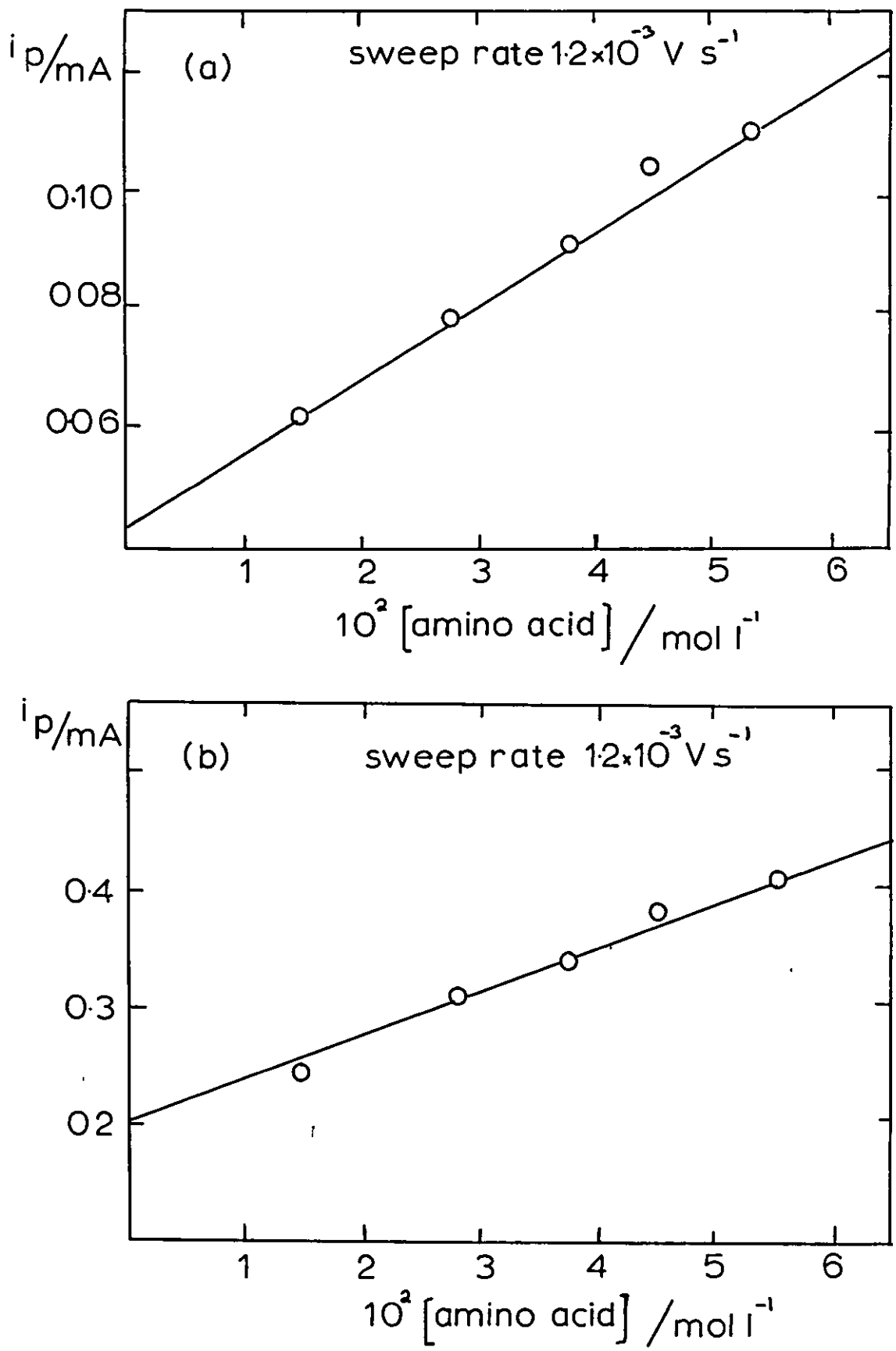

FIG 18 Dependence of i_p on $\sqrt{SR}$

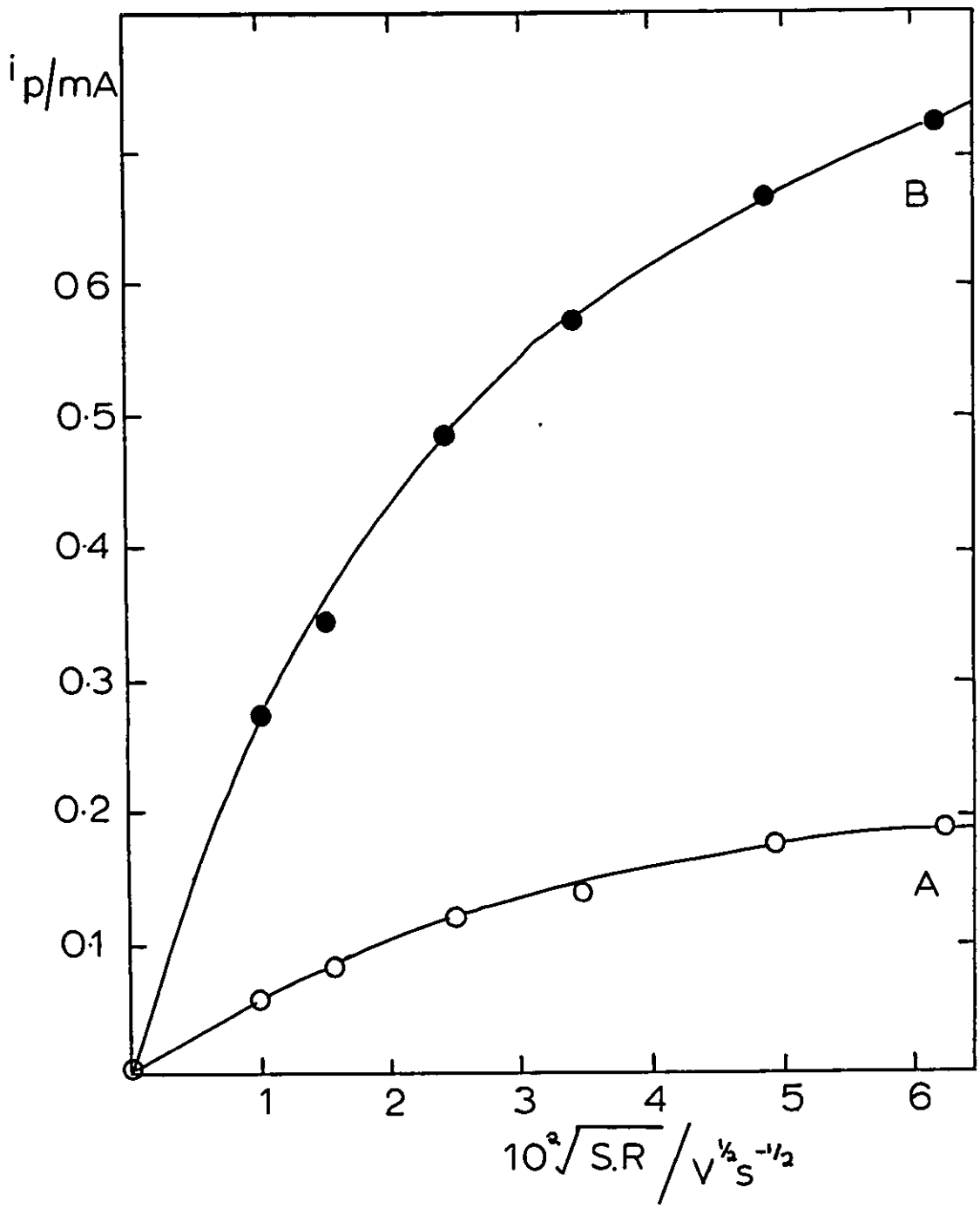

Electrolyte concentrations

1·0 mol l^{-1} NaOH

4·1 mol l^{-1} 2-amino butyric acid $\times 10^{-2}$

FIG 19 Dependence of i_m^{-1} on $w^{-1/2}$

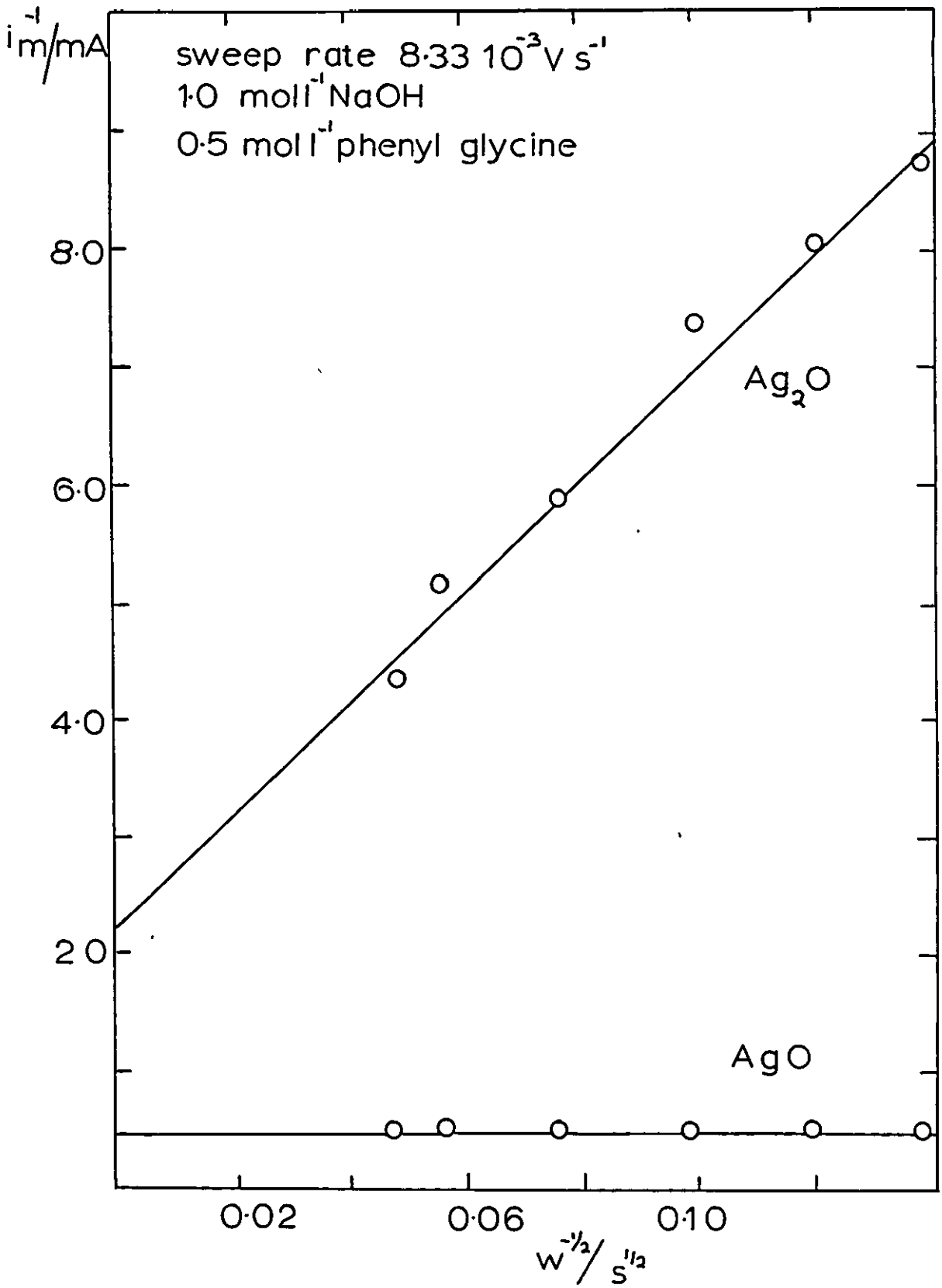

the formation of AgO α-amino acids do not appear to be oxidised to any appreciable extent. Even at the relatively high positive potential of 0.75 V (n.h.e.) the rate of oxidation is found to be slow and cell currents of ~ 1.0 mA cm^2 were observed at this potential.

The reaction rates appear to be dependent on the degree of branching of the α-amino acids and the cell currents measured under identical conditions are given in Table 4.

The products of the oxidation of a series of α-amino acids are shown in Table 5. The major product in every case is the nor-nitrile, with a minor proportion (< 5%) of the nor-aldehyde in the case of the branched chained α-amino acids.

TABLE 4 Cell currents measured after 15 min, electrode area 5.8 cm^2, electrolyte NaOH (1.0 mol l^{-1}) and α-amino acid (0.125 mol l^{-1})

DL α-amino acid	Cell Current (mA)
Alanine	4.60
2-amino butyric acid	2.30
Nor-valine	1.75
Valine	0.97
Nor-leucine	1.45
Leucine	1.12
Isoleucine	1.02
Phenyl glycine	7.90

TABLE 5 Products of the electrochemical oxidation of α-amino acids at silver anodes in NaOH (1.0 mol l^{-1})

DL α-amino Acid	Product	
Alanine	Acetonitrile	
2-amino-butyric acid	Propionitrile	
Nor-valine	Butyronitrile	
Valine	isobutyronitrile	(96%)
	isobutyraldehyde	(4%)
Nor-leucine	Valeronitrile	
Leucine	Isovaleronitrile	(95%)
	Isovaleraldehyde	(5%)
Iso-Leucine	2-me-butyronitrile	(95%)
	2-me-butyraldehyde	(5%)
Phenyl glycine	Benzonitrile	(98%)
	Benzaldehyde	(2%)

The variation of the products obtained with changes in the potential, base electrolyte concentration and the concentration of the α-amino acid are shown in Table 6.

6.4. Discussion

The changes in the shape of the potential/current curves in the presence of the α-amino acid can be explained by the formation of Ag/complexes at the electrode interphase, which blocks the electrode for further reactions in the case of the Ag(I) complex, but only partially blocking the electrode in the case of

TABLE 6 Dependence of oxidation products on electrode potential, $[OH^-]$ and [amino acid]. Oxidation of nor-valine (0.125 mol l^{-1}) in NaOH (1.0 mol l^{-1}) for 4 hours except:

a) 2 mol l^{-1} NaOH

b) 0.25 mol l^{-1} nor-valine.

Potential V (n.h.e.)	Product
0.65	None
0.75	Butyronitrile
0.85	Butyronitrile (97%) Butyraldehyde (3%)
0.85 (a)	Butyronitrile (96%) Butyraldehyde (4%)
0.95 (b)	Butyronitrile (97%) Butyraldehyde (3%)
0.95	Butyronitrile (96%) Butyraldehyde (4%)
1.05	Butyronitrile (97%) Butyraldehyde (3%)

the Ag(II) complex. Therefore on completion of the Ag_2O layer the reaction ceases (current falls to zero) in a similar manner to that observed when secondary amines are oxidised at silver anodes[59], where the reaction only occurs at "clean" growing crystallites. At the higher potentials corresponding to the formation of AgO any complex that is formed is progressively oxidised. This explains the occurrence of the faradaic current flow after the formation of the AgO layer, indicative of a reaction occurring at the electrode surface. This behaviour resembles that observed with primary amines[58], although in the case of the oxidation of the amines the continuous reaction was so rapid that current waves were observed instead of the peaks observed in this case.

When the potential sweep is changed an analysis of the i_p vs $\sqrt{S.R.}$ data gives rise to curved plots. The curve of these graphs being towards the $\sqrt{S.R.}$ axis indicating that processes in addition to diffusion are rate controlling. This appears to be the blocking of the electrode surface by the formation of a complex, or the adsorption of a reactant, product or intermediate on the electrode. It is observed that this effect is more pronounced in the case of the Ag_2O reaction than in the case of AgO. This is in agreement with the observations that the Ag_2O complex is more effective in blocking the electrode than the AgO complex, indicated by the occurrence of the faradaic current at potentials greater than that required for AgO formation.

Examination of the reaction peak heights with changing rotation speed of the electrode system in the presence of phenyl glycine show that there is clearly a difference in the effect of the rotation speed upon the two reactions (see Figure 19). The peak height of the $Ag\,|Ag_2O\,|OH^-$, phenyl glycine reaction increases with an increase of rotation speed whereas the $Ag|AgO|OH^-$, phenyl glycine reaction peak appears to be independent of rotation speed. This reflects a difference in the rate controlling mechanisms, the latter being dependent upon a process in the solid phase whereas the former reaction is dependent upon the transport of the rate determining species through the solution.

The reaction rates of the oxidation of the α-amino acid at the AgO peak potential appear to be dependent on both the chain length and the degree of branching of the α-amino acids (see Table 4). For example the rate of oxidation of

alanine is approximately twice that of 2-aminobutyric acid and the rate of oxidation of nor-valine is approximately twice that of valine. This reflects a difference in the availability of the reactants at the electrode interphase, probable as a result of increased steric compression of the adsorbed species.

The products of the oxidations of the α-amino acids are the nor-nitrile as the major product in every case, with a minor proportion (<5%) of the nor-aldehyde in the case of the more bulky α-amino acids. For example 2-amino butyric acid yields propionitrile whereas valine yields isobutyronitrile and a small quantity of isobutyraldehyde (4%). These observations are in sharp contrast to the reaction of the same α-amino acids with AgO, in isolation from the electrode system, where the oxidations yielded the nor-acid. The nor-aldehyde being the probable initial product which is then further oxidised by unchanged argentic oxide.

The oxidation of primary amines[58] at silver anodes have been shown to follow the reaction path:

$$R \cdot CH_2 \cdot NH_2 \xrightarrow[-2H^+]{-2e^-} R \cdot CH = NH \xrightarrow[-2H^+]{-2e^-} \underline{\underline{R\,C\,N}} \qquad (6.1.)$$

$$R \cdot CH = NH \xrightarrow{OH^-} \underline{\underline{R \cdot C\,H\,O}}$$

Since the nor-aldehyde and the nor-nitrile are the only products from the oxidation of the α-amino acids it is reasonable to assume that the mechanism may again involve an imine intermediate. In the case of the oxidation of the α-amino acids only a

trace of the nor-aldehyde is isolated. This implies that further oxidation of the imine occurs more readily than hydrolysis in the present experiments. Hydrolysis under the conditions used would most likely occur by attack of OH^- upon the imine carbon atom, this could either occur upon adsorbed imine or imine free in the bulk of the solution. It seems probable that the α-amino acid is bonded to the electrode surface through the nitrogen atom as well as the carboxyl oxygen, the imine intermediate also being bonded to the electrode surface. The greater steric compression in the case of the branched chained α-amino acids tending to drive any equilibrium between adsorbed and free imine towards the free state. This explains the slightly slower oxidation of these branched chained compounds and also the increased yield of aldehyde, but is is obvious that the effect is only slight. Further since there is no increase in the aldehyde yield when the concentration of the OH^- is doubled, it appears that the amount of imine free in solution controls the magnitude of the aldehyde yield, there being little, if any, attack of OH^- upon the adsorbed imine. The overall reaction can be written as:-

$$RCH(NH_2)\cdot CO_2^- \xrightarrow[-2H^+]{-2e} RCH=NH \xrightarrow[-2H^+]{-2e} \underline{\underline{RCN}} \qquad (6.2.)$$

(fast)

(slow, OH^-)

$$\underline{\underline{RCHO}}$$

It has been observed that the oxidation products are independent of the sodium hydroxide concentration, α-amino acid concentration and the electrode potential

once the AgO peak potential has been obtained. This is further evidence that the reaction occurs in an adsorbed state at the electrode.

Any mechanism for these reactions must account for these observations and for the higher proportion of aldehyde found in the oxidation of primary amines. The results accord well with the behaviour which might have been predicted. Silver forms strong complexes with amino acids such as picolinic acid (where the ligand is stable towards oxidation) involving both Ag-N and Ag-O bonds and similar behaviour with other amino-acids would not be unexpected. The differences between the oxidation of α-amino acid and primary amines may be accounted for if the imine intermediate is set free in the latter case, but remains in an adsorbed state in the α-amino acid oxidations. Imine formation in the oxidation of primary amines necessarily involves the transfer of electrons with the cleavage of the Ag-N bond, this cleavage may or may not be base assisted (see reaction (6.3.)).

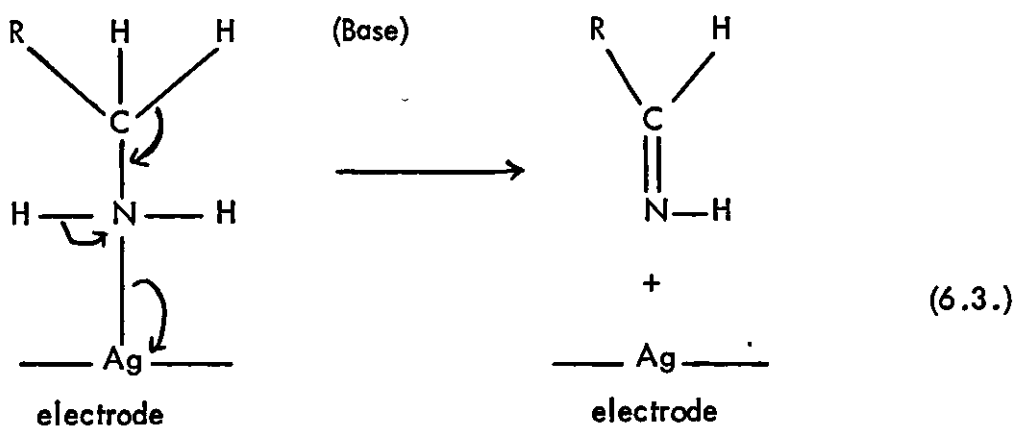

(6.3.)

This clevage of the Ag-N bond is not necessary in the oxidation of the α-amino acid where only one of either the Ag-N or Ag-O bonds need to be broken for the formation of the imine intermediate (see reaction (6.4.)).

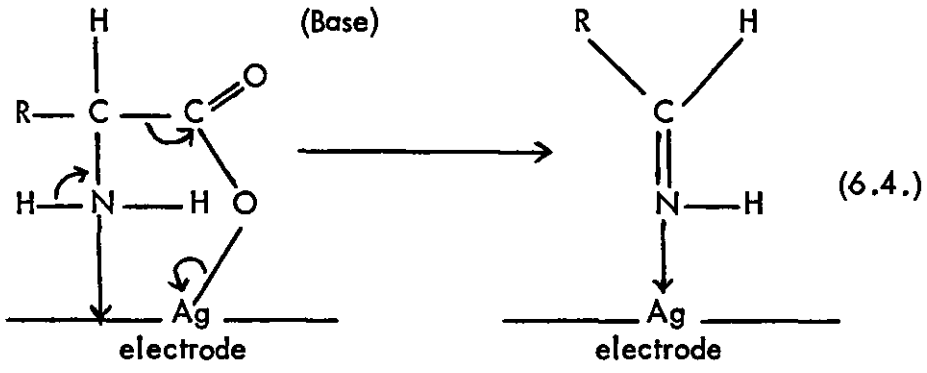

(6.4.)

In the first case where the imine is set free into the solution it may either readsorb at the electrode or remain in the electrolyte. Since a major reaction product is the nor-aldehyde it is likely that the bulk of the imine remains in the free state in the electrolyte where it is hydrolysed, only when the imine is readsorbed does further oxidation of the nor-nitrile product occur.

In the case of the oxidation of α-amino acids further oxidation of the imine occurs rapidly and we may assume that only when steric factors favour some release of the bonded imine do we get the formation of the nor-aldehyde.

The system may be schemmatically represented as reactions (6.5.) and (6.6.), where the equilibrium (C) lies well to the left even for the most bulky α-amino acid investigated:

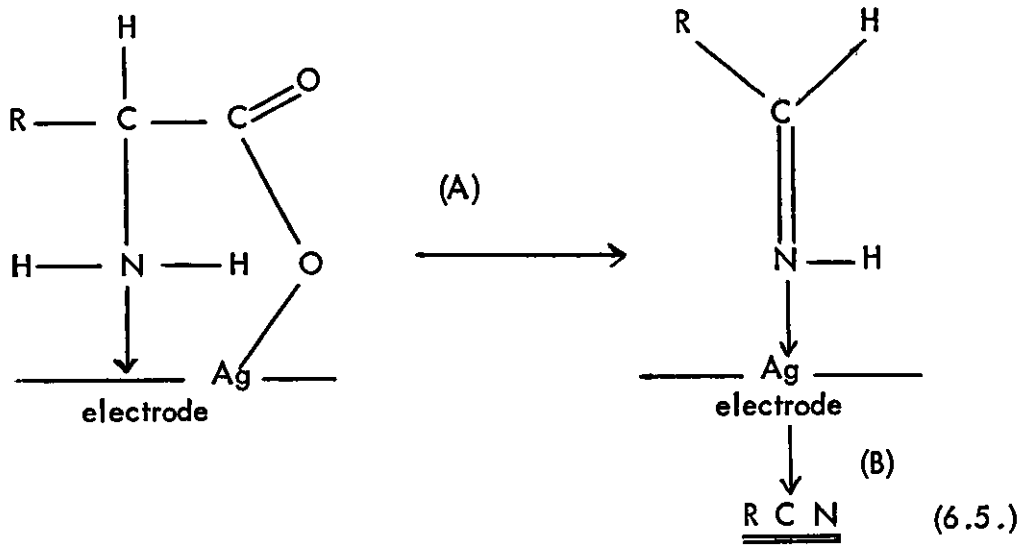
H
R — C — C
O
H — N — H
O
Ag
electrode
(A)
R
H
C
N — H
Ag
electrode
(B)
R C N

(6.5.)

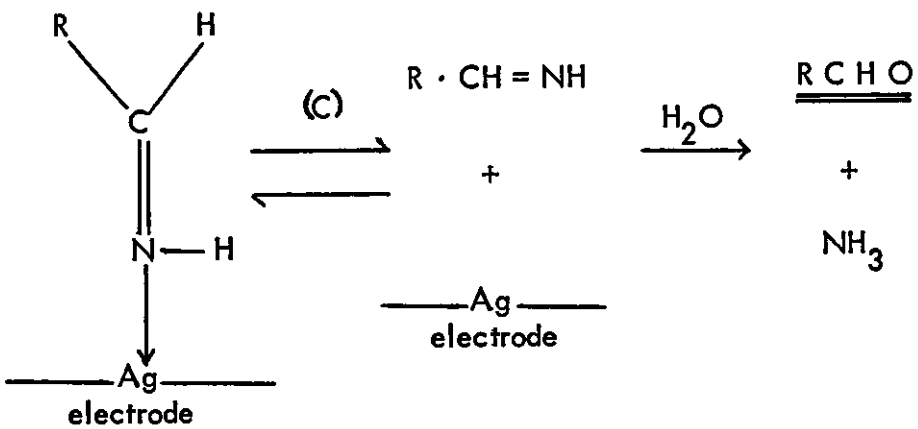
R
H
C
N — H
Ag
electrode
(C)
R · CH = NH
+
Ag
electrode
H2O
R C H O
+
NH3

(6.6.)

CHAPTER 7

A REVIEW OF THE REACTIONS AT ANODIC COPPER IN ALKALINE SOLUTIONS

The study of reactions occurring at anodic copper electrodes in alkaline solutions has been made by various workers over the last fifty years[64-85]. The nature of the reactions that occur is still open to considerable discussion and the following summary of the major experimental work shows the diversity of the proposed electrode products under different experimental conditions.

The first major investigation of the system was carried out by Muller[64] who used an anodizing circuit with which he detected the formation of three oxides at anodic copper electrodes. The sequence of reactions that he proposed consisted of the formation of Cu_2O, followed immediately by the formation of either CuO or $Cu(OH)_2$ at the oxide electrolyte interphase and the continued formation of Cu_2O at the oxide electrode interphase. These two reactions were observed under all experimental conditions, but in more concentrated hydroxide solutions a further oxide was produced at the electrode. In the stronger base the cupric oxide or hydroxide dissolves to an appreciable extent leading to the formation of a higher oxide, Cu_2O_3 at ~ 0.7 V (n.h.e.). This oxide was unstable and decomposed to give oxygen and cupric oxide.

Using a similar technique Feitknecht and Lenel[65] confirmed Mullers'

conclusions regarding the formation of the Cu(I) and Cu(II) oxides but they found no evidence for the existence of a higher oxide. The nature of the Cu(II) oxide was found to be very dependent upon convective transport in solution. In quiet solutions $Cu(OH)_2$ was deposited at the electrode and it was supposed that the formation of the $Cu(OH)_2$ continued in the electrolyte, immediately adjacent to the anode, until local saturation was reached thus precipitating the $Cu(OH)_2$ and hence passivation. If the solution was stirred the electrode was passivated by a film of CuO and not $Cu(OH)_2$, since the hydroxide is swept away into the solution.

A comprehensive study of the system, recording charging curves as oscillograms, was carried out by Hickling and Taylor[66]. The charging curves indicated that the sequence of the reactions, after the charging of the double layer, was the formation of Cu_2O that was almost immediately converted to CuO. The film of CuO continued to grow until it had attained sufficient thickness to protect the copper metal from further attack, at this point the evolution of oxygen commenced. The nature of the Cu(II) oxide was specified as CuO and not $Cu(OH)_2$, this conclusion was based on the measurement of the potentials involved with the formation of the oxide layer. In agreement with the previous workers no evidence of the presence of Cu_2O_3, as postulated by Muller, was obtained. The cathodic curves that were also obtained indicated a successive reduction of the cupric oxide first to cuprous oxide and then finally to copper.

The composition of the anodic oxide films formed on the copper

electrodes was first extensively studied by Halliday[67], who used an electrometric method and electron diffraction. The effect of the current density and electrolytic concentration on the film forming processes was also examined as was the effect of stirring the various solutions. Initially the copper anode was found to be covered by a layer of Cu_2O, this in turn was covered with CuO or $Cu(OH)_2$, which formed on the top of the Cu_2O, until the electrode became passive. In more concentrated hydroxide solutions (4.0 mol l^{-1} NaOH) Cu $(OH)_2$ becomes more soluble and the passivation processes vary for stirred and unstirred solutions. In the latter case local saturation of $Cu(OH)_2$ in the close vicinity of the electrode causes passivation of the electrode due to a precipitated film of this oxide. If the solutions were stirred then the $Cu(OH)_2$ was swept away and the formation of a film of CuO was the electrode passivating process. In these experiments it was again concluded that the reduction of the Cu(II) oxide film involves two processes: reduction of the cupric oxide to cuprous oxide and then the reduction of the cuprous oxide to copper.

The effect of temperature upon the primary oxidation processes at copper anodes in alkaline solutions was studied by L'Vov and Fortunatov[68] who also investigated the effect of electrolyte concentration and current density on these processes. The first anodic process consisted of the formation of Cu_2O and it was found that the yield of this oxide increased with increases in the electrolyte concentration and temperature and with a decrease in the current density. From calculations of the quantity of electricity consumed during the oxidation process, for the formation of Cu_2O at 85°C, it was found that the oxide layer consisted of a film of greater than

fifty molecules in depth. The second anodic process was thought to be due to the formation of $Cu(OH)_2$ from the base copper. The yield of this oxide was at least ten times greater than that of the Cu_2O. It was found to have a similar dependence upon changes in the electrolyte concentration, temperature and current density.

Faizallice et al[69] recorded that there was a change in the oxidation products with changes in the temperature at which the oxidation was carried out. In all solutions and at all the temperatures studied the primary oxidation product was Cu_2O. The formation of the second oxide was found to be dependent on both the temperature and the electrolyte concentration. In dilute solutions and low temperatures ($\sim 20^{\circ}C$) the oxide formed was $Cu(OH)_2$, whereas if the temperature was increased ($> 45^{\circ}C$) the oxide layer was found to be a mixture of both $Cu(OH)_2$ and CuO. $Cu(OH)_2$ was again the sole product of oxidations in concentrated electrolytes at $20^{\circ}C$ but at higher temperatures ($65^{\circ}C$) the passivating film was found to be CuO. These workers also reported the formation of a higher oxide that resulted from the oxidation of soluble Cu(II) species.

Evidence for the existance of a Cu(III) species has been reported by several workers[70-74], apart from Muller and Faizullice. Shams El Din and co-workers[71] in attempts to repeat Muller's work obtained evidence for the presence of the higher oxide Cu_2O_3. In their experiments if fresh anodes were used for the polarizations then only Cu_2O and $Cu(OH)_2$ were found to be present in the oxide layer. When the electrodes were subjected to repeated recycling evidence of further

oxidations was discovered. They stated that this further oxidation was due to the formation of Cu_2O_3 and that it occurred only when there were cuprite ions in the electrolyte.

Miller[73] has examined the anodic oxidation of copper using rotating ring and split-ring disc electrodes. Using this technique a soluble Cu(III) species has been identified in the anodic region at the onset of oxygen evolution.

The most recent study of the system has been carried out by Leckie[74], who identified three reactions occurring during galvanostatic charging of a copper anode. These reactions occurred at -0.57 V, - 0.32 V and 0.00 V (s.c.e.). The reactions were thought to be the formation of Cu_2O, $Cu(OH)_2$ and the cuprite ion respectively. Potential decay curves showed the presence of a reduction plateau at 0.52 V (s.c.e.) and this has been attributed to a reaction involving Cu_2O_3. Leckie postulated the following series of reactions to account for the formation of the various reaction products:-

$$2\,Cu + 2OH^- \longrightarrow Cu_2O + H_2O + 2e \qquad (7.1.)$$

$$Cu_2O + 2OH^- + H_2O \longrightarrow 2\,Cu(OH)_2 + 2e \qquad (7.2.)$$

$$Cu(OH)_2 + OH^- \rightleftharpoons HCuO_2^- + H_2O \qquad (7.3.)$$

$$HCuO_2^- + OH^- \rightleftharpoons CuO_2^{-2} + H_2O \qquad (7.4.)$$

$$Cu + 3OH^- \longrightarrow HCuO_2^{-2} + H_2O + 2e \qquad (7.5.)$$

$$HCuO_2^{-2} + OH^- \rightleftharpoons CuO_2^{-2} + H_2O \qquad (7.6.)$$

$$2CuO_2^{-2} \longrightarrow Cu_2O_3 + H_2O + 4e \qquad (7.7.)$$

CHAPTER 8

OXIDATIONS AT COPPER ELECTRODES IN ALKALINE SOLUTIONS:

8.1. Differential Capacitance Measurements

8.1. (i) Experimental The electrical circuit used for these measurements has been described in section 3.2. (i). The electrolytic cell was of the type shown in Figure 4 (a). The electrolyte was purified by continuous circulation through the purification limb for at least four weeks. The test electrode was of spectroscopically pure polycrystalline copper wire and was prepared in the manner described in section 3.1. (i). The test electrode was cleaned on roughened glass and then chemically etched with HNO_3 (15%) before every series of readings. The counter electrode was of platinum gauze and the reference electrode was a saturated calomel electrode, contained in a special reference compartment (see Figure 4 (a)).

8.1. (ii) Results A plot of faradaic current against the applied potential is shown in Figure 20. An experimentally accessible polarizable region extends from - 0.10 V to - 0.80 V (n.h.e.). At the negative limit of the polarizable region hydrogen evolution occurred whilst at the positive limit a solid phase was formed at the electrode.

Within this experimental polarizable region the resistive component of the electrode impedance was observed to remain satisfactorily constant. However, at the positive limit it increased markedly. Figures 21 and 22 show typical differential capacitance curves in the concentration range 0.925 - 0.007 mol l^{-1} NaOH. The shape of these curves was similar for all concentrations and show two maxima at $\sim$ -0.3 V and $\sim$ -0.65 V (n.h.e.). The relative magnitude of these peaks increased with the electrolyte concentration. The associated minima at $\sim$ - 0.5 V and $\sim$ - 0.8 V (n.h.e.) decreased with decreasing electrolyte concentration. The potentials at which the maxima and minima occurred were concentration dependent, becoming slightly more negative with increasing concentration. At potentials more positive than about - 0.2 V (n.h.e.) the capacitance decreased very markedly becoming time dependent and after a sufficient time, very small.

The electrode capacitance showed considerable frequency dispersion and a tenfold change in capacitance resulted from a frequency change of 1 000 to 100 Hz.

8.1. (iii) Discussion A number of investigations concerning the p.z.c. of solid copper electrodes in aqueous solutions have been reported. Contact angle[86], friction[87], immersion[88,89], charging curves[90], capillary rise with contact angle[91], electroreduction[92] and electrode impedance[93-96] methods have been employed to identify Ez. Results, however, have varied from 0.11 V[90] to - 0.26 V[87] (n.h.e.) This potential range is outside the experimental region investigated here and so no

FIG 20 Faradaic current curve

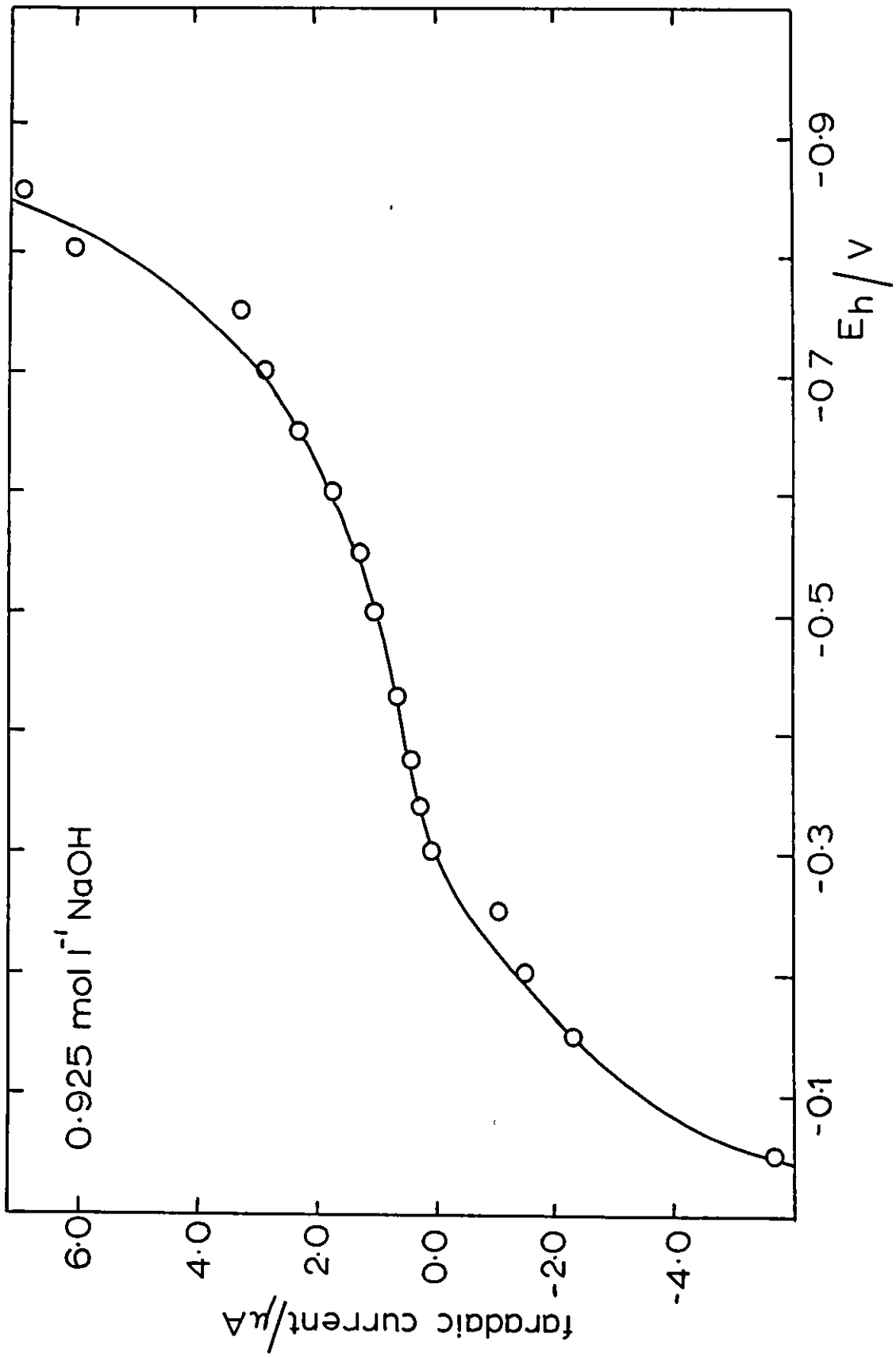

FIG 21 Differential capacitance curves

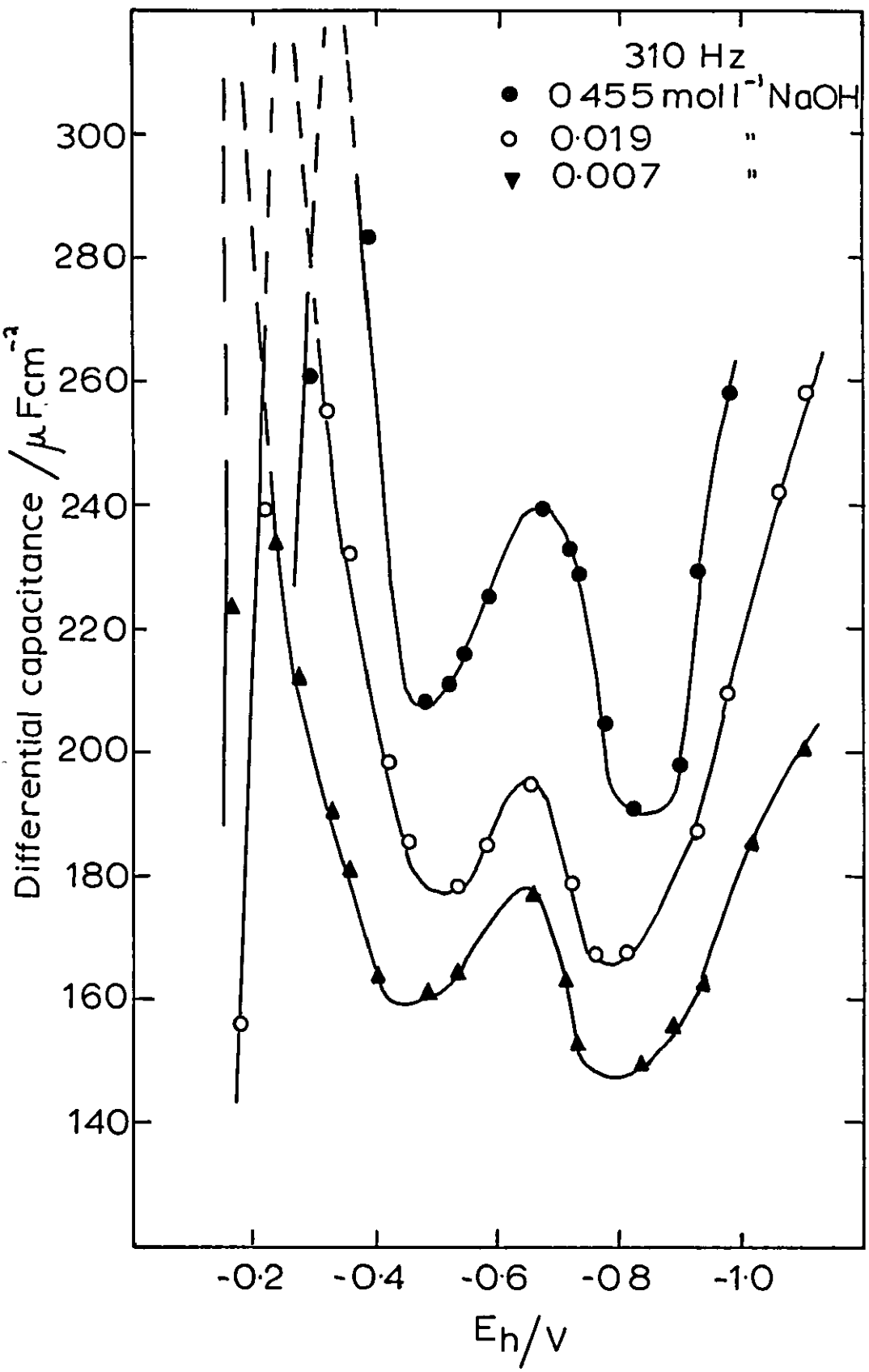

FIG 22 Dependence of capacitance on frequency

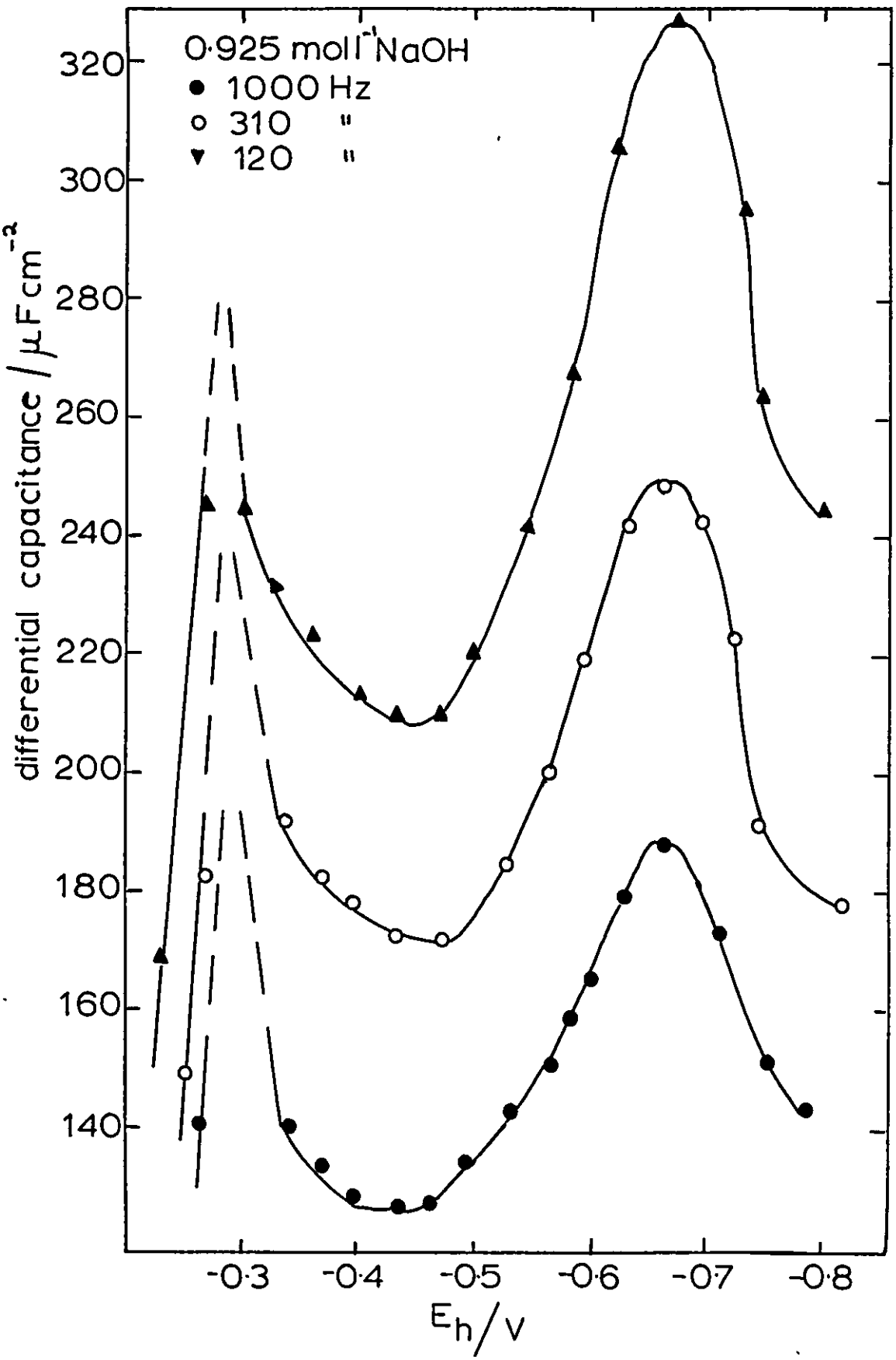

information concerning Ez for the Cu|aqueous solution interphase can be gained from this present study due to obscuring by the lattice dissolution process. It should be noted, however, that no capacitance minimum, characteristic of the diffuse double layer, was observed with solutions of sufficient dilution.

An examination of the capacitance curves (see Figure 21) show that the potential ($\sim$ -0.3 V) at which the first capacitance peak occurs corresponds to the equilibrium potential for the formation of cuprous oxide. It can be concluded therefore that this peak represents the formation of a film of Cu(I) oxide or hydrated oxide at the electrode surface. The maximum of this pseudo capacitance peak corresponds to half-monolayer formation. This maximum should be of the order of 10^2 μF cm^2, however, such high values were never obtained as stable readings since the non-polarizability of the electrode resulted in rapid changes of capacitance with potential. Once the film completely covers the electrode surface the observed decrease in capacitance is due to the thickening of the oxide film, so that values decrease with film thickness in accordance with the flat plate capacitor theory.

The second peak at $\sim$ 0.65 V lies between the potential of lattice disruption and the potential of hydrogen evolution. The only possible process involving available species that can occur within these limits is that between hydrogen ions and the copper electrode. This can be considered either as the formation of an adsorbed layer of hydrogen ions at the electrode or the formation of a layer of copper hydride. If the latter is considered then it must be emphasised

that this layer does not thicken since the capacitance remains high. This is confirmed by the fact that the occurrence of this capacitance peak at ~ -0.65 V is not accompanied by any very significant change in the electrode resistance. It is likely therefore that this peak represents monolayer coverage of the electrode. The fall of capacitance after this peak to a minimum at ~ -0.8 V indicates that no further interaction occurs at the electrode until the capacitance begins to rise at the potential corresponding to hydrogen evolution.

The extent of the frequency dispersion (see Figure 22) is considerably greater than that reported by Armstrong et al[96]. An analysis of the frequency dispersion was made according to de Levie[98]. The relationship of the measured capacitance was linear with $\omega^{-\frac{1}{2}}$. The dispersion of frequency may therefore be considered as arising from the inhomogeneity of the surface in the sense of de Levie[99] rather than faradaic effects. Had the latter been present the simple $\omega^{-\frac{1}{2}}$ dependency would not have been observed and the consistency of the magnitude of frequency dispersion throughout the experimentally polarizable region unlikely. The magnitude of the capacitances presented (generally greater than 160 μF cm^{-2}) are higher than those observed for acid and neutral nitrate and perchlorate electrolytes (generally less than 100 μF cm^{-2}). This further supports the presence of extra electrode capacitance components in the electrode analogue, over and above those corresponding to the model of Nernst[13], which can be assigned to adsorption.

8.2. Linear Sweep Voltammetric Measurements

8.2. (i) Experimental The experimental techniques and the electrical circuit

have been discussed in section 3.2.(i). The electrolytic cells used were of the types shown in Figures 4(b) and 5(a). In the former case the cell was filled with purified electrolyte (NaOH) that was further purified by circulation through the purification limb for at least four weeks. In the second type of cell the electrolyte was clean electrolyte solution, however the further purification with charcoal was omitted. The test and counter electrodes were of spectroscopically pure copper wire and were prepared in the manner described in section 3.2 (i). The test electrode pretreatment was that described in section 8.1. (i). The reference electrode was again a saturated calomel electrode.

8.2. (ii) Results A typical current/potential curve corresponding to the application of an anodic potential gradient to a solid copper electrode in sodium hydroxide electrolyte is shown in Figure 23 (a). The potential was swept from the potential for the hydrogen evolution reaction to that for the oxygen evolution reaction. The curve exhibits two current peaks indicating that at least two electrochemical reactions are occurring in the experimental potential range. The shape of the larger peak is not symmetrical and incorporates a shoulder on the negative side of the peak, indicating a further (third) electrochemical reaction.

Figure 23(b) shows the result of reversing the direction of the sweep, from a potential more positive than that corresponding to reaction peak (iii), but less positive than the potential of the oxygen evolution reaction. It can be seen that there are three negative current peaks, two broad and one sharp. This suggests

that there is a two stage reduction of the products formed at potentials ~ 0.00 V (n.h.e.) and then a single stage reduction of the products formed at the peak (i) potential.

When the potential gradient was changed there were corresponding changes in the peak heights of reaction peaks (i) and (iii). An analysis of the results can be seen in Figures 24 and 25, where the peak heights are plotted against the sweep rate (S.R.) and $(S.R.)^{\frac{1}{2}}$ respectively for reaction peaks (i) and (iii).

A comparison of results of the dependence of the peak height for reaction peak (iii) on $(S.R.)^{\frac{1}{2}}$ was made between an electrolytic system that had been finally purified by circulation through activated charcoal and a clean electrolytic system. Figure 26 shows the similarity of the two systems and the majority of the experimental work was therefore carried out without the final charcoal purification. This emphasises the fact that when the electrode reaction being studied involves oxidation of many thousands of atomic layers, purity requirements are not so great as when only surface properties (e.g. double layer) are being investigated.

An interesting effect of the dependence of the reaction peak heights, for reactions (ii) and (iii), upon sweep rate is shown in Figure 27 where higher sweep rates are employed. At the fast sweep rate of 25×10^{-3} V s^{-1} the two reactions occurring at potentials ~ 0.0 V (n.h.e.) are more clearly displayed on the current/potential traces, the large reaction peak being resolved into two distinct reaction peaks. At even higher sweep rates ~ 50×10^{-3} V s^{-1} the portion of the peak at the

more positive potential decreased in absolute magnitude whereas the smaller reaction peak (ii) increased.

A detailed analysis of the variation of peak heights for reactions (i), (ii) and (iii) with changes in both sweep rate and the electrolyte concentration ~~are~~ is shown in Figures 28, 29 and 30 respectively.

It is interesting to note that the maximum peak height for reaction (i) appears to be dependent to some extent on the potential from which the potential sweep is commenced (see Table 7).

TABLE 7 Dependence of i_p on starting potential for reaction peak (i). Sweep rate 1.25×10^{-3} v s^{-1}, 1.0 mol l^{-1} NaOH and 23°C.

Electrode Pretreatment	i_p Reaction (i)	i_p Reaction (iii)
A	0.028 mA	0.430 mA
B	0.043 "	0.600 "
C	0.014 "	0.428 "
D	0.008 "	0.426 "

A, mechanically polished, chemically etched, starting at -0.75 V

B, reduced, completely oxidised electrode, " " "

C, as A starting at - 0.50 V

D, as A starting at - 0.30 V

FIG 23 L.S.V. curve for $Cu|OH^-$

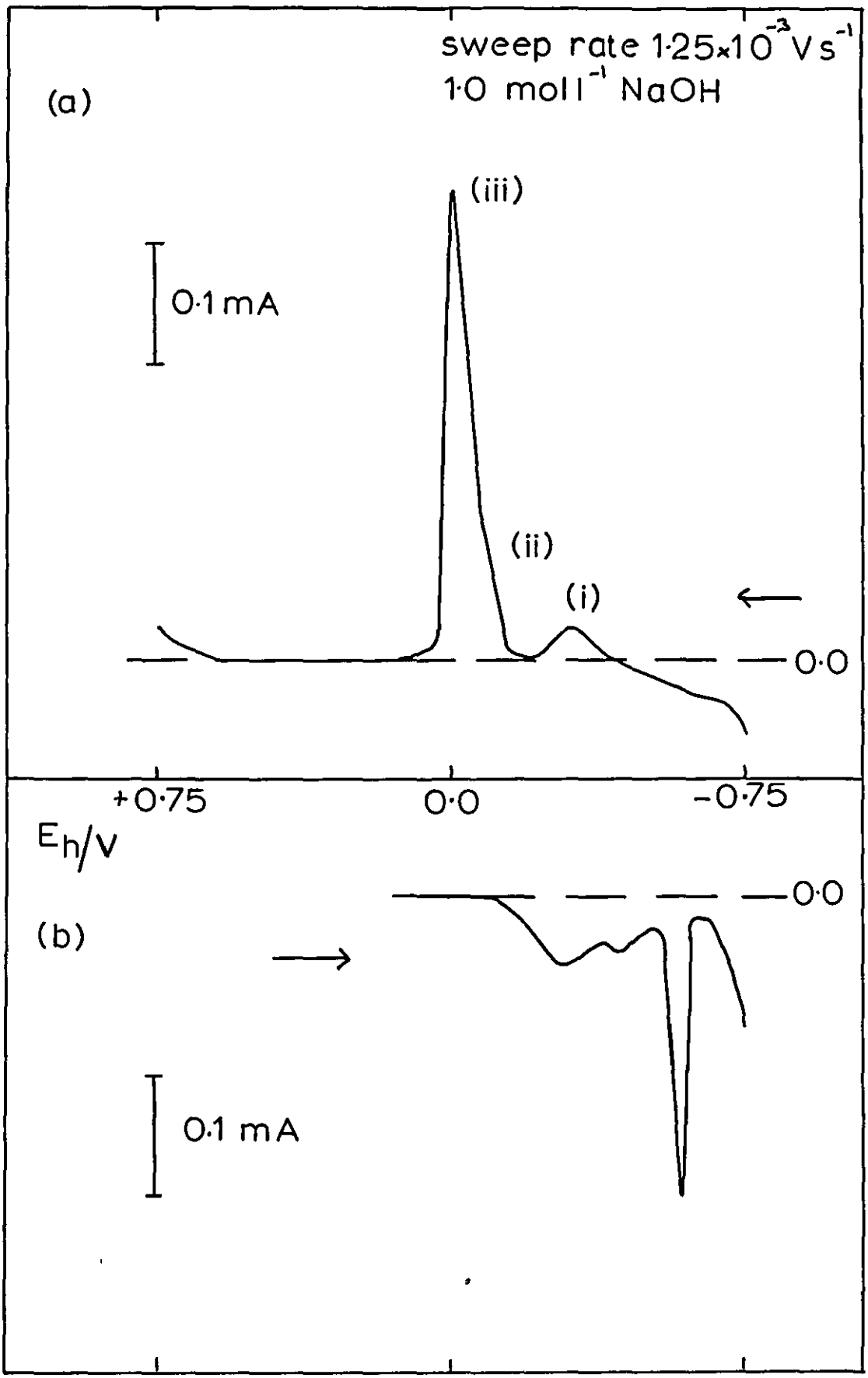

FIG 24 Dependence of i_p on (S.R.)

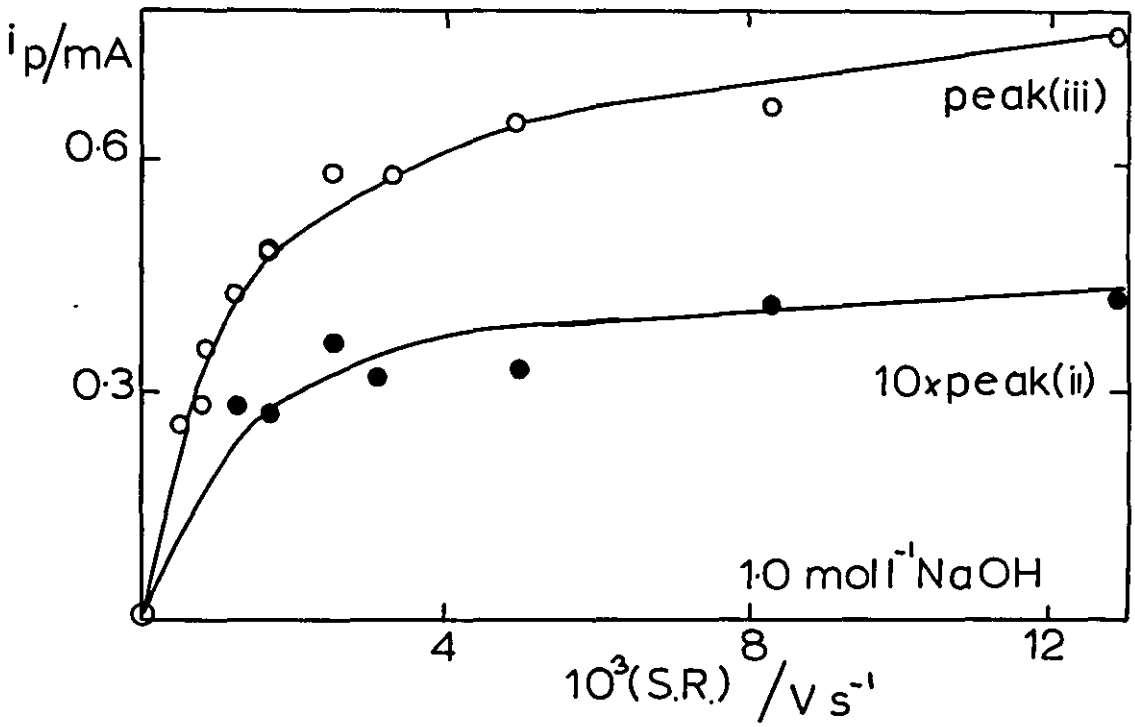

FIG 25 Dependence of i_p on $\sqrt{S.R.}$

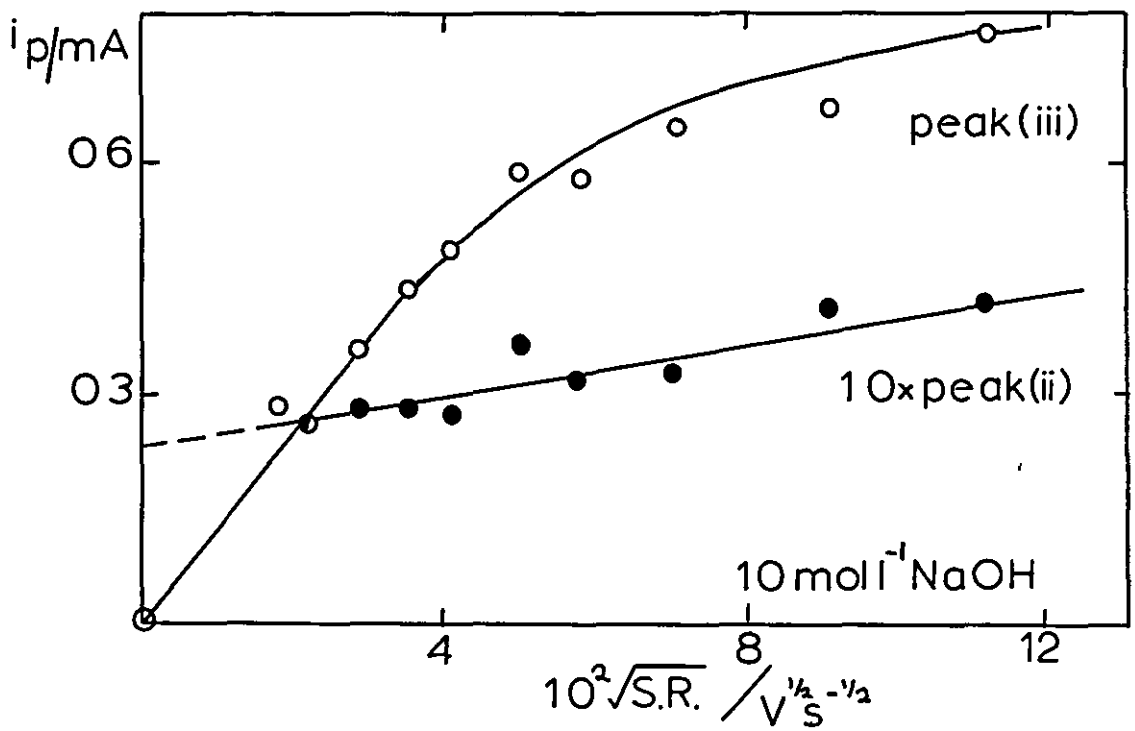

FIG 26 Comparison of electrolytes

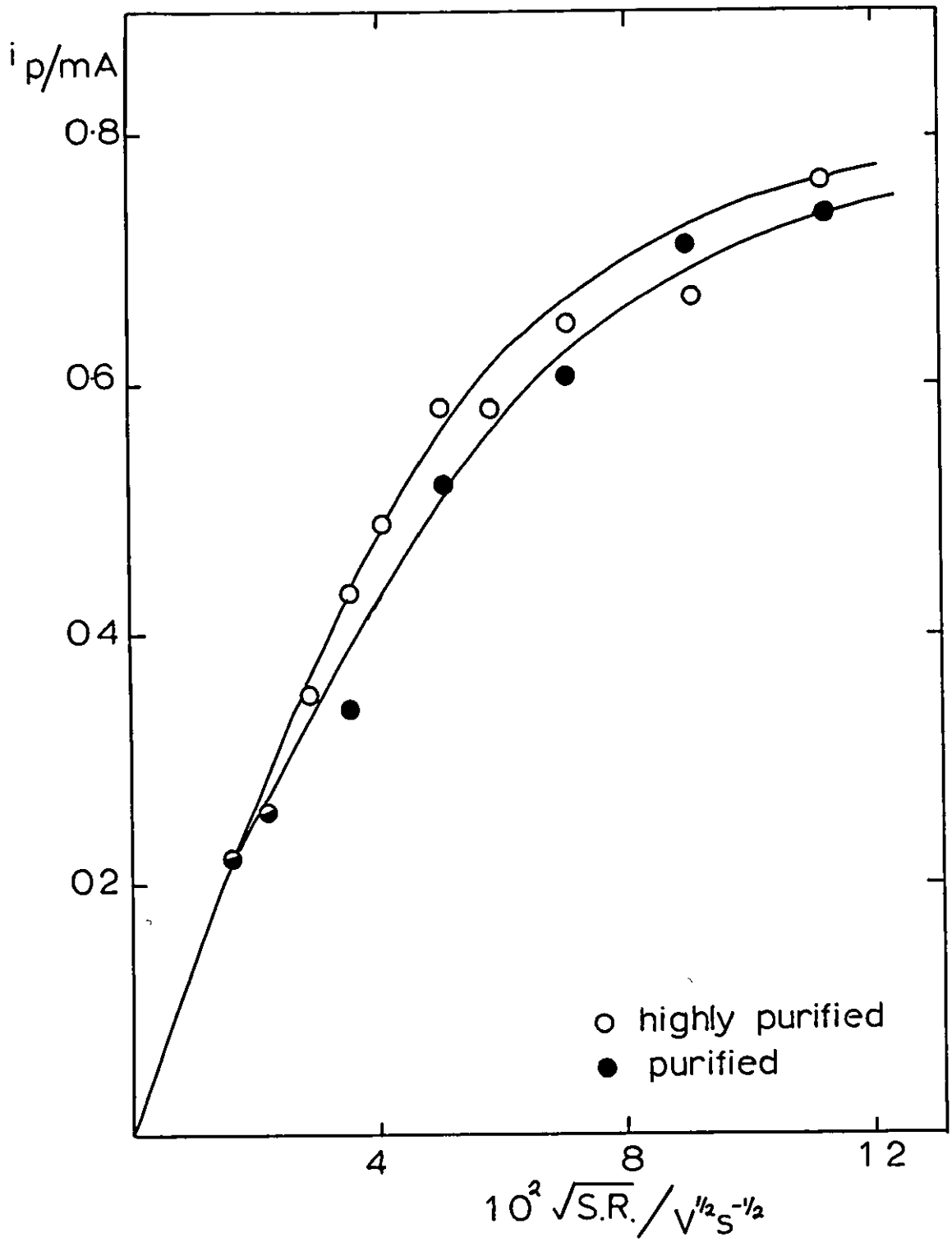

FIG 27 L.S.V. curves at fast sweep rates

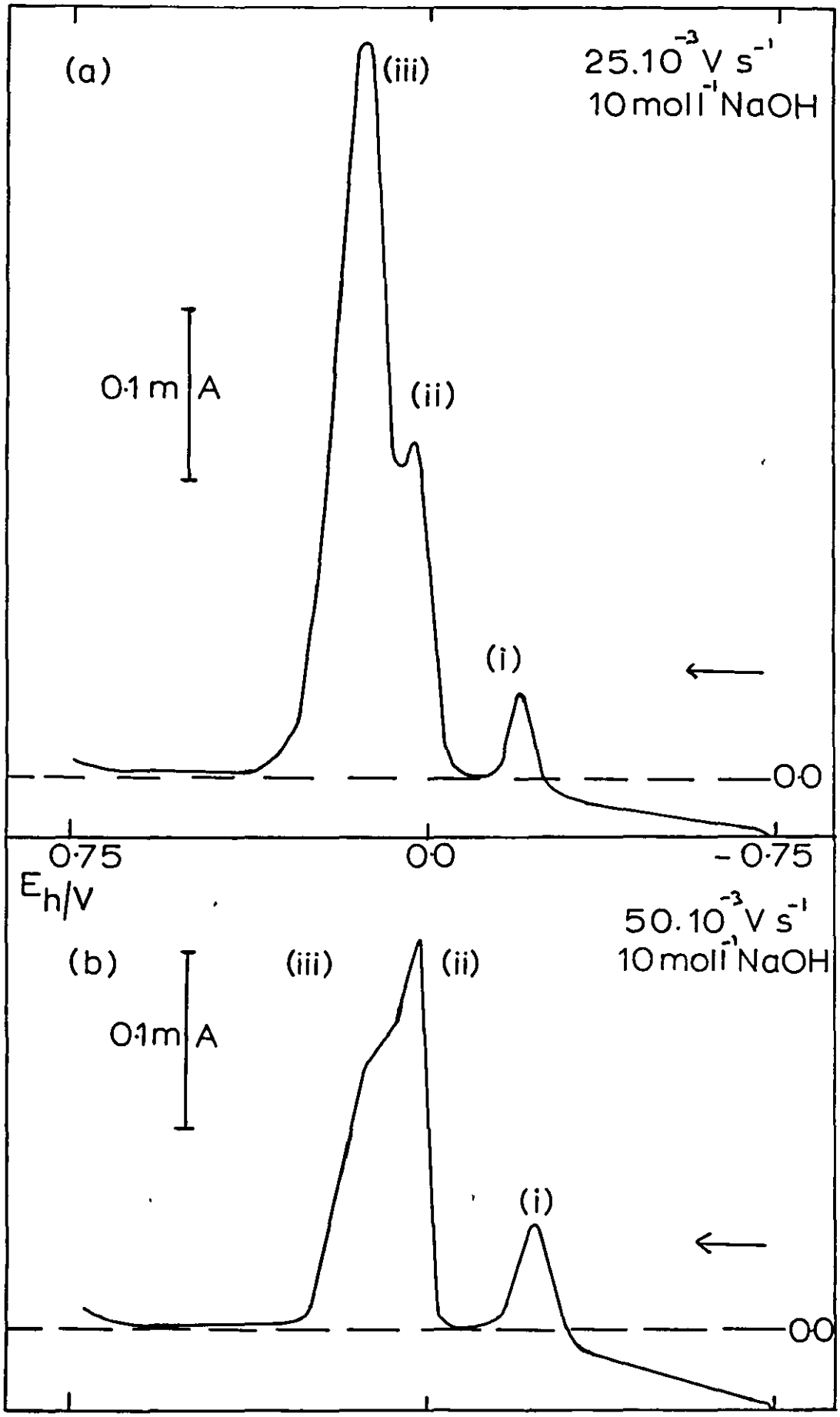

FIG 28 Dependence of i_p on $\sqrt{S.R.}$ for peak (I) at a series of $[OH^-]$

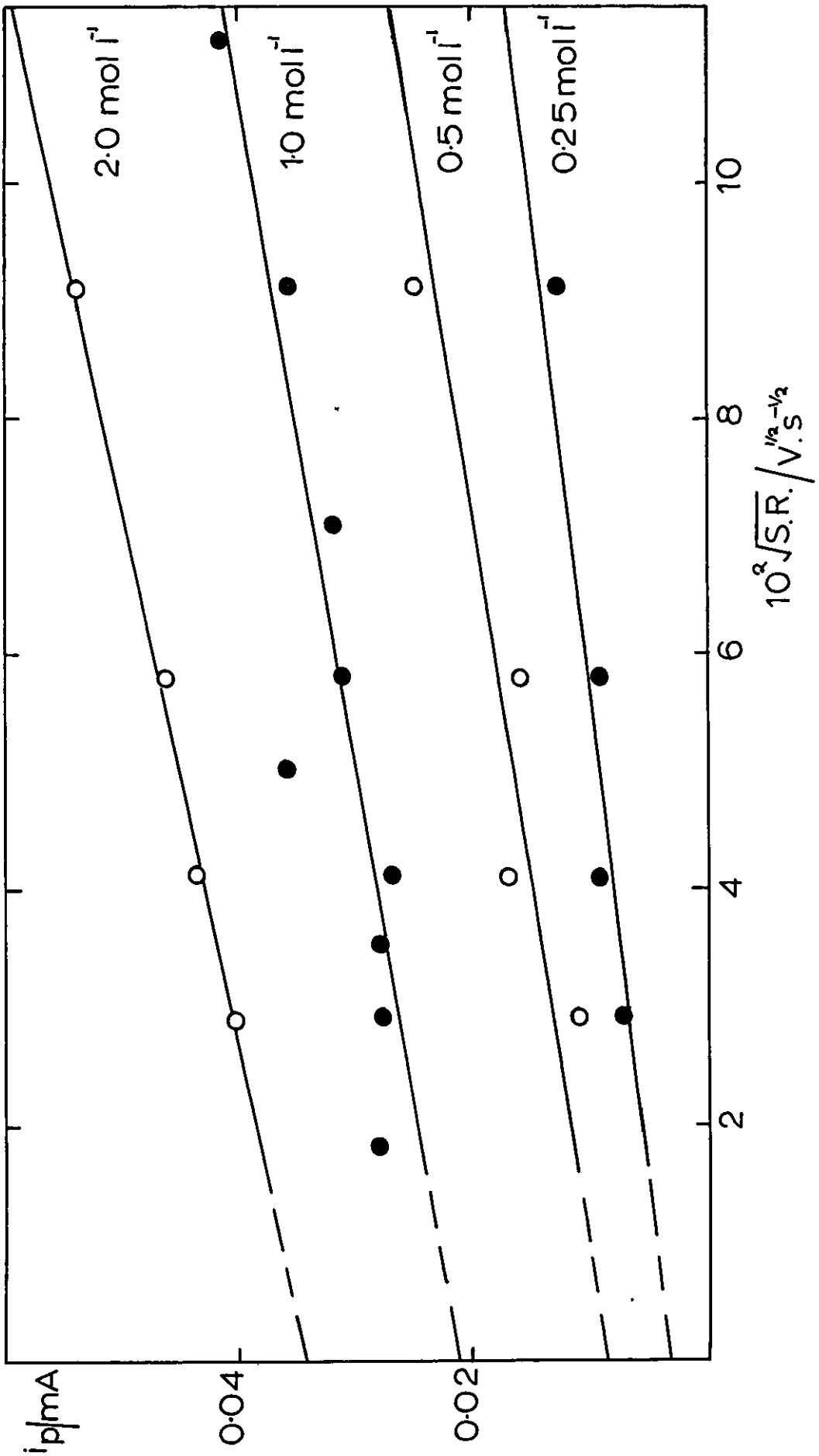

FIG 29 Dependence of i_p on $\sqrt{SR}$ for peak(ii) at a series of $[OH^-]$

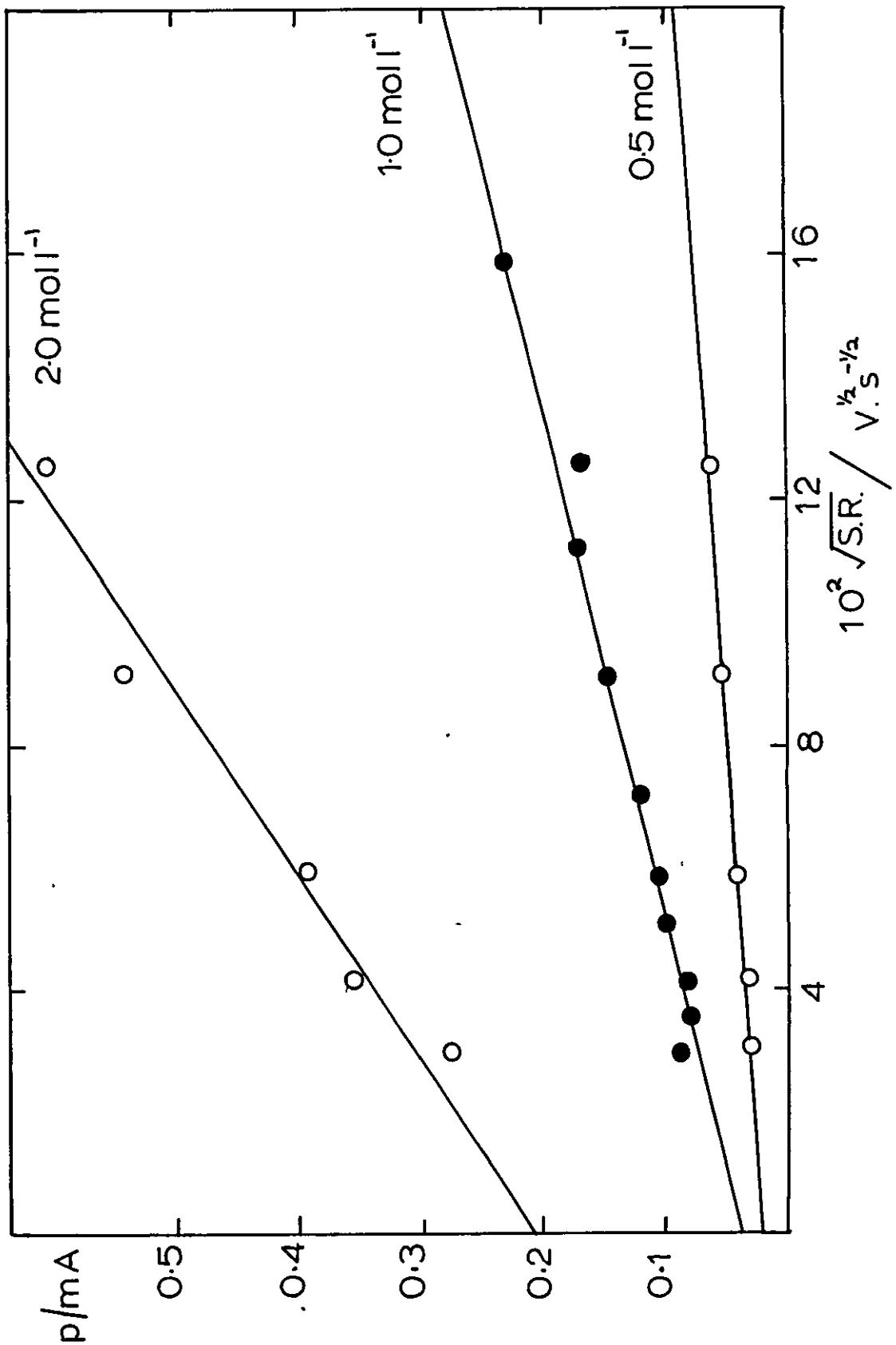

FIG 30 Dependence of i_p on $\sqrt{S.R.}$ for peak(iii) at a series of $[OH^-]$

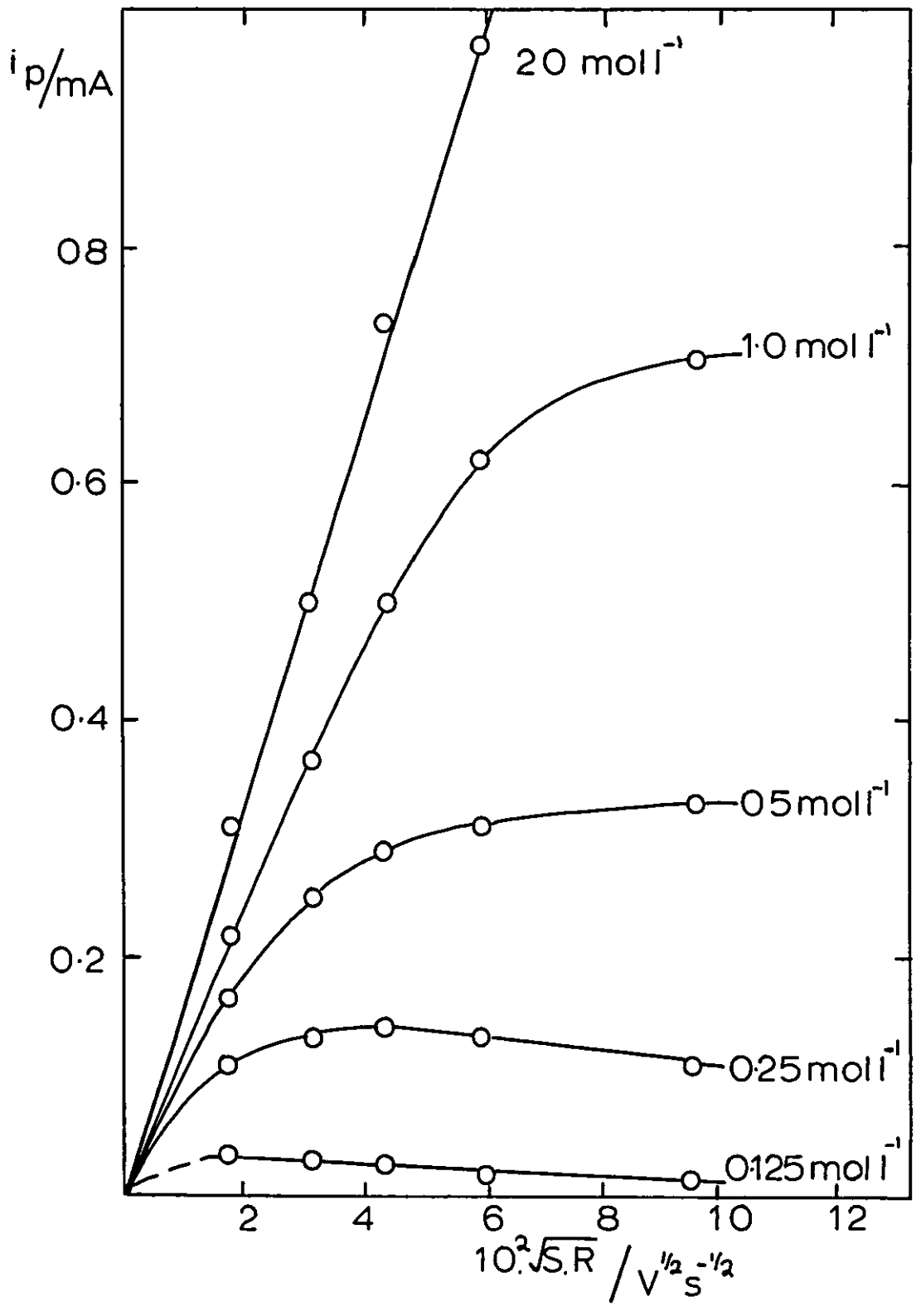

8.2. (iii) Discussion

Reaction peak (i) ($\sim$ - 0.268 V (n.h.e.)) The reaction that occurs in this potential region is the oxidation of copper to Cu_2O. This potential region is not too far removed from the reduction potential for reaction (8.1.), - 0.358 V (n.h.e.) and is in good agreement with a value of $\sim$ - 0.25 V (n.h.e.) found by Miller[73] for the corresponding oxidation at comparable sweeping rates (20 mV s^{-1}).

$$2\,Cu + 2OH^- \longrightarrow Cu_2O + H_2O + 2e \qquad (8.1.)$$

The dependence of the peak height corresponding to this reaction upon the starting potential is shown in Table 7. This may indicate that the peak height is influenced by adsorbed species at the electrode. The species most likely to participate in such a reaction is hydrogen, which has been shown to be adsorbed at copper electrodes in neutral potassium sulphate at $\sim$ 0.15 V (n.h.e.) by Champion et al[100]. It is not likely however that adsorbed hydrogen reacts to give Cu_2O

$$2\,Cu\,H_{ads} + 4OH^- \longrightarrow Cu_2O + 3H_2O + 2e \qquad (8.2.)$$

since there is neither a significant shift in peak potential with changes in the initial sweeping potential, nor the presence of a significant peak that can be identified with the formation of this species. The cause of this dependence of the peak height upon the initial potential is more likely due to differences in the electrode surface,

resulting from the formation of active copper species on the surface, these species arising during polarisation at negative potentials. This effect has been observed previously; thus Bockris and Kita[101] report that "the effect of cathodic pulses is remarkable in the case of copper and that this is due to an increase in active surface area due to the formation of fine particles of Cu". The enhanced peak currents obtained from cycled electrodes (see Table 7) supports this agreement.

Figure 28 shows a family of i_p vs $(S.R.)^{\frac{1}{2}}$ plots at different electrolyte concentrations. The resultant set of straight lines show that the reaction is diffusion controlled, the lines are parallel (slope independent of $[OH^-]$) and do not extrapolate through the origin. Attempts to calculate an apparent diffusion coefficient, using the equations discussed by Delahay[24] for a system controlled by semi infinite diffusion, give apparent values with an upper limit of 1×10^{-8} cm^2 s^{-1}. This value is too small for diffusion in solution to be rate controlling and it is suggested that the transference of ionic species in the solid phase is the rate controlling process, the most likely species being Cu^+. The intercepts on the i_p axis under these conditions are a measure of the charge associated with the formation of the layer of active species at the copper electrode.

Reaction peaks (ii) and (iii) ($\sim$ - 0.10 V (n.h.e.)) An examination of an L.S.V. potential/current trace obtained at a slow sweeping speed (1.25×10^{-3} V s^{-1}) shows an overall oxidation peak that on first examination might be interpreted

as the formation of a single Cu(II) oxide. On closer examination it is possible to see a shoulder on the more negative side of this reaction peak. This effect becoming more noticeable at faster sweeping speeds (25×10^{-3} V s^{-1}) where the larger reaction peak is resolved into two distinct reaction peaks. The products of these two reactions could be CuO, $Cu(OH)_2$ or a mixture of the two.

It is unlikely that the component reactions corresponding to this twin peak are the two stage oxidation of Cu to Cu(II) via a Cu(I) intermediate, the difference in the E^o values of the two reactions being 0.27 V, which is larger than the extent of the region in which the faradaic current flows ($\sim$ 0.15 V). Another possibility is that reaction (ii) is the oxidation of Cu(I) to Cu(II) accompanied by reaction (iii) which is the oxidation of Cu(O) to Cu(II). This does not seem likely since reaction (ii) cannot simply be the oxidation of Cu(I) to Cu(II) since the peak area (for the same sweep speed) of reaction (ii) is much greater than that of reaction peak (i), although reaction (iii) is quite likely the oxidation of Cu(O) to a Cu(II) oxide. It appears most likely that in this potential region we have the formation of two Cu(II) oxides.

An analysis of the reaction peak heights and changing sweep rate data for reaction (ii) is shown in Figure 29. From the slopes of the plots of i_p vs $(S.R.)^{\frac{1}{2}}$ an apparent diffusion coefficient of this reaction was calculated and found to be $\sim$ 1-2 $\times 10^{-8}$ cm^2 s^{-1}. Since the slopes of these plots are dependent upon the concentration of the electrolyte, the diffusion control may be due to the diffusion of OH^- through an adsorbed layer at the electrode/electrolyte interphase.

The apparent diffusion coefficient being too low for diffusion in solution to be the rate controlling process.

A similar analysis of the i_p and $(S.R.)^{\frac{1}{2}}$ data for reaction (iii) (see Figure 30) shows that this reaction is very dependent upon both the potential sweeping rate and the electrolyte concentration. It is not possible to draw any definite conclusions about the rate controlling mechanisms for this reaction, other than at slow sweep rates and at high electrolyte concentrations (> 1.0 mol l^{-1} NaOH), where it appears that diffusion of OH^- is rate controlling. Attempts to apply the equations formulated by Delahay[24] give values for an apparent diffusion coefficient of the rate controlling species that approach that expected for the diffusion of OH^- in solution ($2 - 4 \times 10^{-5}$ cm s^{-1}). It is suggested that this reaction may be controlled by the diffusion of OH^- in solution at high electrolyte concentrations and low sweeping rates. At higher sweeping speeds and lower electrolyte concentrations the control appears to be due to the development of a film of Cu(II) oxide on the electrode surface. This is indicated by the curving of the i_p vs $(S.R.)^{\frac{1}{2}}$ plots towards the $(S.R.)^{\frac{1}{2}}$ axis at the higher values of $(S.R.)^{\frac{1}{2}}$. These changes in peak height with sweep rate can be explained as follows: at the slow sweeping rates the soluble product has adequate time to leave the electrode surface; at faster sweeping rates a layer of Cu(II) oxide is developed at the electrode and the current is limited by the formation of this solid phase. An extreme case is shown in Figure 27(b) where very little Cu(II) passes out into solution. The most likely reactions that

would be in agreement with these experimental findings are:-

$$Cu + 2OH^- \longrightarrow CuO + H_2O + 2e \qquad (8.3.)$$

$$Cu + 2OH^- \longrightarrow Cu(OH)_2 + 2e \qquad (8.4.)$$

8.3. Rotating Disc Electrode Measurements

8.3. (i) Experimental This method has been fully discussed in section 3.2. (iii). The electrolytic cell used was of the type shown in Figure 5(b). The electrolyte was of pure NaOH; no charcoal purification was used in these experiments. The rotating disc electrode has been described and is shown in Figure 3. The active electrode surface was cleaned on fine emery paper and then on roughened glass, using bidistilled water as a lubricant, followed by chemical etching in HNO_3 (15%). The counter and reference electrodes were those used in the L.S.V. experiments.

8.3. (ii) Results A preliminary investigation of the system was made using L.S.V. applied to a copper disc electrode. Current/potential curves were obtained with the electrode rotating at a fixed rotation speed and a slowly varying potential. A typical trace of the system is shown in Figure 31. The variation of the reaction peak height, i_m, of the two electrochemical reactions indicated by these traces, with rotation speed, ω, is shown in Figure 32.

FIG 31 L.S.V. curve for Cu r.d.e. in OH^-

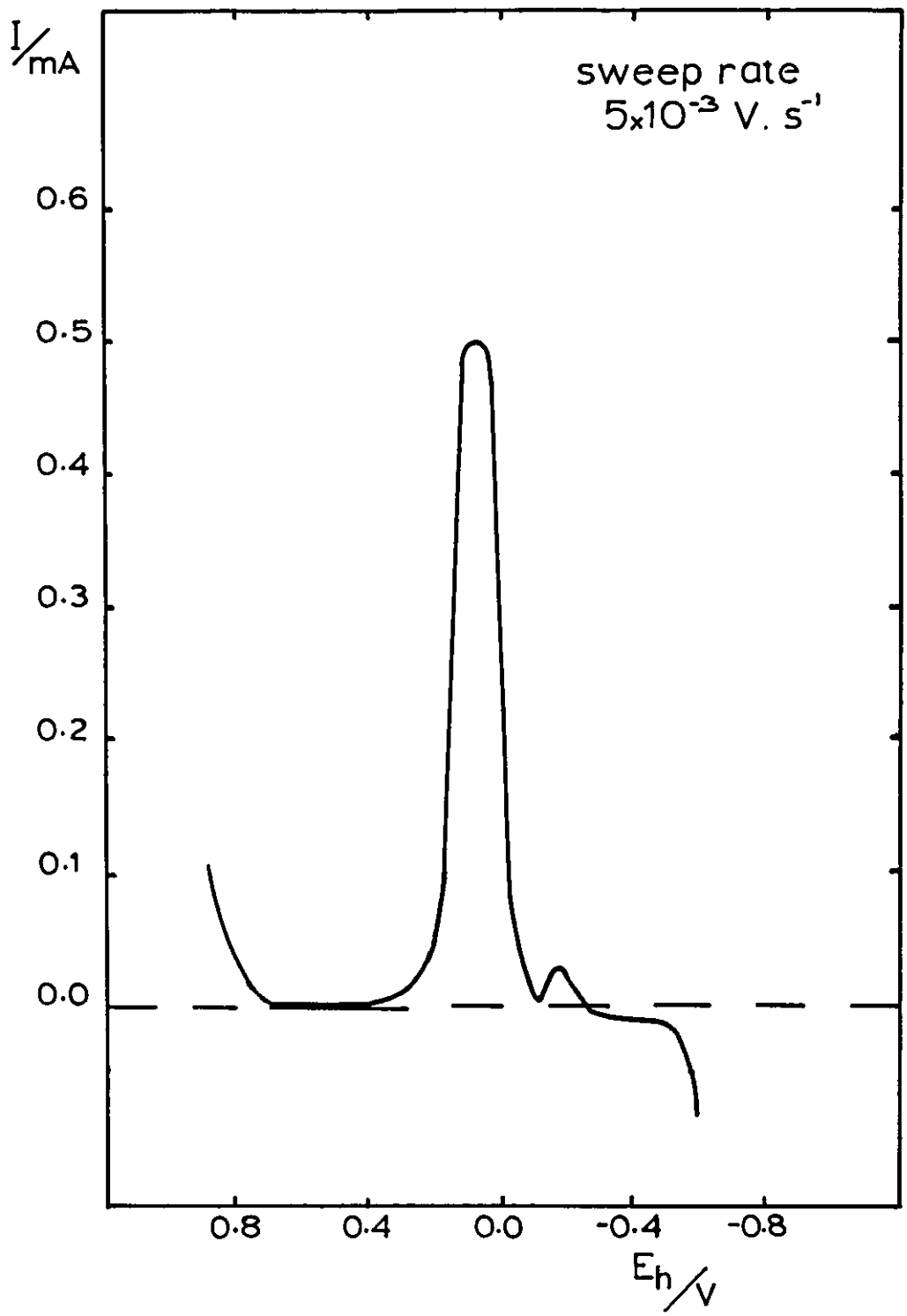

FIG 32 Dependence of i_m^{-1} on $w^{-1/2}$

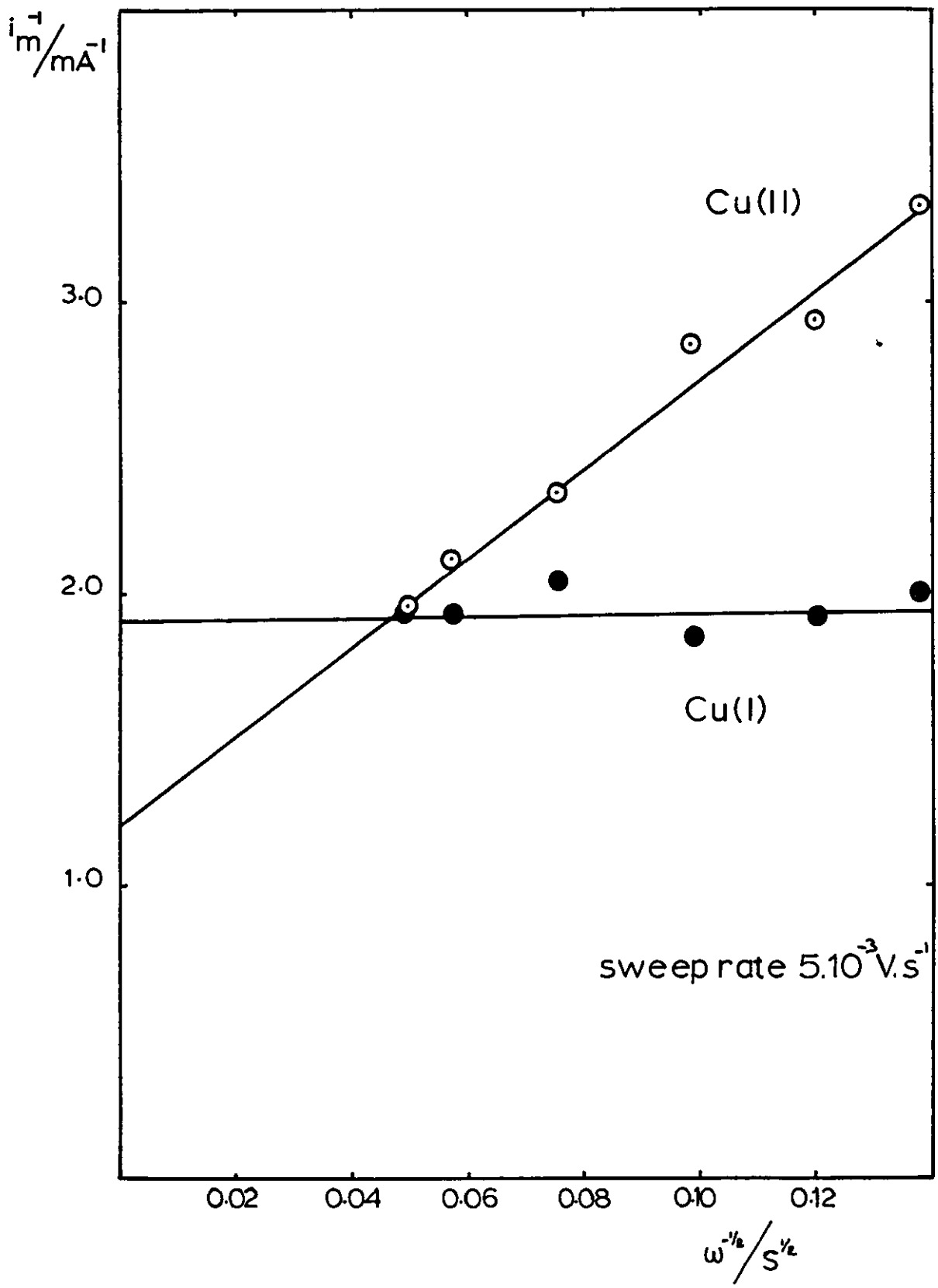

A further preliminary investigation was made in which the rotation speed of the copper disc was kept constant (1,000 r.p.m.) and the rate of the potential sweep varied. Figure 33 shows the resulting plot of the reaction peak height, i_p, against $(S.R.)^{\frac{1}{2}}$.

It can be seen from these preliminary investigations that the reactions, identified by the two current peaks, differ in the nature of their rate controlling processes. The height of the smaller peak (Cu(I)) does not vary with a change in the rotation speed but it does vary with a change of sweep rate. The height of the larger peak (Cu(II)) varies quite markedly with the rotation speed of the copper disc but remained constant when the sweep rate was changed.

Of the two observed peaks only that due to the formation of Cu(II) species showed the behaviour of an electrode process influenced by mass transport in solution and so further experiments with the r.d.e. were confined to an investigation of this reaction.

A more detailed examination of the Cu | Cu(II) oxide | OH^- system was made over the potential range - 0.15 V to 0.30 V (n.h.e.). Figure 34 shows the variation of current with potential at a fixed rotation speed, every current reading being taken with a freshly prepared electrode at a fixed potential. There appear to be four distinct regions in the curve and these are designated as:-

(a) rapid increase of current with increasing potential,

(b) current independent of potential,

(c) rapid decrease of current with increasing potential,

FIG 33 Dependence of i_m on $\sqrt{S.R.}$

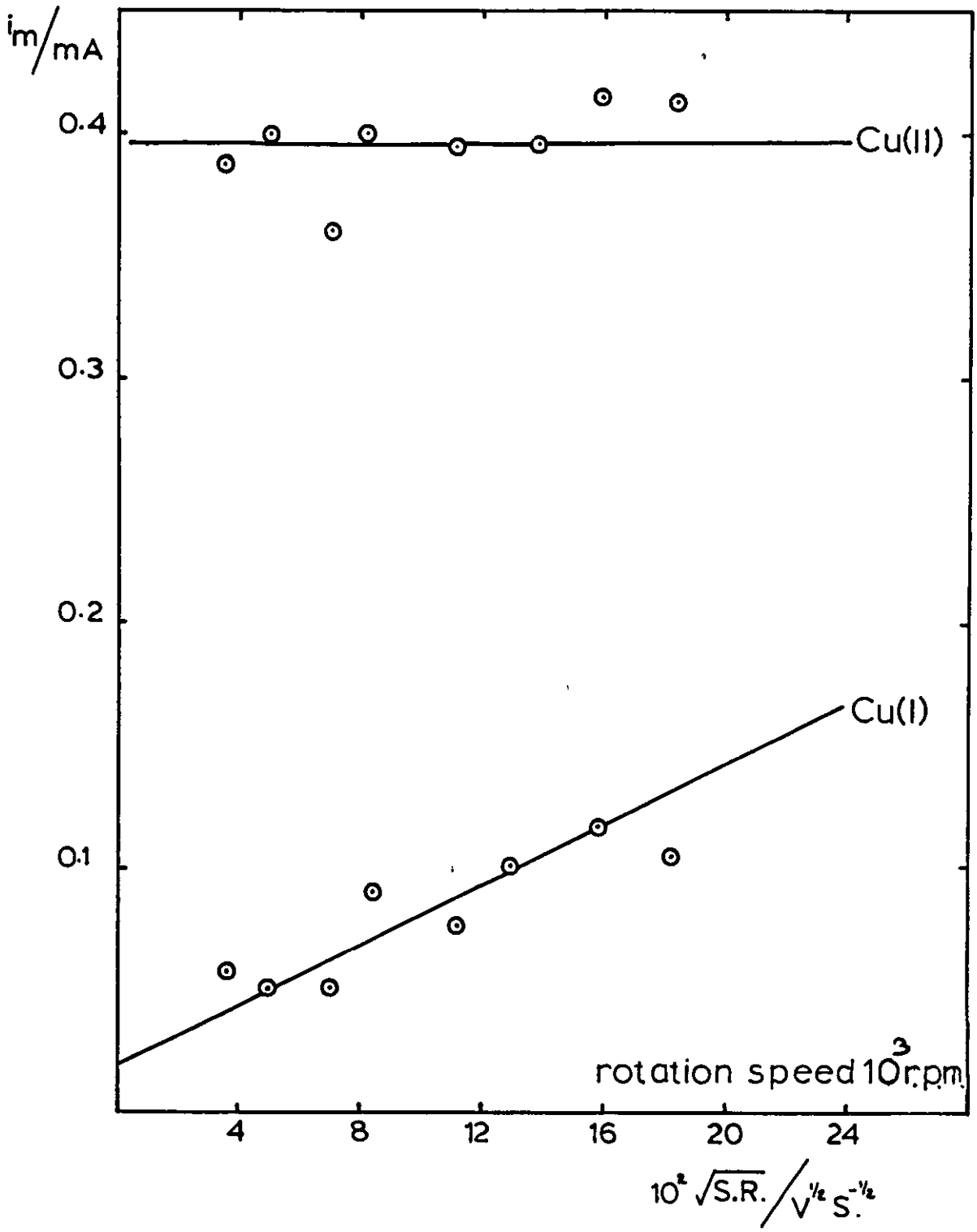

FIG 34 Variation of steady state current with potential

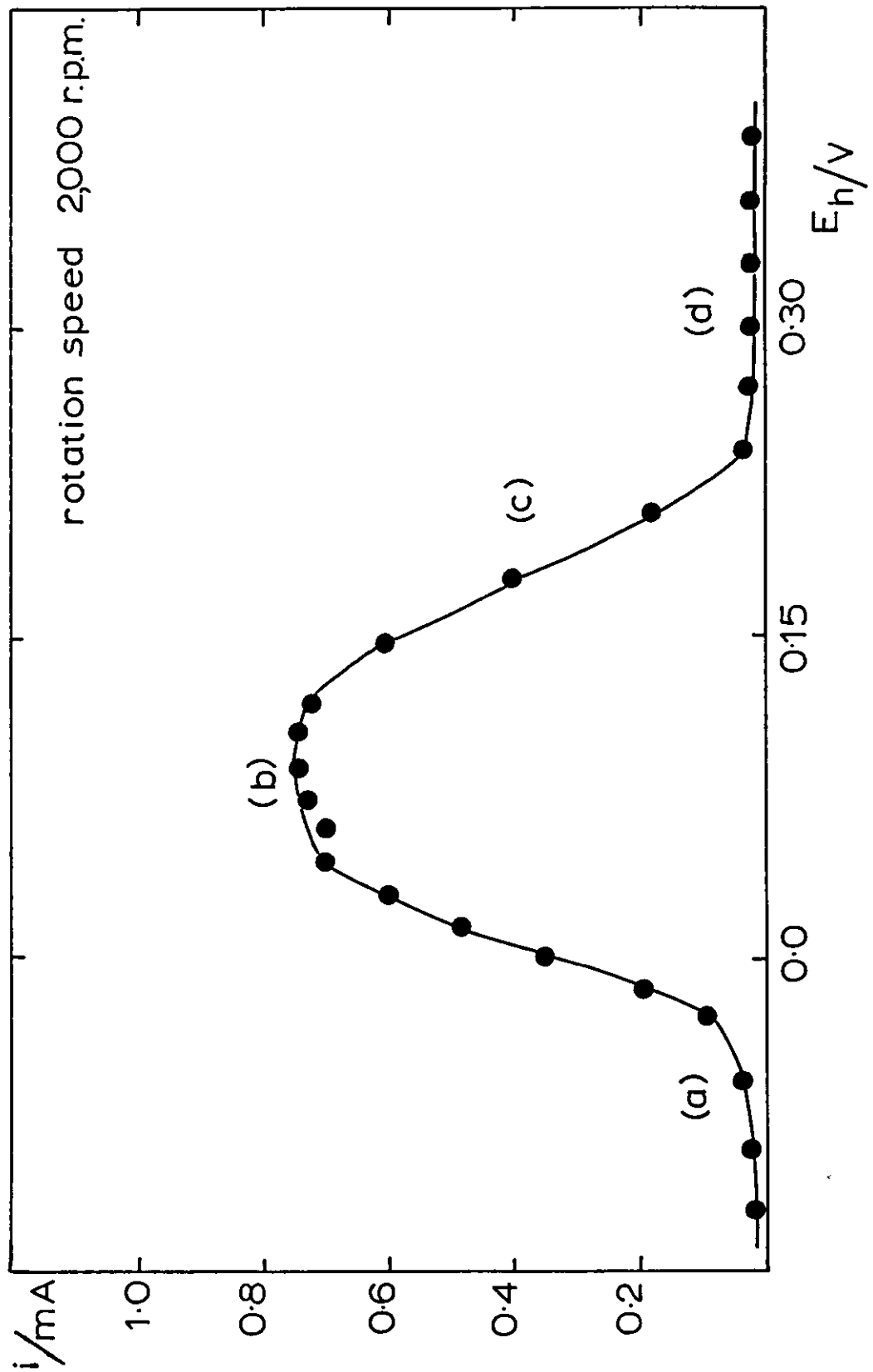

(d) current (low) independent of potential.

In the first of these regions, corresponding to the active dissolution of the copper electrode, the measured current increases rapidly with a small increase in the applied potential (Tafel region).

The current in the second (plateaux) region appears to be almost independent of the applied potential, but is very dependent upon the rotation speed of the copper disc electrode. It would appear that we have two competing effects that are just balancing each other out. The first effect is the formation of a Cu(II) oxide at the electrode, this being dependent on the applied potential. The second effect is the removal of this Cu(II) oxide from the electrode into the solution and this is dependent on the rotation speed of the disc electrode. The net result of these competing effects is the observed independence of the current upon the applied potential. This "limiting" current is not a true limiting current in the sense of Levich where

$$i_L = 0.02\, n\, F\, A\, C_o^b\, D^{\frac{2}{3}}\, \nu^{-1/6}\, \omega^{\frac{1}{2}} \qquad (8.5.)$$

since intercepts are obtained from i_L vs $\omega^{\frac{1}{2}}$ plots (see Figure 35). It seems likely that these intercepts at zero rotation speed are due to the formation of an oxide phase at the electrode surface. Also in this potential region an interesting effect is observed with the more dilute electrolyte solutions, which are absent at higher concentrations, is shown in Figure 36. At low rotation speeds a shoulder was present

FIG 35 Variation of i_L with $\omega^{1/2}$

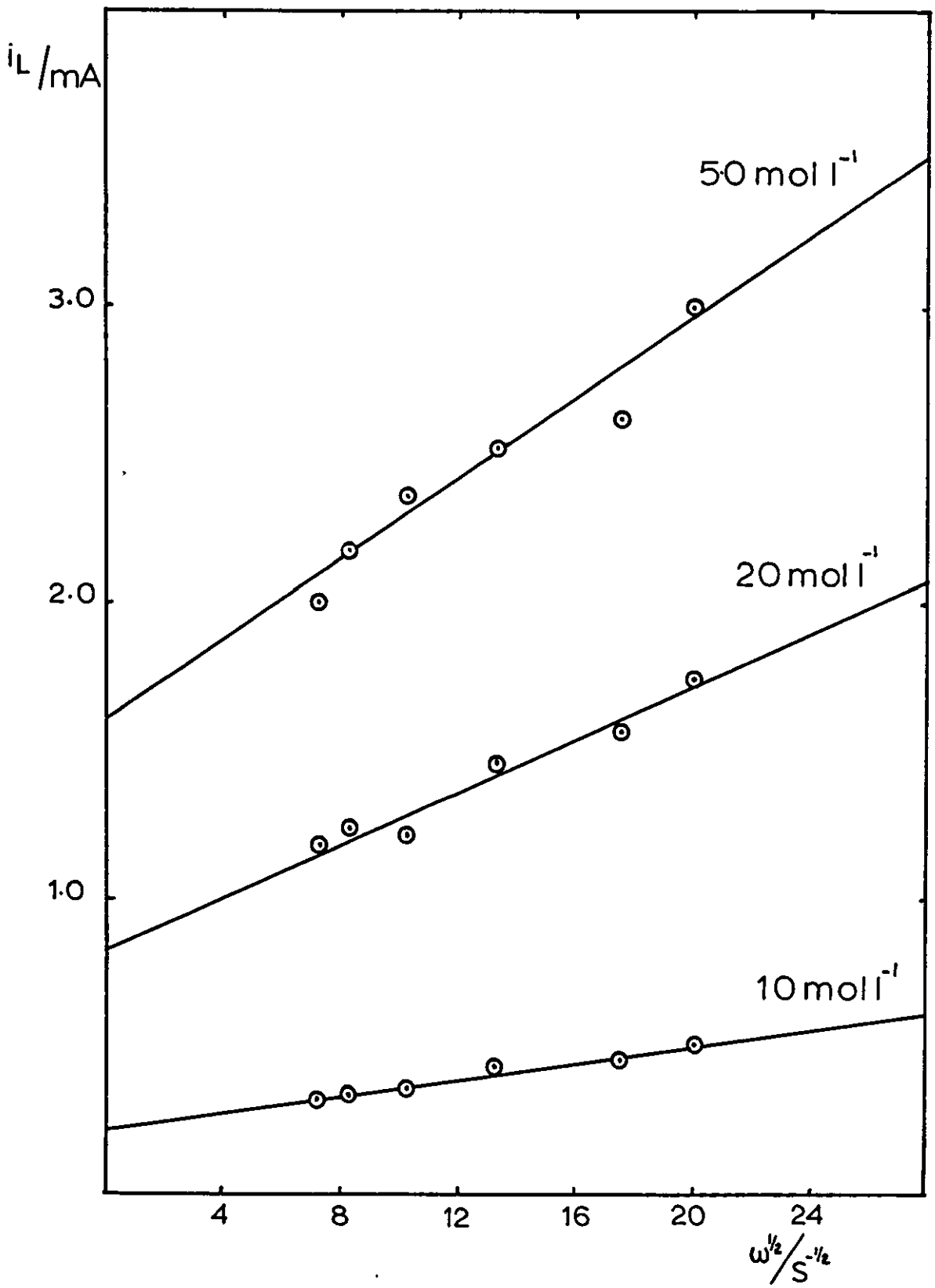

FIG 36 LSV. curve of a Cu r.de. in 05 mol l^{-1} NaOH, sweep rate 5×10^{-3} V. s^{-1}.

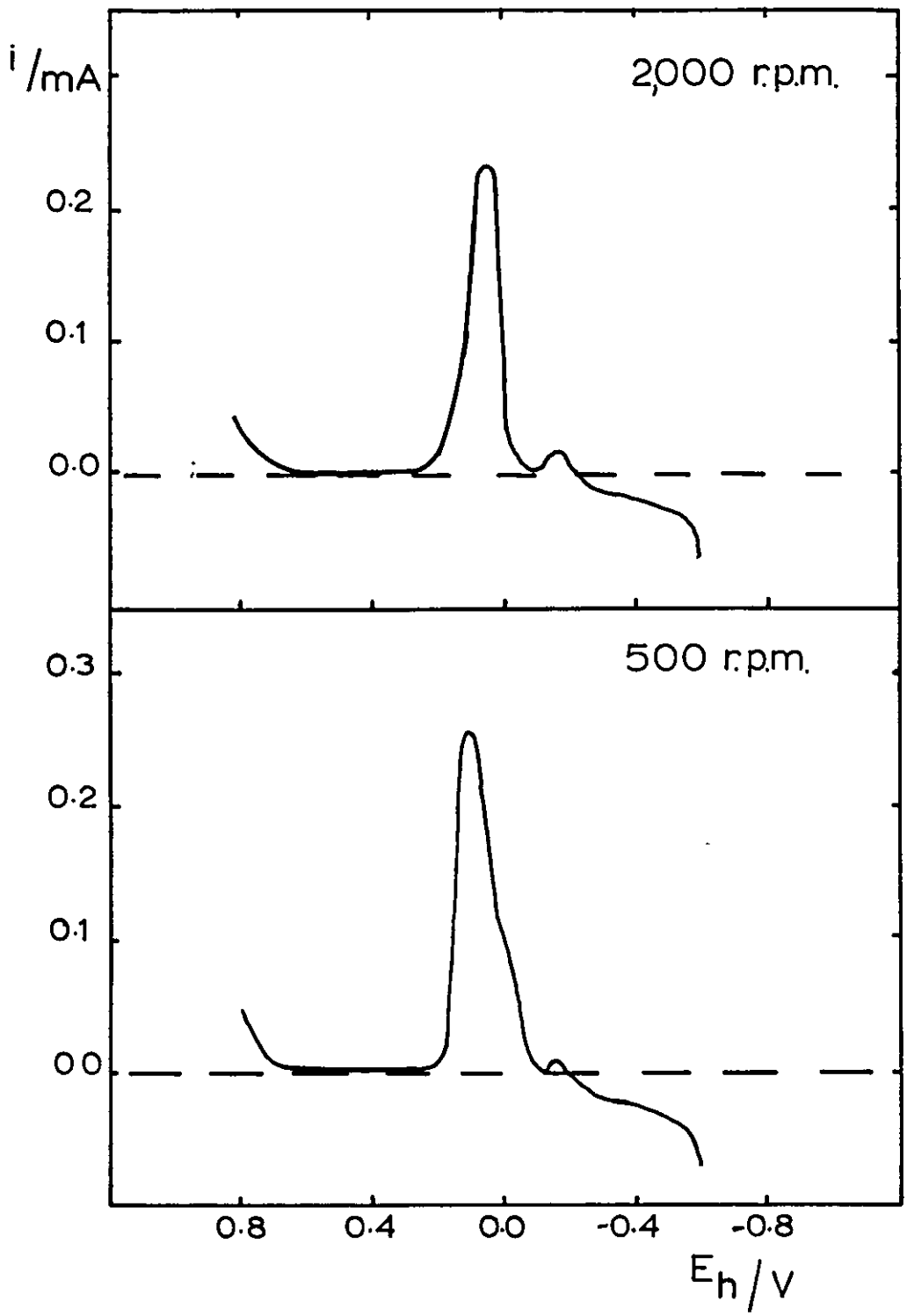

on the negative side of the Cu(II) reaction peak; at higher rotation speeds this shoulder becomes the major reaction peak and there is a noticeable degree of tailing on the positive side of the Cu(II) reaction peak. The dependence of the overall peak height on the rotation speed for this system is shown in Table 8. At concentrations $>$ 0.5 mol l^{-1} NaOH shoulders were not detected under the experimental conditions.

TABLE 8 Dependence of overall peak height for the Cu(II) reaction on rotation speed. 0.5 mol l^{-1} NaOH, sweep rate 5×10^{-3} V s^{-1}, electrode area 3.14×10^{-2} cm^2

ω	i_m
500 r.p.m.	0.26 mA
650 "	0.27 "
1 000 "	0.23 "
2 000 "	0.24 "
3 000 "	0.23 "

The third potential region (c), where it was observed that there was a rapid decrease of the current with any increase in potential, is due to the passivation of the electrode by the presence of an oxide film.

The fourth (d) and most positive potential region shows the transpassive dissolution of the copper electrode. The magnitude of the dissolution is almost independent of the applied potential.

It is possible to obtain kinetic data for the active dissolution of the copper from a study of the r.d.e. system under potentiostatic control. It should be noted that the current values were found to be time dependent. This effect was most noticeable at the lower rotation speeds and an extreme example is shown in Figure 37. The current values that were used in this investigation were the maximum values that were obtained. Typical E vs i data are shown in Figure 38 for the 1.0 mol l^{-1} NaOH electrolyte solution. The variation of i^{-1} with $\omega^{-\frac{1}{2}}$, at constant potential, is shown in Figure 39. The dependence of the slopes of those straight line plots upon the applied potential is shown in Figure 40. A least squares fit through these points gives a 55 $\pm$ 5 mV per decade dependence of these slopes upon the applied potential. If however only the lowest potential readings are considered then this dependence becomes 31.5 mV per decade. Similar values of this dependence were also obtained for other electrolyte concentrations and a summary of these results using the same treatment is given in Table 9.

TABLE 9 Variation of slope dependence with concentration of the electrolyte.

$[OH^-]$	Slope Dependence
1.0 mol l^{-1} NaOH	31.5 mV per decade
2.0 " "	48.0 " "
5.0 " "	24.0 " "

If the plots, shown in Figure 39, are extrapolated to $\omega^{-\frac{1}{2}} = 0$ the intercepts give the value of the current at infinite rotation speed, i_∞. The variation

FIG 37 Dependence of steady state current on time

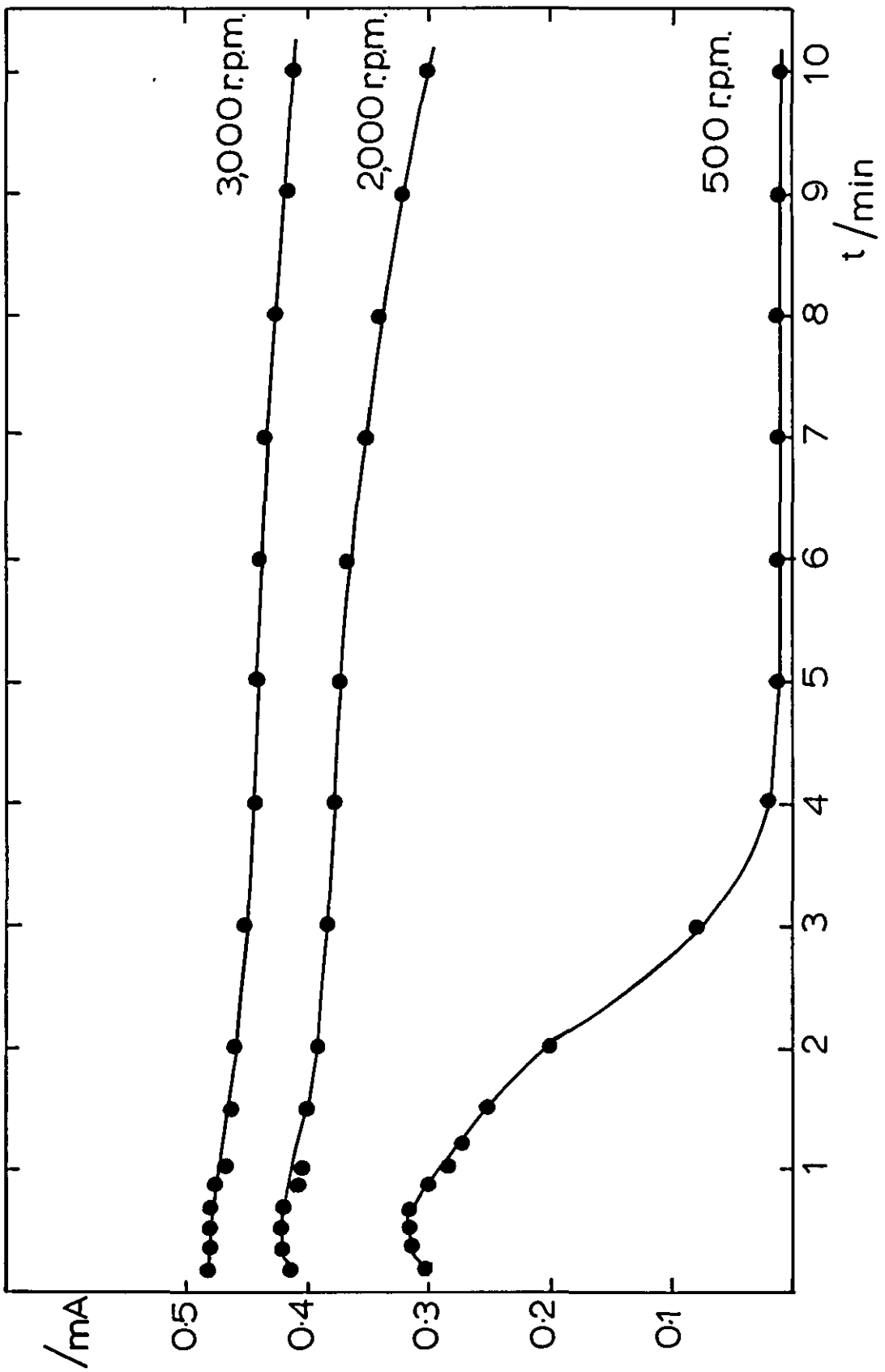

FIG 38 Variation of steady state current with potential

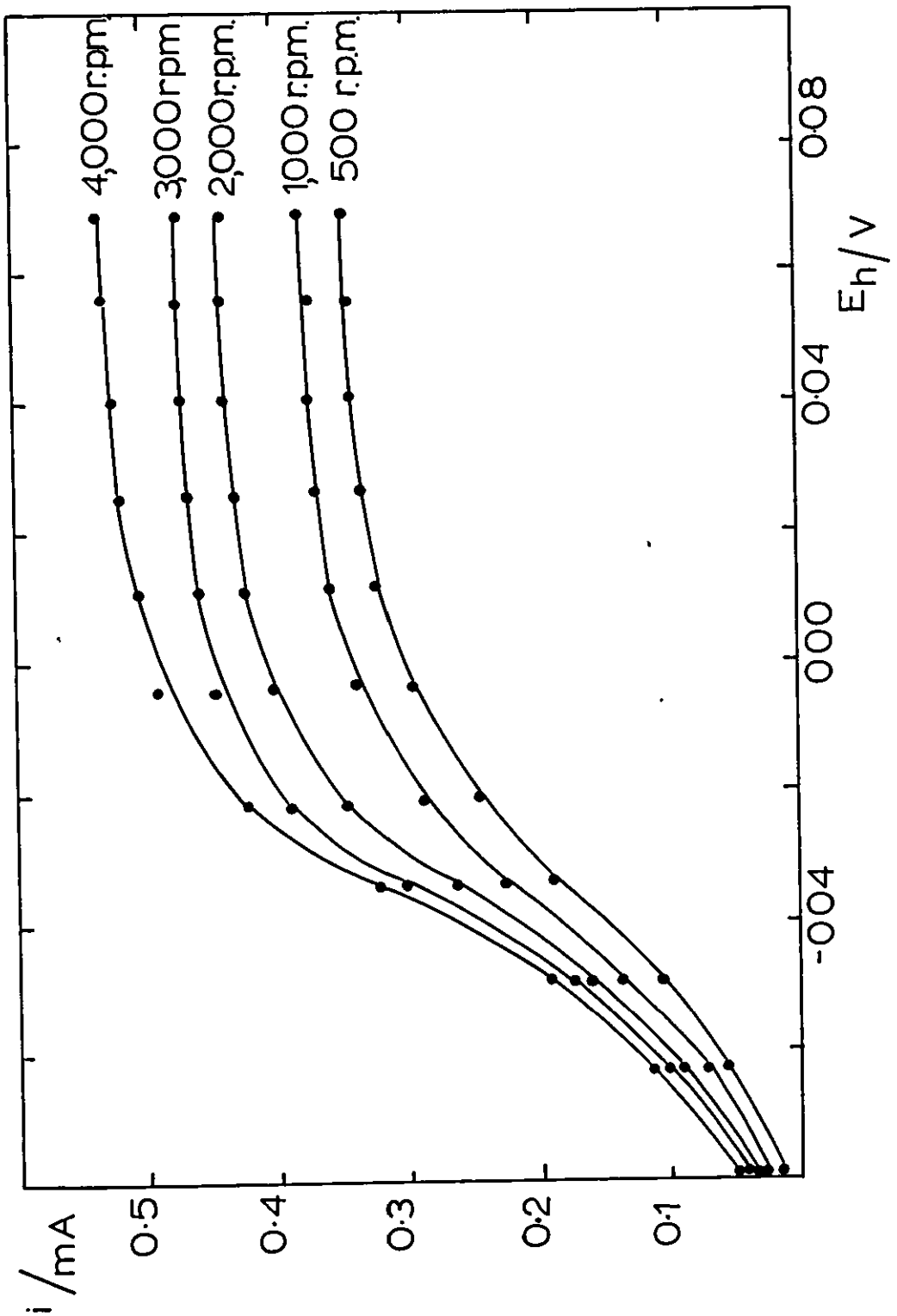

FIG 39 Variation of i^{-1} with $\omega^{-1/2}$ at a series of potentials

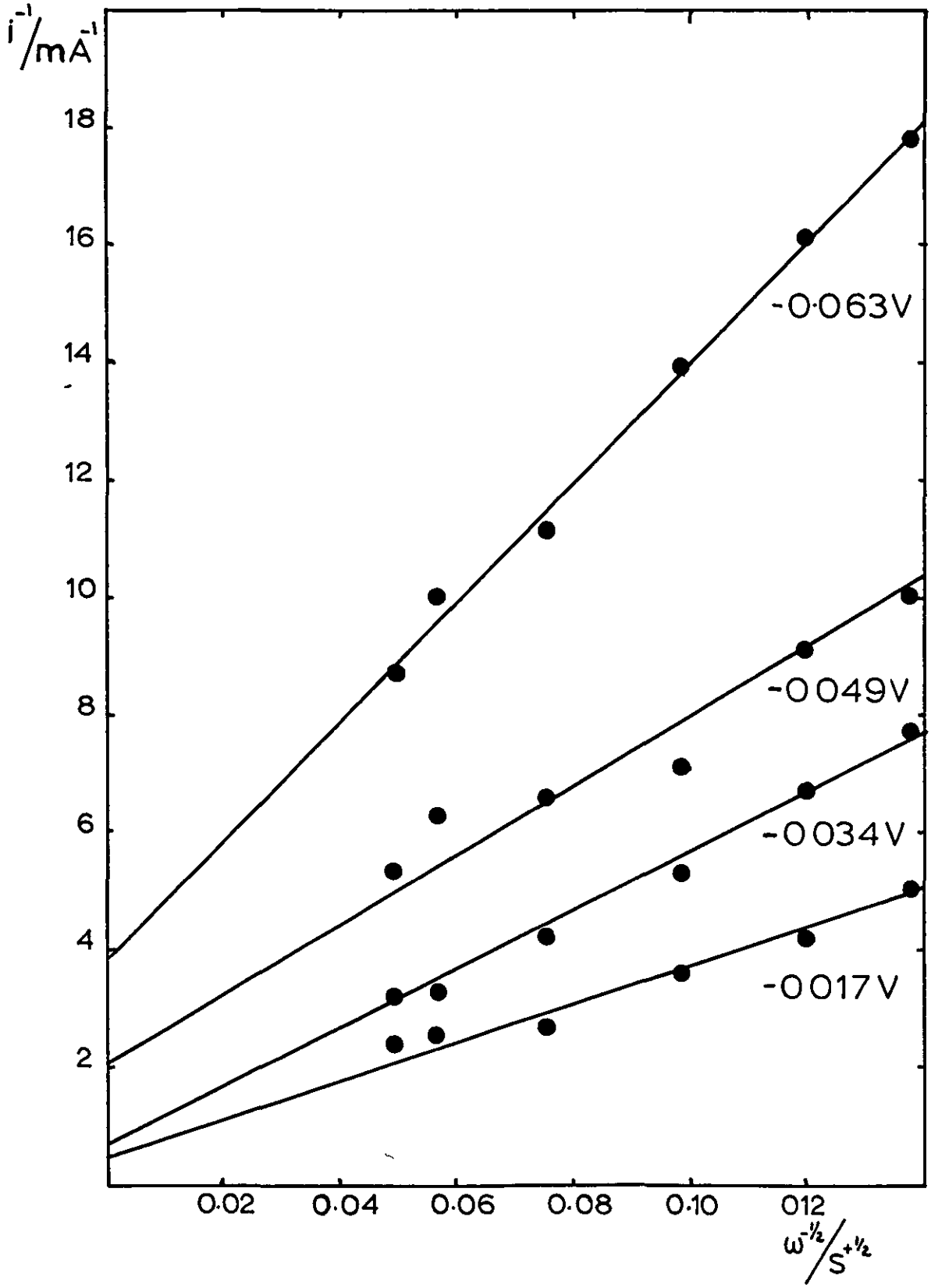

FIG 40 Dependence of slope on potential

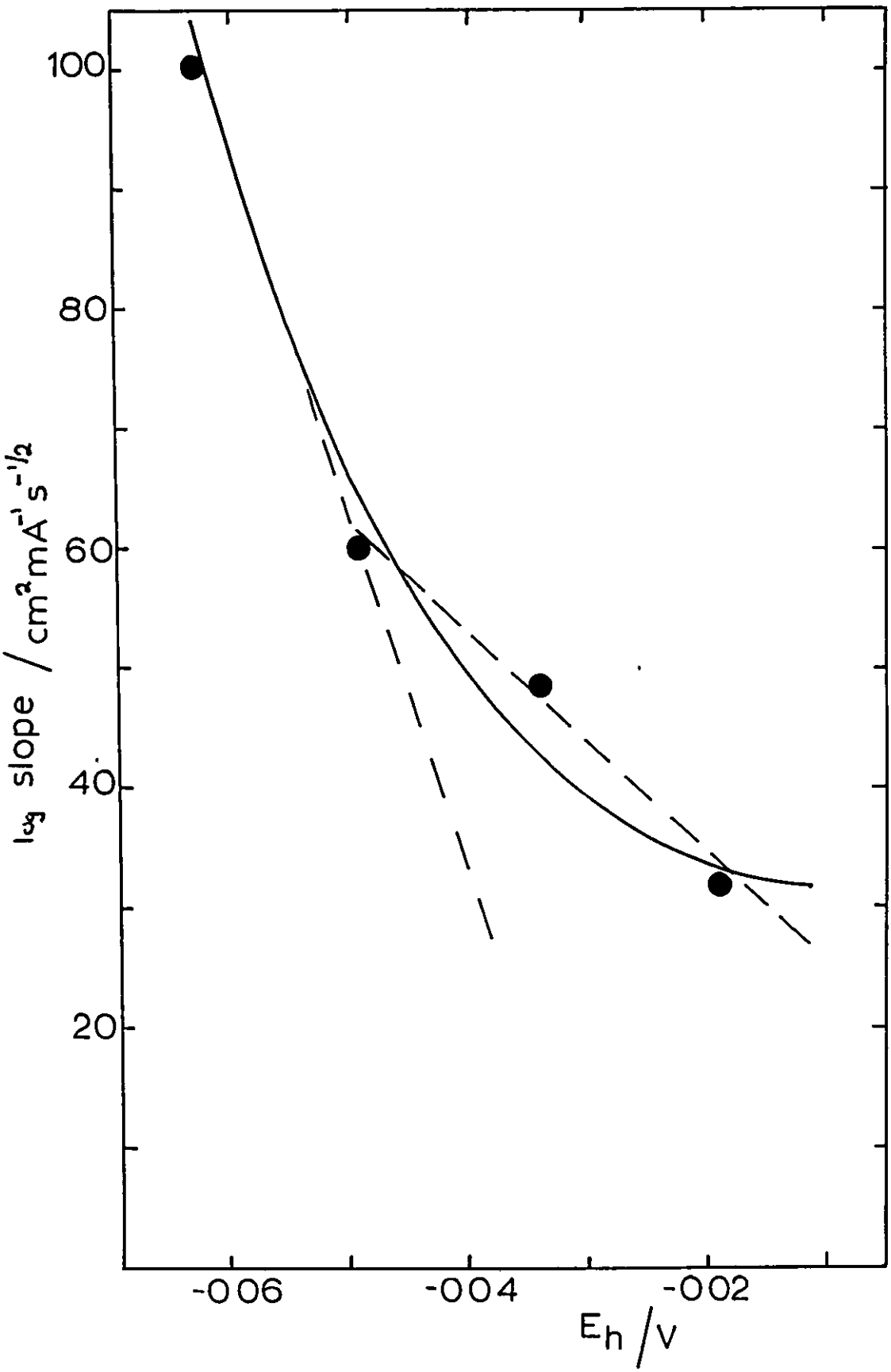

FIG 41 Dependence of log i_{∞} on potential

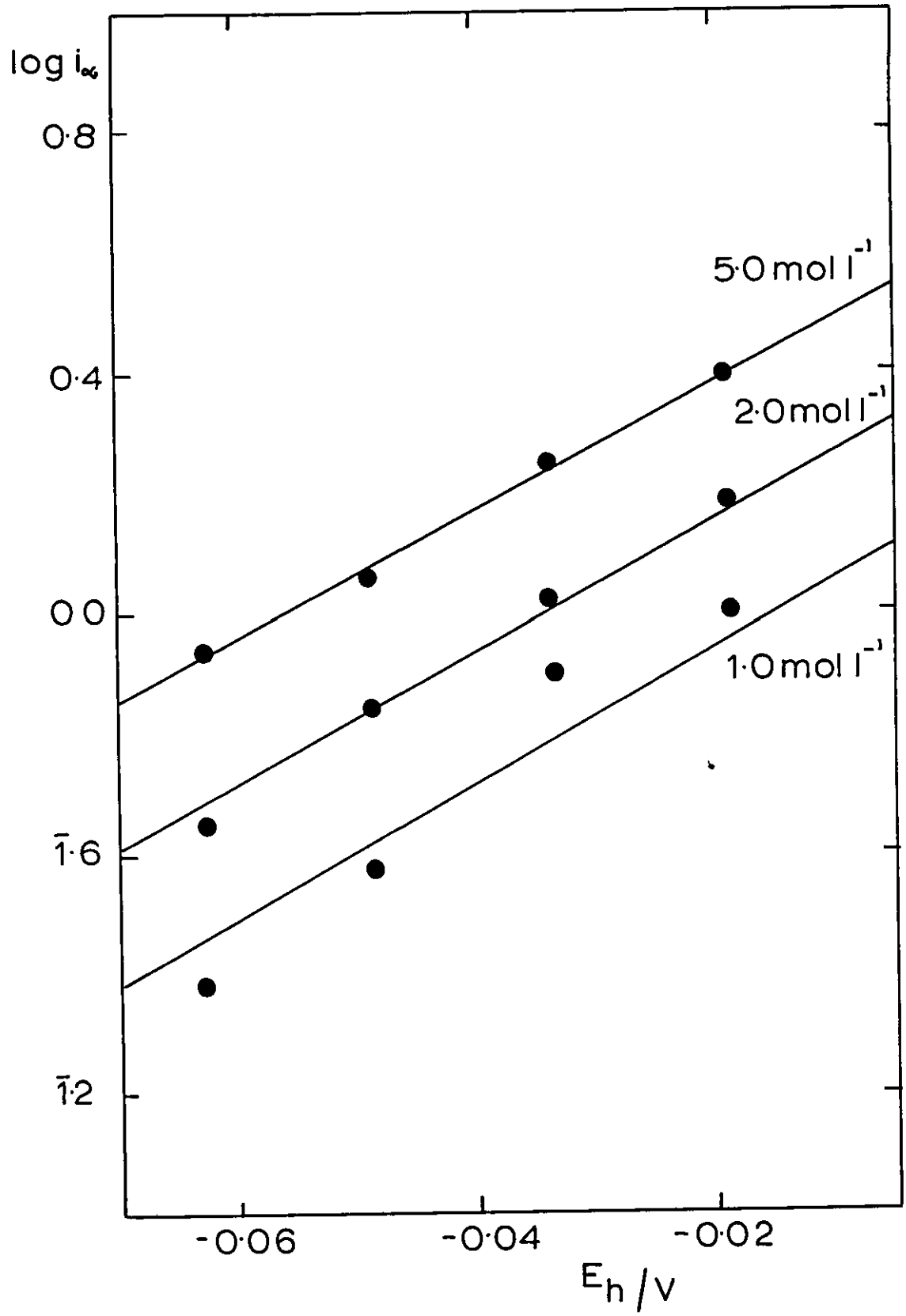

FIG 42 Dependence of i_∞ on $[OH^-]$

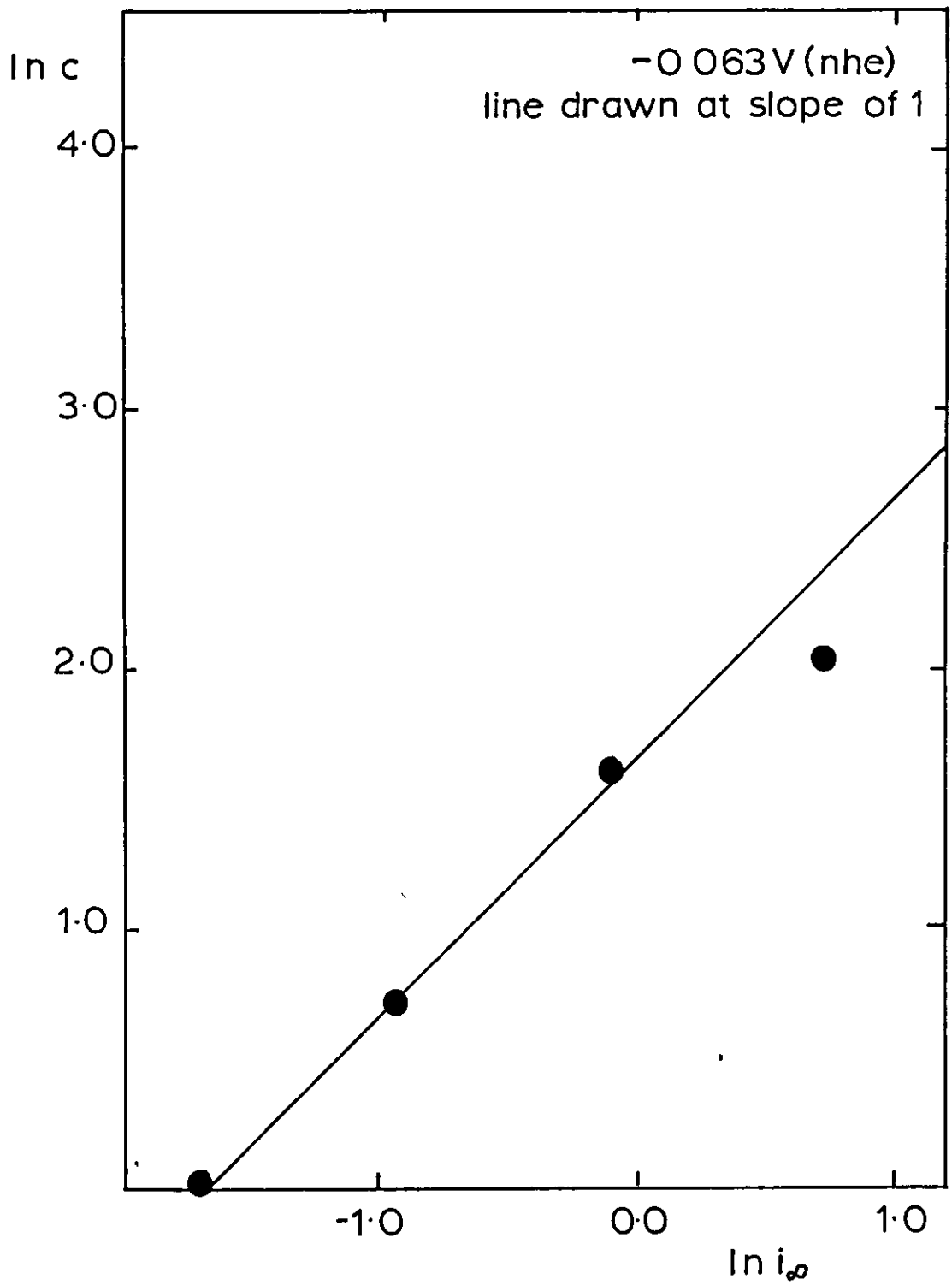

of i_{∞} with potential is shown in Figure 41 for a series of electrolyte concentrations. The corresponding Tafel slopes were 75 $\pm$ 5 mV per decade. The dependence of i_{∞} upon $[OH^-]$ at a constant potential follows from the data in Figure 41 and indicates that i_{∞} is first order with respect to $[OH^-]$. (see Figure 42).

8.3. (iii) Discussion

Sweeping potential experiments From Figure 31 it is evident that two major electrochemical reactions occur in the potential region bounded by the h.e.r. and the o.e.r. and it has been established that these are due to the formation of Cu(I) and Cu(II) oxides. Compared with stationary electrodes, under the same experimental conditions, it is noticeable that at higher NaOH concentrations rotating the electrode has the effect of removing the shoulder from the negative side of the Cu(II) peak. In these experiments with copper disc electrodes only at concentrations < 0.5 mol l^{-1} NaOH is the symmetrical Cu(II) peak distorted by the occurrence of a shoulder on the negative side of the peak. Under these conditions it is difficult to attach quantitative significance to the data, however the fact that the height of this shoulder/peak remains constant with changing rotation speed (see Table 8) suggests the presence of a parallel solid phase reaction. Under these conditions it is possible that this solid phase reaction is the formation of CuO.

Figure 33 shows the effect of changing the potential sweep rate on the maximum currents. The variation of the peak height, corresponding to the formation of Cu_2O, at disc electrodes rotating at 1000 r.p.m. is very similar to that occurring

for stationary electrodes and supports the conclusion that the process controlling the current flow is the transport of species through a solid phase. For the case of the Cu(II) peak the maximum current is independent of the potential sweep rate.

Rotation speed experiments From Figure 32 it can be seen that the Cu(II) reaction peak height has a marked dependence upon rotation speed and this is strong evidence for the control of this reaction by solution phase processes. For electrolyte concentrations greater than 0.5 mol l^{-1} NaOH quantitative examination of the controlling mechanism can be made by an analysis of the current/potential response at a spectrum of rotation speeds (see Figure 38 and 39).

For a 2 e charge transfer reaction the dependence of the slope $[\partial i^{-1} / \partial \omega^{-\frac{1}{2}}]$ of the plots shown in Figure 39 should be tenfold for a potential shift of $2.3\,RT/2\,F$ (~ 30 mV). For a copper disc electrode rotating at a constant speed in the potential region Cu|Cu(II) and where $i < i_L$

$$i = \underset{\rightarrow}{i} - \underset{\leftarrow}{i} \qquad (8.6.)$$

where $\underset{\rightarrow}{i}$ is the dissolution current at infinite rotation speed, i_∞, and $\underset{\leftarrow}{i}$ depends on the concentration of Cu(II) species at the electrode according to

$$\underset{\leftarrow}{i} = n F \overleftarrow{k} C_o^s \qquad (8.7.)$$

hence

$$\frac{1}{i} = \frac{1}{i_\infty - nF\overleftarrow{k}C_o^s}$$

$$= \frac{1}{i_\infty}\left[1 - \frac{nF\overleftarrow{k}C_o^s}{i_\infty}\right]^{-1} \qquad (8.8.)$$

expanding by the binomial as far as the second term

$$\frac{1}{i} = \frac{1}{i_\infty}\left[1 + \frac{nF\overleftarrow{k}C_o^s}{i_\infty}\right] \qquad (8.9.)$$

Using the diffusion layer concept for the dissolution of Cu in NaOH

$$i_\infty = nFDC_o^s/\delta$$

where $\delta = 1.61\, D^{\frac{2}{3}}\, \nu^{1/6}\, \omega^{-\frac{1}{2}}$

substituting in (8.9.)

$$\frac{1}{i} = \frac{1}{i_\infty} + \frac{\overleftarrow{k}\,\delta}{i_\infty D} \qquad (8.10.)$$

at equilibrium $i_\infty = nF\overleftarrow{k}C_o^b$

and (8.9.) varies according to

$$E = E^{o} - \frac{RT}{nF} \log_e \frac{C_o^b}{C_o^E}$$

Hence

$$\frac{1}{i} = \frac{1}{i_\infty} + \frac{1}{0.62\, \omega^{\frac{1}{2}} D^{\frac{2}{3}} \nu^{-1/6} n F C_o^E \exp \frac{nF}{RT}(E-E^{o})} \qquad (8.11.)$$

A plot of i^{-1} vs $\omega^{-\frac{1}{2}}$ should be linear with an intercept of $1/i_\infty$ and a slope dependence on potential of 30 mV per decade.

The least squares fit of the data for the 1.0 mol l^{-1} NaOH gave a 55 $\pm$ 5 mV per decade dependence of the slope on the potential. This value is not possible and hence it was necessary to investigate the data further. The 31.5 mV per decade dependence found for the lower potential readings indicated that the higher potential readings were suspect. A similar slope dependence was found for 2.0 and 5.0 mol l^{-1} NaOH solutions and so equation (8.11.) was in fact verified by the experimental results. The possible cause for this discrepancy at the higher potential readings is that in these cases $i \longrightarrow i_L$ and hence the expression (8.6.) does not hold as demanded by the theory.

Figure 41 shows the dependence of log i_∞ upon the applied potential There is a 75 $\pm$ 5 mV per decade dependence of the slopes of these plots upon the applied potential.

If we consider the reaction sequence

$$Cu(O) \longrightarrow Cu(I) \longrightarrow Cu(II)$$

there are two possible reaction mechanisms:-

$$Cu \underset{\text{fast}}{\rightleftharpoons} Cu(I) \underset{\text{slow}}{\longrightarrow} Cu(II) \qquad (8.12.)$$

$$Cu \underset{\text{slow}}{\longrightarrow} Cu(I) \underset{\text{fast}}{\rightleftharpoons} Cu(II) \qquad (8.13.)$$

A decision of which reaction may rate control can be obtained from the Tafel slope

If the step $Cu \rightleftharpoons Cu(I)$ is fast and $Cu(I) \longrightarrow Cu(II)$ is slow, as proposed by Bockris et al[102,103] then:

considering (8.12.)

$$i = n F \vec{k} [\, Cu(I) \,] \qquad (8.14.)$$

and

$$E = E^{o} + \frac{RT}{nF} \frac{[Cu(I)]}{[Cu]} \qquad (8.15.)$$

$$[Cu(I)] = [Cu] \exp \frac{F (E - E^{o})}{RT}$$

let

$$E - E^{o} = \eta$$

then

$$[\, Cu(I) \,] = [Cu] \exp \frac{F\eta}{RT} \qquad (8.16.)$$

substituting (8.16.) in (8.14.)

$$i = n \vec{k} F \ [Cu] \ \exp \frac{F\eta}{RT}$$

$$= n F \vec{k}_o \exp \frac{(1-\alpha) F \eta}{RT} \ [Cu] \ \exp \frac{F\eta}{RT}$$

$$= n F \vec{k}_o \ [Cu] \ \exp \frac{(2-\alpha) F \eta}{RT}$$

$$\therefore \quad \frac{\partial \log i}{\partial \eta} = \frac{F(2-\alpha)}{RT}$$

$$= \frac{2-\alpha}{60} = \frac{1}{75} \text{ mV}$$

i.e. $\underline{\alpha = 1.2}$

This is an impossible value of α and hence this mechanism must be incorrect

Considering (8.13.)

$$i = n F \vec{k} \ [Cu] \qquad (8.17.)$$

$$= n F \ [Cu] \ \vec{k}_o \ \exp \frac{(1-\alpha) F \eta}{RT}$$

$$\therefore \quad \frac{\partial \log i}{\partial \eta} = \frac{(1-\alpha) F}{RT}$$

$$= \frac{1-\alpha}{60} = \frac{1-}{75} \text{ mV}$$

i.e. $\underline{\alpha = 0.2}$

Application of the method of Lovrecek[104], as considered by Wright[105], to the Tafel slopes leads to the same conclusion.

Figure 42 shows the dependence of i_∞ on the hydroxide concentration. From this plot it can be seen that the order of the reaction with respect to $[OH^-]$ is unity.

The electrode reaction is therefore

$$Cu \underset{\text{slow}}{\longrightarrow} Cu(I) \underset{\text{fast}}{\longrightarrow} Cu^{Cu(II)}(II)$$

where the slow step Cu → Cu(I) involves a single hydroxide ion and may be

$$Cu + OH^- \longrightarrow Cu(OH) + e \qquad (8.18.)$$

followed by:

$$Cu(OH) \longrightarrow Cu(OH)^+ + e \qquad (8.19.)$$

$Cu(OH)^+$ being a likely product due to its high stability constant.

8.4. Galvanostatic Measurements

8.4. (i) Experimental This technique has been fully discussed in section 3.2. (iv). The electrolytic cell was of the type shown in Figure 4(b) and the electrolyte was exhaustively purified by pumping through the purification arm. All of the electrodes were pure copper wire and their construction has been described in

FIG 43 Typical Tafel plot

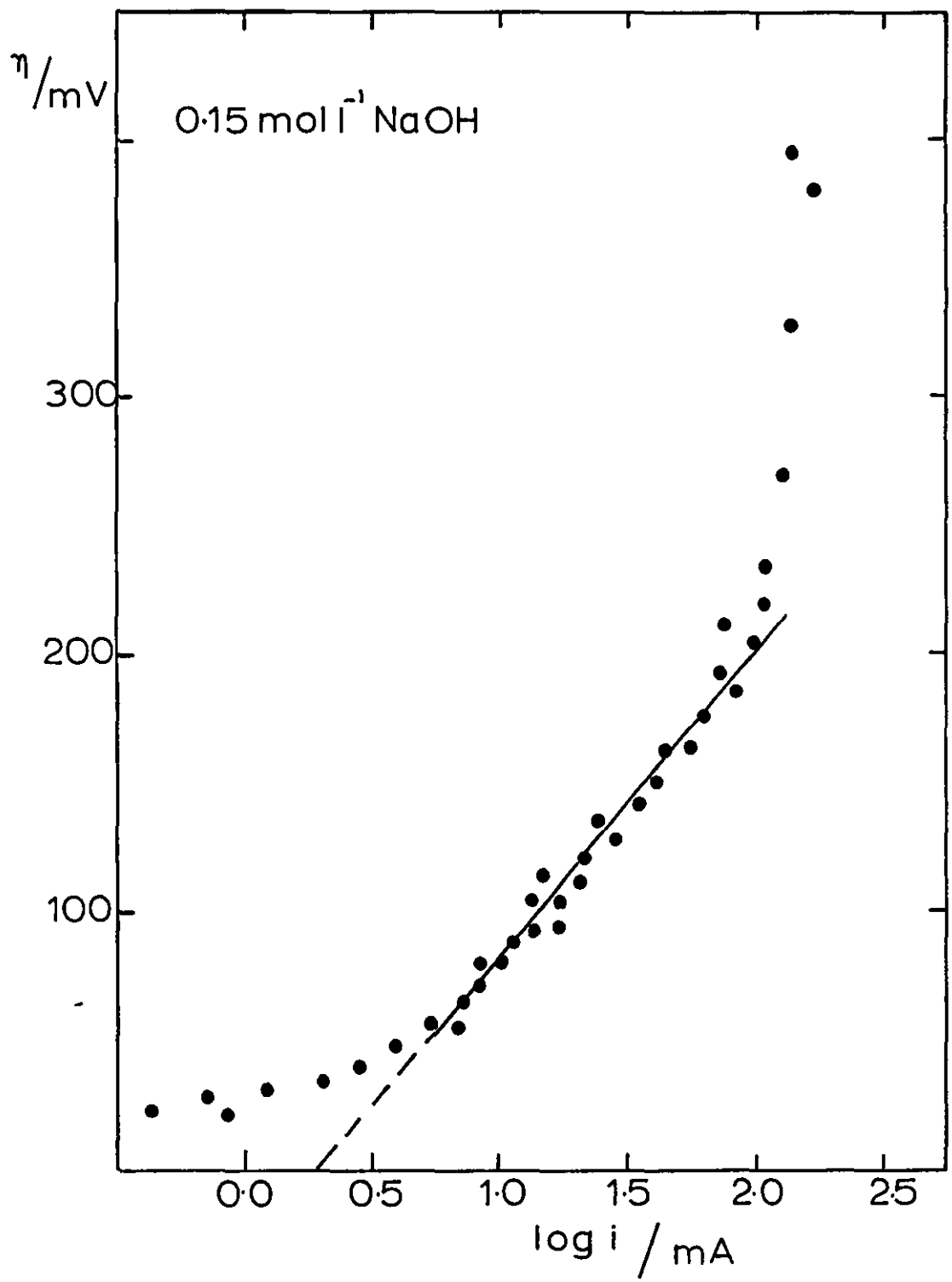

FIG 44 Dependence of i_o on T^{-1}

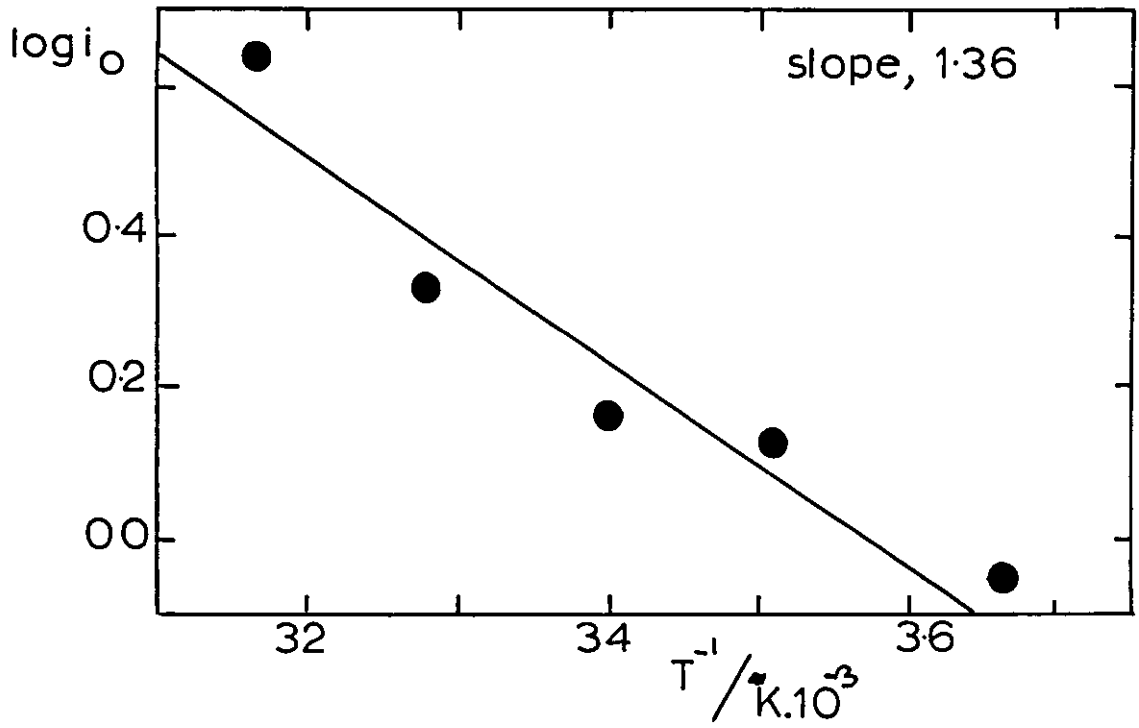

FIG 45 Dependence of i_o on $[OH^-]$

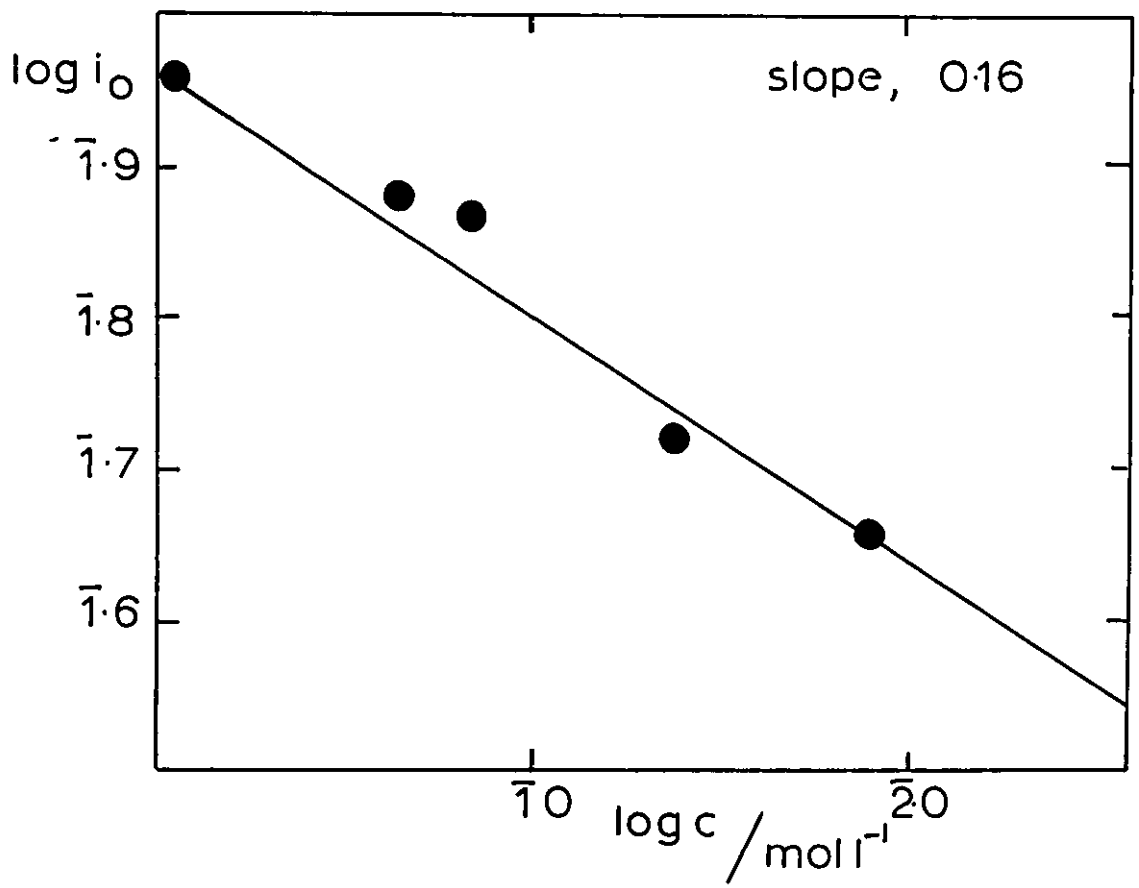

section 3.1. (i). The pretreatment of the test electrode was that described for the L.S.V. measurements in section 8.2. (i). All of the measurements were made against a copper reference electrode that was at a potential of - 0.295 V against a saturated calomel electrode i.e. - 0.047 V (n.h.e.).

8.4. (ii) Results A series of experiments were carried out to obtain η/i data at various electrolyte concentrations and at a range of temperatures. A typical Tafel plot for the system at a fixed electrolyte concentration and temperature is shown in Figure 43. The intercept of the straight line portion of this plot with the log i axis (η = O) gives a value of the exchange current, i_o. The Tafel slopes of these plots were found to be 50 - 80 mV/decade. The variation of i_o with temperature is shown in Figure 44 where an Arhenius plot of log i_o vs 1/T is shown. From the slope of this graph a value of the enthalpy of activation, ΔH, was calculated to be 27 $\pm$ 4 K.J mol^{-1}. The variation of i_o with the electrolyte concentration is shown in Figure 45, where log i_o is plotted against log $[OH^-]$

8.4. (iii) Discussion The slopes of the Tafel plots were found to vary between 50 to 80 mV/decade for different electrolyte concentrations and temperatures. These values are higher than those found by Brown and Thirsk[106], who found that the anodic Tafel slopes in the deposition of copper from cupric sulphate solutions were in the range 40 - 50 mV. These results largely duplicated those of Bockris et al[102] who found anodic Tafel slopes of 40 mV for their galvanostatic measurements

on the same system. The values reported here are however in agreement with those found in the potentiostatic experiments using a rotating disc electrode where a value of 75 $\pm$ 5 mV/decade was observed.

The value of ΔH was found to be 27 $\pm$ 4 K.J. mol^{-1}. This value is somewhat low for a pure charge transfer reaction where a value of $\sim$ 40 K.J. mol^{-1} would be expected. This suggests that the reaction involves adsorbed species, the heat of adsorption lowering the activation enthalpy to 27 K.J. mol^{-1}.

The electrode reaction has been shown to be

$$Cu \xrightarrow[\text{slow}]{} Cu(I) \underset{\text{fast}}{\rightleftharpoons} Cu(II)$$

Now $$i = \overrightarrow{i} - \overleftarrow{i} \qquad (8.20.)$$

where $$\overrightarrow{i} = n F \overrightarrow{k} [Cu] \exp\left[\frac{(1-\alpha) F (E - E^{o})}{RT}\right] \qquad (8.21.)$$

and $$\overleftarrow{i} = n F \overleftarrow{k} [Cu(I)] \exp\left[\frac{-\alpha F (E - E^{o})}{RT}\right]$$

$$[Cu(I)] = [Cu(II)] \exp - \left[\frac{F (E - E^{o})}{RT}\right]$$

$$\therefore \quad \overleftarrow{i} = n F \overleftarrow{k} [Cu(II)] \exp\left[\frac{-(1+\alpha) F (E - E^{o})}{RT}\right] \qquad (8.22.)$$

At the equilibrium potential, E^{o}, $\overrightarrow{i} = \overleftarrow{i} = i_{o}$

$$\therefore \quad i_o = n F \vec{k} [Cu] \exp\left[\frac{(1-\alpha) F E^e}{RT}\right] = n F \overleftarrow{k} \; Cu(II) \; \exp\left[\frac{-(1+\alpha) F E^e}{RT}\right] \qquad (8.23.)$$

For the general case $O + ne \longrightarrow R$

$$i_o = n F k_1^o C_o^o \exp\left[-\frac{\alpha n F E^e}{RT}\right] = n F k_2^o C_R^o \exp\left[\frac{(1-\alpha) n F E^e}{RT}\right]$$

and $$i_o = n F k^o (C_o^o)^{1-\alpha} (C_R^o)^{\alpha}$$

In the above case:

$$i_o = n F k^o [Cu]^{\frac{(1-\alpha)}{2}} [OH^-]^{\frac{(1-\alpha)}{2}} [Cu(II)]^{\frac{(1+\alpha)}{2}}$$

Now we have the further reaction:

$$Cu(II) + OH^- \rightleftharpoons Cu(OH)_2$$

hence

$$[Cu(II)] = \frac{1}{K} \frac{[Cu(OH)_2]}{[OH^-]}$$

$$\therefore \quad i_o = n F k^o [Cu]^{\frac{(1-\alpha)}{2}} [OH^-]^{\frac{(1-\alpha)}{2}} \times \frac{[Cu(OH)_2]^{\frac{(1+\alpha)}{2}}}{K \; OH^{-\frac{(1+\alpha)}{2}}} \qquad (8.24.)$$

$$\frac{a \log i_o}{a \log [OH^-]} = \frac{(1-\alpha)}{2} - \frac{(1+\alpha)}{2}$$

$$= \underline{\underline{-\alpha}}$$

Examination of Figure 45 shows that the experimental value of $\partial \log i_o / \partial \log [OH^-]$ is ~ 0.2, which is in disagreement with the above theory. It is possible that the order of reaction indicated by the r.d.e. experiments is in error so that the exchange current dependency corresponds to a value of 2_α, which although it is not in agreement of the observed value it is at least of the correct sign. However, a critical examination of the accuracy of these experiments did not reveal any obvious shortcomings. On the other hand the exchange current studies depend on a constant concentration of copper throughout the experimental range of $[OH^-]$. This necessitates a constant low concentration of copper in solution so that the most dilute solution would remain unsaturated with Cu^{+2}. Analysis before and after experimental runs showed that this condition was rarely achieved and it is quite likely that with the presence of adsorption the constancy of Cu^{+2} at the interphase was never achieved.

8.5. Constant Potential Measurements

8.5. (i) Experimental Preparations were carried out to produce the various copper oxide films so that an examination of their crystal structure, using a stereoscanning technique, could be carried out. The electrolytic cell was of the type shown in Figure 5(c). The test electrode has been described in section 3.(ii) The counter electrode was of copper wire and the reference electrode was a saturated calomel electrode.

FIG 46 Electrode films

Cu (1)

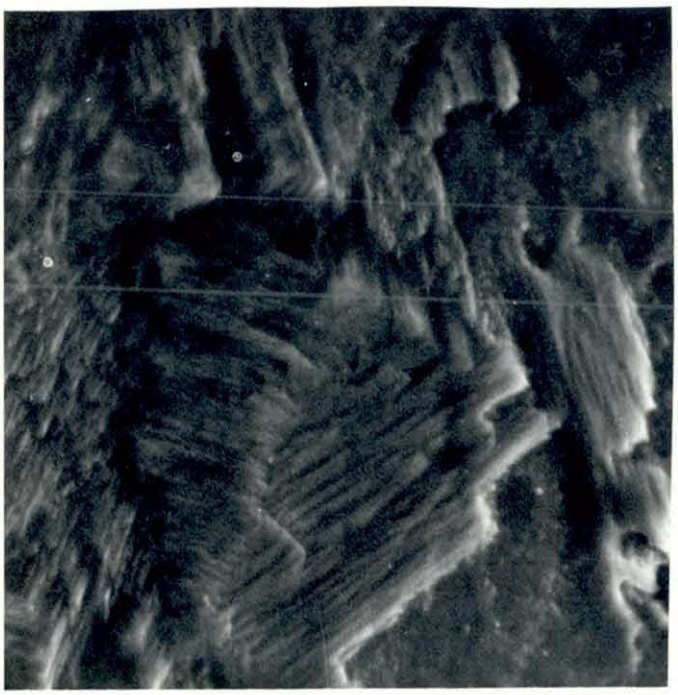

Cu (11)

x 5,000

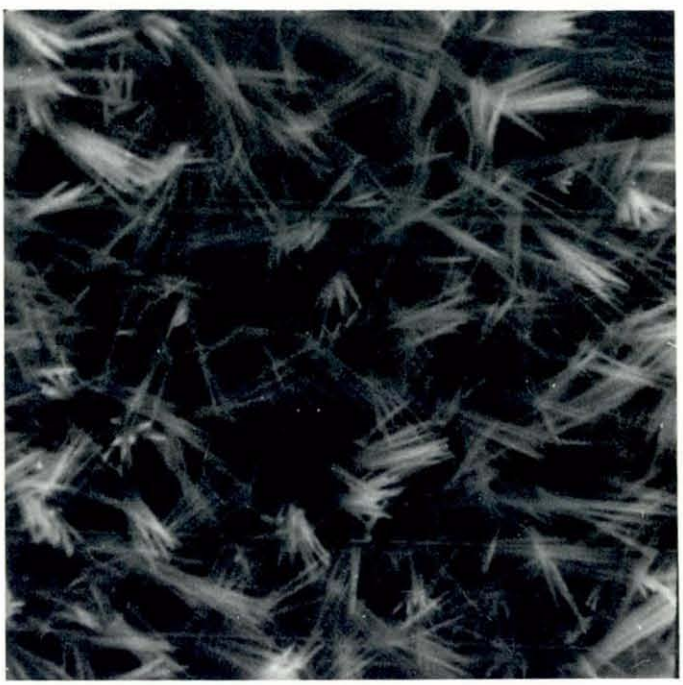

8.5. (ii) Results Photographs of the electrode surface obtained by this technique are shown in Figure 46, for Cu(I) and Cu(II) oxide films on the electrode.

8.5. (iii) Discussion The two electrochemically produced copper oxide films differ considerably in their crystalline shape. The cuprous oxide appears to form plate-like crystals. The surface being completely covered with this oxide and there were areas where the crystal plates are stacked one upon the other (see Figure 46). The cupric oxide forms needle-like crystals that grow out from the electrode surface. The electrode surface was again found to be completely covered by this crystalline growth, that appeared to extend in some depth, since adjustments made to the focus controls brought further crystals into focus, that were present at a greater depth.

CHAPTER 9

THE OXIDATION OF α-AMINO ACIDS AT COPPER ANODES

9.1. Experimental

All the experimental conditions of the various techniques used in this investigation have been described previously in the relevant sections.

9.2. Results

9.2. (i) Differential capacitance measurements A typical double layer capacitance curve, for the system Cu $|OH^-$, in the potential region between h.e.r. and Cu(I) oxide formation, is shown in Figure 47 (a). Figure 47(b) shows the effect of adding α-alanine to the electrode/electrolyte system.

9.2. (ii) Linear sweep voltammetric measurements A typical current/potential curve, corresponding to the application of a linear potential gradient to a polished etched copper electrode, initially at equilibrium with sodium hydroxide electrolyte, is shown in Figure 48(a). Figure 48(b) shows the effect of the addition of an α-amino acid to the same system under otherwise identical conditions.

Figure 49, 50 and 51 show the dependence of the reaction peak currents upon the α-amino acid concentration, for all four of the reaction peaks indicated in Figure 48(b), at a constant base electrolyte concentration and a constant sweeping rate.

FIG 47 Differential capacitance curve for Cu|OH,∝alanine

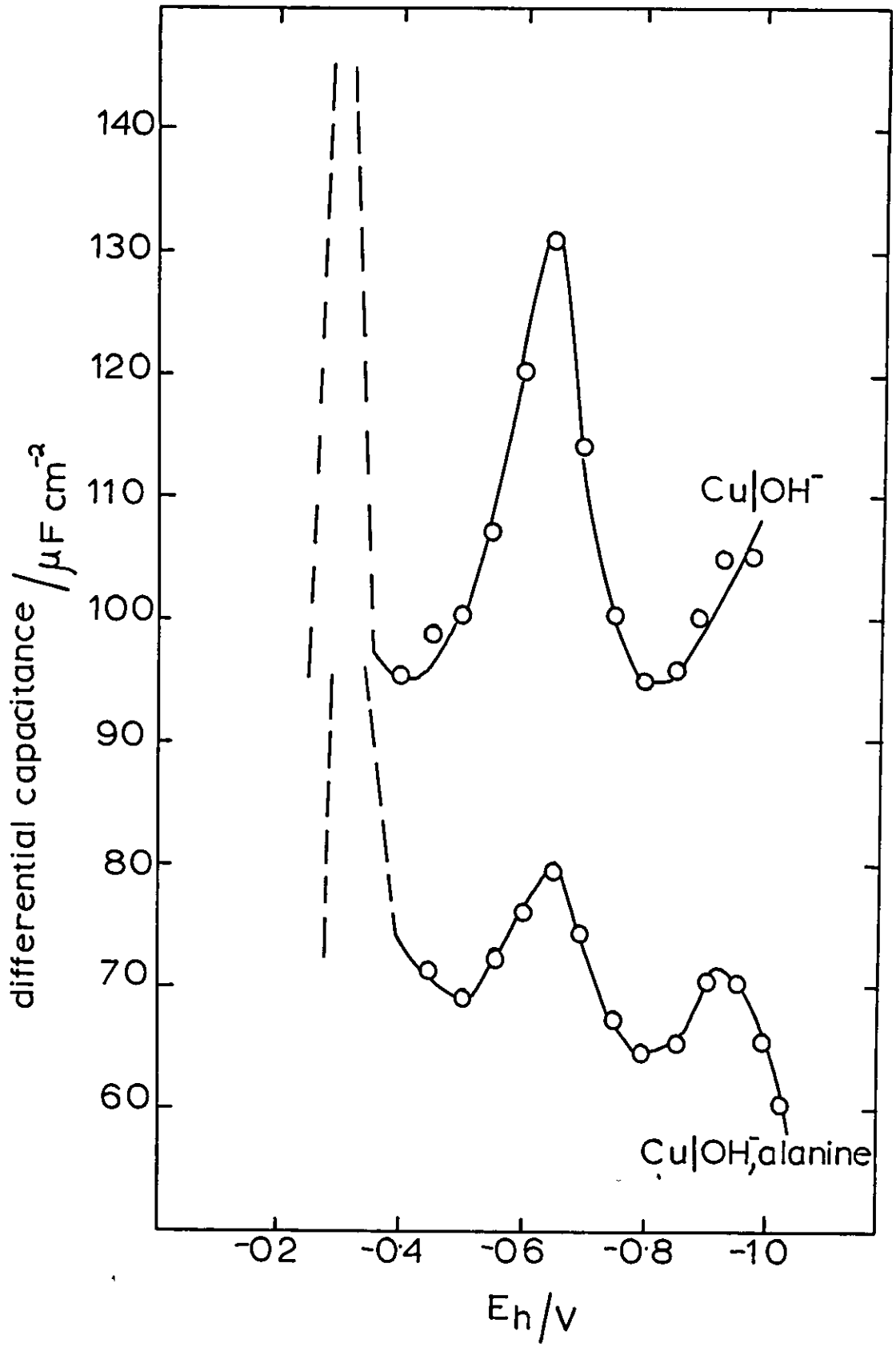

FIG 48 L.S.V. curves for (a) Cu|OH

(b) Cu|OH, alanine

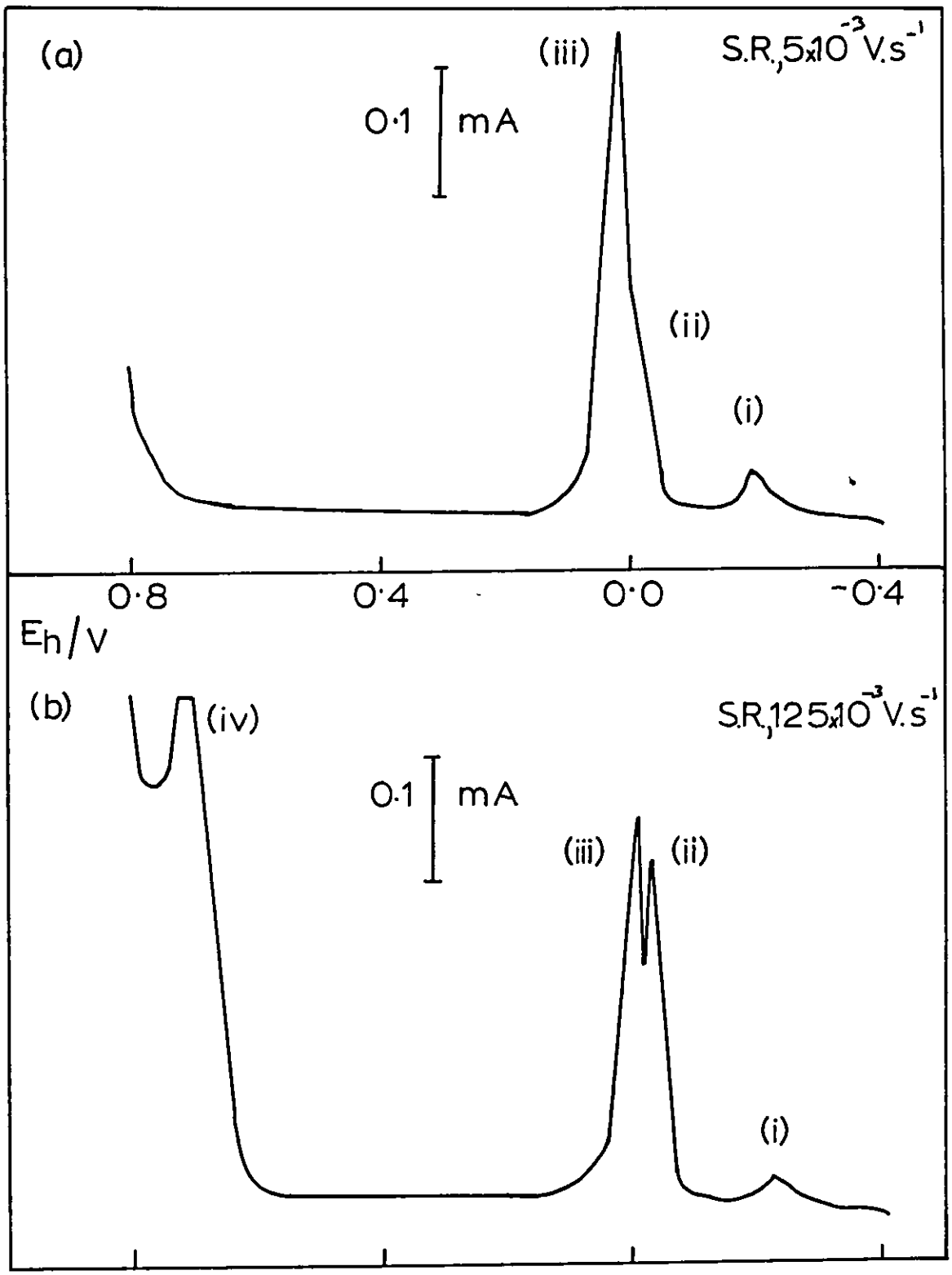

FIG 49 Dependence of i_p on [amino acid] for peak (i)

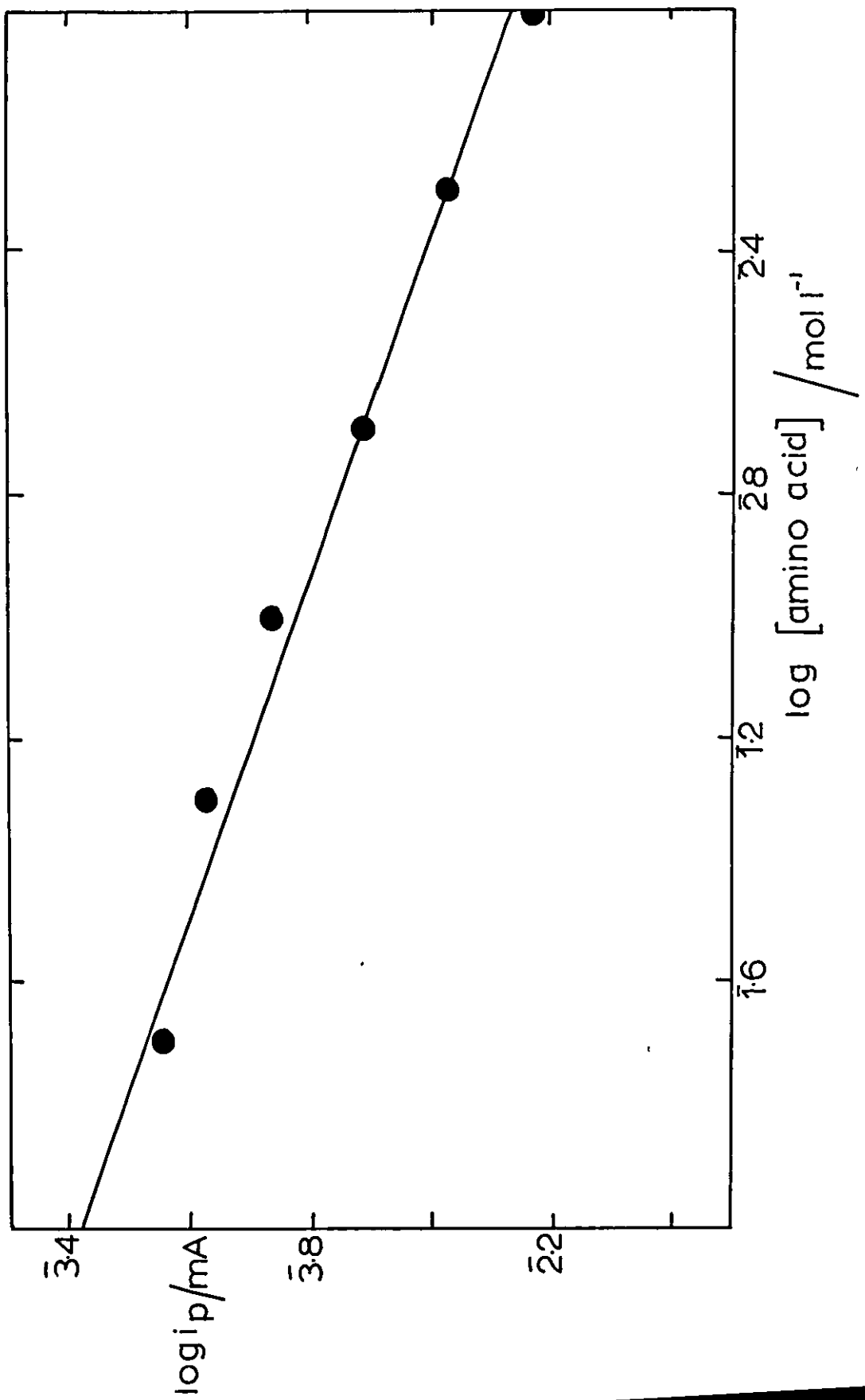

FIG 50 Dependence of i_p on [amino acid]

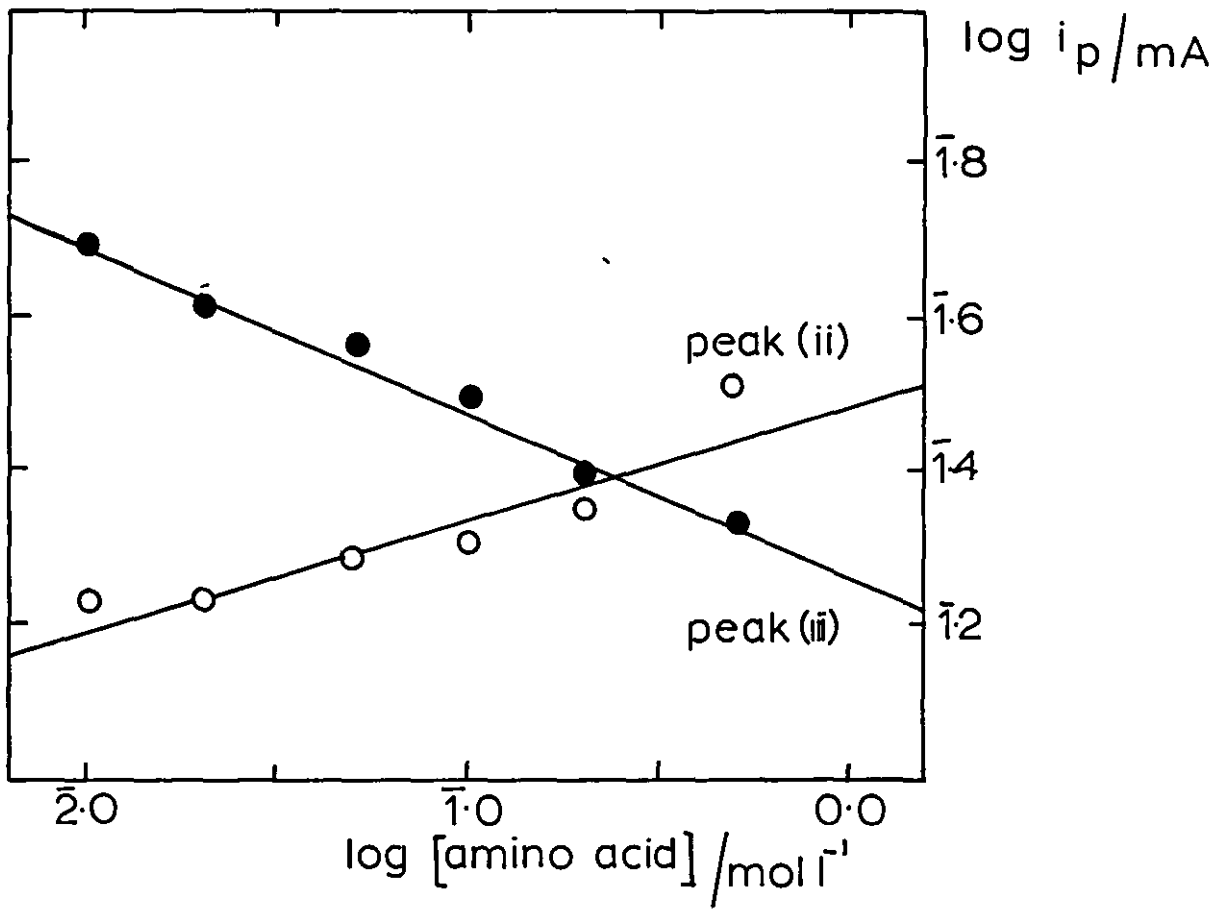

FIG 51 Dependence of i_p on [amino acid]

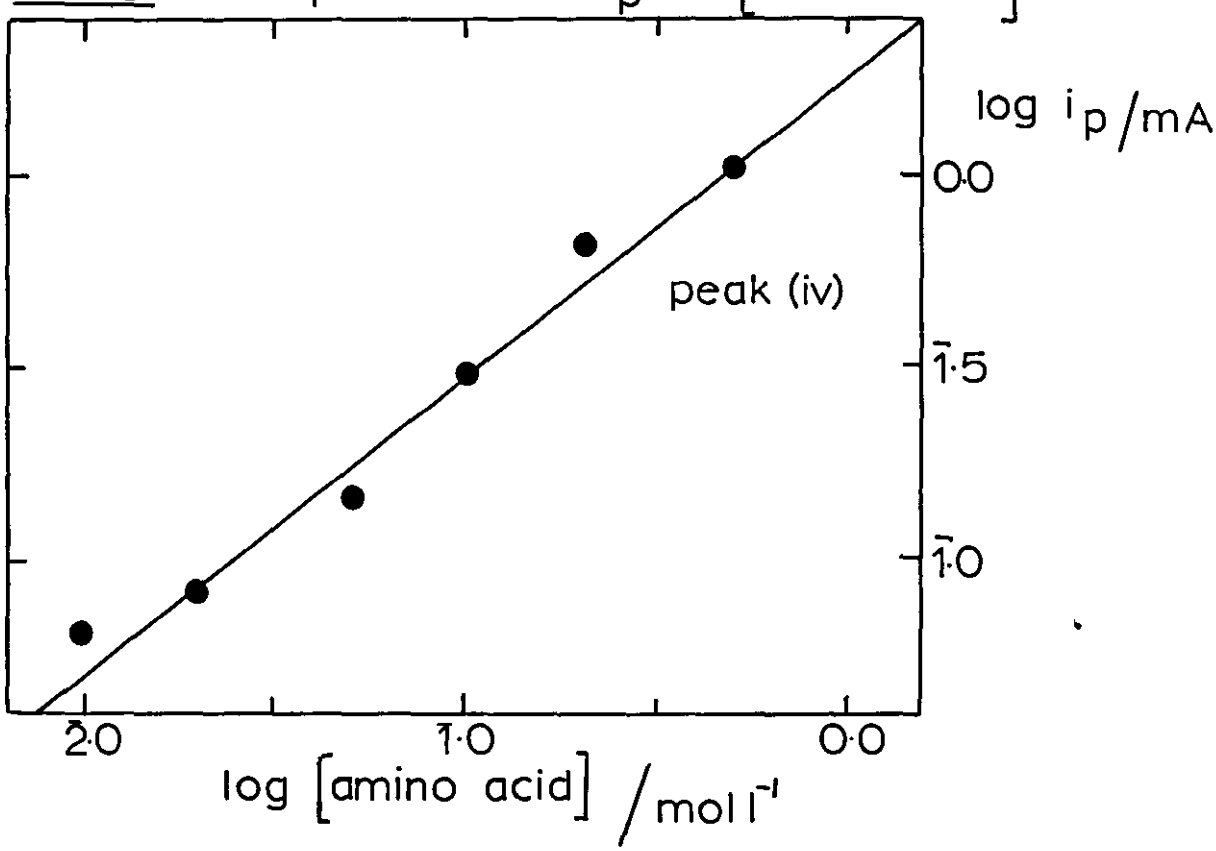

The effect of changing the sweep rate on the reaction peak heights of reactions (ii) and (iv) is shown in Figures 52 and 53. The data are shown for a series of α-amino acid concentrations. The peak current for the reaction due to the α-amino acid, in the case of reaction (ii), were obtained by subtracting the peak current of the reaction in the absence of the α-amino acid from the total reaction current, for each of the sweep rate determinations.

9.2. (iii) Constant potential measurements The most significant electrode reaction of α-amino acids at copper electrodes occurs in the potential region prior to oxygen evolution, hence preparative oxidations were carried out in this potential region. Two types of electrodes were used in these preparative experiment. The first was a clean and etched copper electrode; the second electrode was prepared in the same manner and then subjected to a slow potential sweep in a cell containing the base electrolyte. The major organic reaction occurred in a potential region more positive than that corresponding to the system Cu|Cu(II) oxide $|OH^-$, hence, where as the first type of electrode was covered by a "thin" oxide film (not visible with the naked eye, but readily detected by electron microscopy), the sweeping process produced a "thick" oxide film (visible with the naked eye). A summary of the oxidations using both "thick" and "thin" oxide covered electrodes, for a series of α-amino acids, is shown in Table 10.

FIG 52 Dependence of peak current on $(S.R)^{1/2}$ for organic reaction at peak (ii) potential at different [alanine]

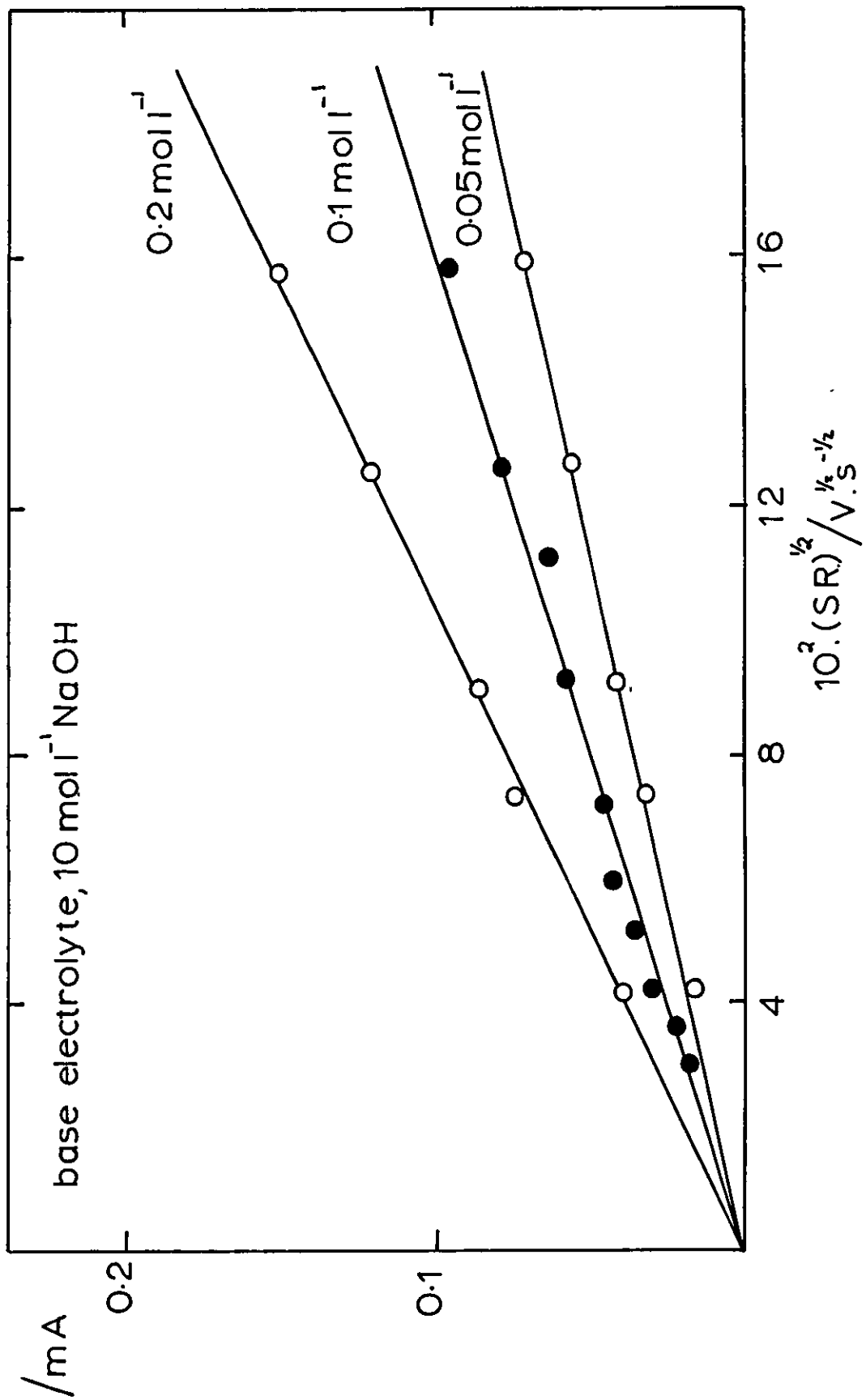

FIG 53 Dependence of i_p on $(S.R)^{1/2}$ for peak (iv)

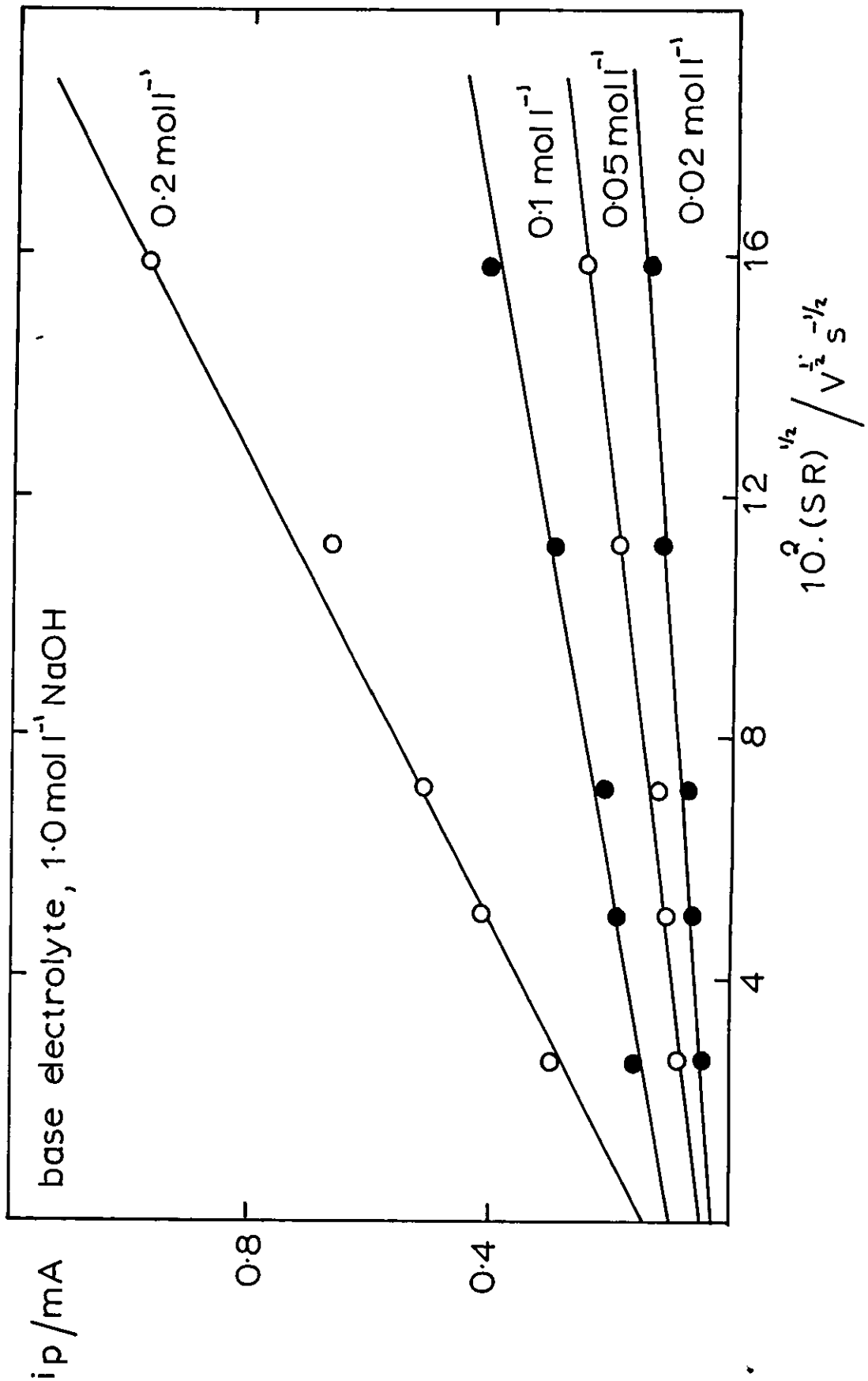

TABLE 10 Products of electrochemical oxidations at Cu electrodes.

Supporting electrolyte 1.0 mol l^{-1} NaOH, 0.75 V (n.h.e.),

2 hrs., electrode area ~ 6.0 cm^2, α-amino acid ~ 0.1 mol l^{-1}

α-Amino Acid	Thick Oxide Electrode		Thin Oxide Electrode	
	Product	limiting current/mA	Product	limitingting current/mA
alanine	acetonitrile	14.0	acetonitrile	6.2
2-aminobutyric	propionitrile	9.8	propionitrile	6.0
nor-valine	butyronitrile	9.0	butyronitrile	4.8
valine	isobutyronitrile	6.8	isobutyronitrile	3.0
nor.-leucine	valeronitrile	6.8	valeronitrile	4.2
leucine	isovaleronitrile	6.2	isovaleronitrile	2.2
iso-leucine	2-me-butyro-nitrile	5.6	2-me-butyro-nitrile	1.6
phenylglycine	benzonitrile	15.0	benzonitrile benzaldehyde	2.9

9.2. (iv) Rotating electrode measurements The effect of the addition of an α-amino acid to the electrode/electrolyte system upon the potentiodynamic/current curves is shown in Figure 54. It can be seen from this diagram that there is an additional reaction peak compared to the corresponding curve in the absence of the α-amino acid. The major electrode reaction in the case of a rotating electrode is the reaction that occurs ~ 0.0 V (n.h.e.). This is in contrast to the similar stationary electrode system, where the major reaction occurs at potentials slightly negative

FIG 54 L.S.V. curve for Cu|OH, alanine

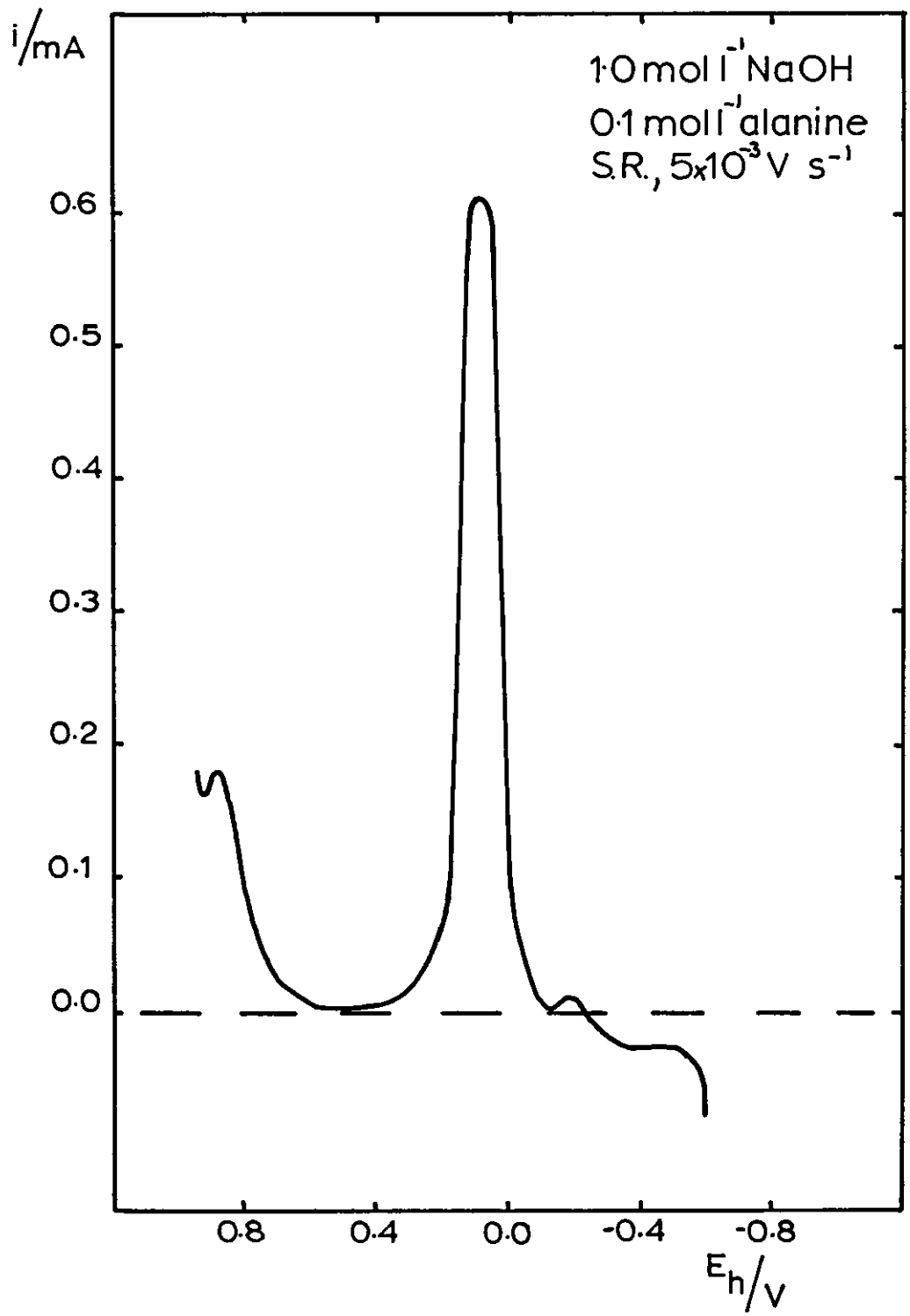

of that of the oxygen evolution reaction. The variation of the three reaction peak heights with rotation speed is shown in Figure 55.

Preparative oxidation of α-amino acid at a rotating copper electrode in sodium hydroxide base electrolyte were carried out and the results of these experiments are shown in Table 11. These oxidations were carried out at the Cu(II) and Cu(III) reaction peak potentials of 0.038 and 0.750 V (n.h.e.) respectively.

TABLE 11 Oxidation of α -amino acids at rotating Cu electrodes. Supporting electrolyte 1.0 mol l^{-} NaOH, 2 hrs, electrode area 5.0 cm^2

Potential	α -amino acid	Product
0.038 V (n.h.e.)	0.05 mol l^{-1} valine	no product
0.038 V (n.h.e.)	0.05 mol l^{-1} phenylglycine	no product
0.750 V (n.h.e.)	0.05 mol l^{-1} phenylglycine	benzonitrile benzaldehyde

The difference of the two types of electrodes that were used are best seen by the use of stereoscan microscopy. Figure 56 shows the electrode surface of an oxide film grown at 0.75 V, in the presence of valine (0.05 mol l^{-1}). This is equivalent to the electrode surface of a "thin" oxide electrode used in the preparative oxidations. The electrode surface of a "thick" oxide electrode was found to be the same as that shown in Figure 46(b).

FIG 55 Variation of i_m^{-1} with $\omega^{-1/2}$

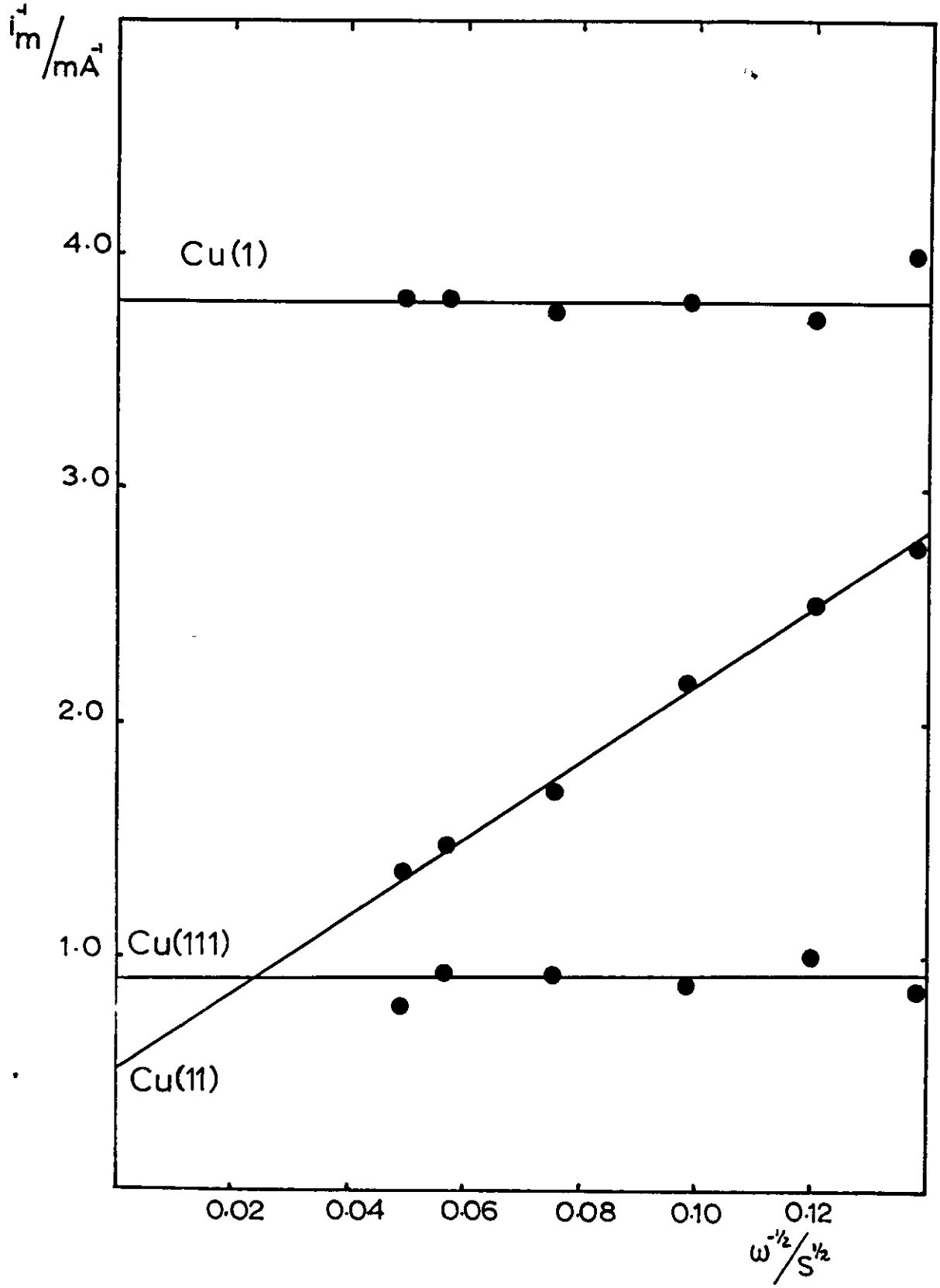

FIG 56 Thin oxide layer electrode

x 5,000

9.3. Discussion

9.3. (i) Differential capacitance measurements The differential capacitance curves for solutions containing an α-amino acid (see Figure 47) show a capacitance peak that is absent in the α-amino acid free system. This peak represents an electrode process (occurring at ~ 0.95 V (n.h.e.))in the same potential region as the desorption and evolution of hydrogen from the copper electrode in the absence of the organic molecule. The additional process is considered to result from the adsorption of the α-amino acid on the copper electrode since no complementary current flow could be ascribed to the occurrence of a faradaic reaction. The reduction in magnitude of the electrode capacitance in the presence of the α-amino acid tend to confirm the presence of an adsorbed layer at the electrode throughout the experimentally polarizable region. Since copper α-amino acid salts are quite stable it is not likely that the α-amino acid is desorbed at potentials more positive than the copper lattice dissolution potential.

9.3. (ii) Potentiodynamic measurements The effect of the addition of an α-amino acid upon the reactions occurring at a copper electrode in alkaline solutions can be seen in Figure 48. The most noticeable differences are that there are now four distinct electrode reaction peaks in the potential/current curves of the system containing the α-amino acid. This is a result of a better resolution of reaction peaks (ii) and (iii) in the electrode/electrolyte system containing the α-amino acid.

The most prominent of the electrochemical processes is represented by reaction peak (iv), occurring at potentials slightly negative to that of the oxygen evolution reaction. Not only is this the most significant of all the electrochemical processes indicated by these curves, but it also appears in a potential region devoid of electrode reactions in the absence of the α-amino acid. Two possibilities exist for a reaction at this potential; a reaction involving a Cu(II) species at the electrode surface, or a reaction between the α-amino acid and a Cu(III) species produced by a reaction of the type:

$$2\,CuO + 2\,OH^- \longrightarrow Cu_2O_3 + H_2O + 2e \qquad (9.1.)$$

It is not possible to decide between these two alternatives from the present results, but the fact that we get a significant electrode reaction even when there is no appreciable coverage of the electrode by an oxide film indicates that the Cu(III) mechanism is the more likely.

It is interesting to note that the dependencies of the reaction heights upon the concentration of the α-amino acid differ. That is that the peak height corresponding to reaction peaks (i) and (iii) decrease with an increase in the α-amino acid concentration (see Figures 49 and 50), whereas the peak heights corresponding to reaction peaks (ii) and (iv) increase with an increase in the α-amino acid concentration (see Figures 50 and 51). In the case of reaction (iv) the variation of peak height with α-amino acid concentration is a straight line graph with a slope of approximately unity; indicating that the electrode process is first order

with respect to the α-amino acid concentration. In the case of reaction peak (i) the presence of the α-amino acid probably produces an insoluble complex at the electrode due to the interaction of the α-amino acid with the reacting copper surface. This complex layer covers the electrode surface more efficiently than the Cu(I) oxide layer, with the resultant progressive lowering of reaction peak (i) with increasing α-amino acid concentration. Formation of a $Cu(II)_{solid}$ oxide/α-amino acid complex (reaction (ii)) is produced at the expense of any other Cu(II)/α-amino acid species. This is consistent with the increase in the peak height of reaction peak (ii), with an increase in the α-amino acid concentration and the corresponding decrease in peak height of reaction peak (iii). The total Cu(II) reaction remaining approximately the same.

A more detailed examination of the processes identified by as reaction peaks (ii) and (iv), once the parasitic oxidation of the copper (rate controlled by diffusion of OH^- in the solid phase) has been taken into account in the case of reaction (ii), was carried out. Figures 52 and 53 show that at a constant hydroxide concentration the reactions appear to be diffusion controlled. An apparent diffusion coefficient, again calculated from the i_p vs $(S.R.)^{\frac{1}{2}}$ data, of both these processes is $\sim 1 \times 10^{-8}$ cm^2 s^{-1}. The diffusion coefficient of an α-amino acid in aqueous solutions would be $\sim 1 \times 10^{-5}$ cm^2 s^{-1}. It is considered therefore that the diffusion control is by the diffusion of reacting species or products through an adsorbed layer at the electrode/electrolyte interphase, not by diffusion in solution.

9.3. (iii) Constant potential measurements At the relatively high positive potential of 0.75 V (n.h.e.) the oxidation of α-amino acids proceeds with current-densities of between 1 and 3 mA cm^{-2}. The product is the corresponding nor-nitrile which is obtained with coulombic yields of greater than 90%. The only exception to this is the oxidation of phenyl glycine at a "thin oxide" layer electrode, where the oxidation products were benzonitrile and a trace (~ 1%) of benzaldehyde. The rates of these oxidations appear to be dependent on both the chain length and the degree of branching of the chain. For example the rate of oxidation of alanine is greater than that of 2-aminobutyric acid and the rate of oxidation of nor-valine is greater than that of valine.

In Chapter 6 it was suggested that the oxidation of α-amino acids at silver electrodes in alkaline electrolytes follows the reaction path

$$R\,C\,H\,(NH_2)\,Co_2^- \xrightarrow[-H^+]{-2e} R\,C\,H = N\,H \xrightarrow[-2H^+]{-2e} \underline{\underline{R\,C\,N}} \qquad (9.2.)$$

(fast)

$R\,C\,H = N\,H \xrightarrow{H_2O}$ (slow) $\underline{\underline{R\,C\,H\,O}}$

The reaction was thought to occur with the α-amino acid in an adsorbed state at the electrode. Similar behaviour at copper electrodes is substantiated by the differential capacitance measurements, discussed above, where the α-amino acid was thought to be adsorbed at the copper electrode. Since the reaction products are so

similar to those obtained at silver electrodes, (where the aldehyde was thought to be produced only by the hydrolysis of imine free in solution) it seems likely that the reaction again involves an imine intermediate and that the reaction occurs almost solely at the copper electrode/aqueous electrolyte interphase. This reflects a stronger adsorption of the α-amino acid at a copper electrode than at a silver electrode. This point is substantiated by an examination of the stability constants of the complexes of both metals with alanine, where the stability constant of the copper complex is twice that of the silver complex[107].

The system may be represented approximately as the reaction scheme:

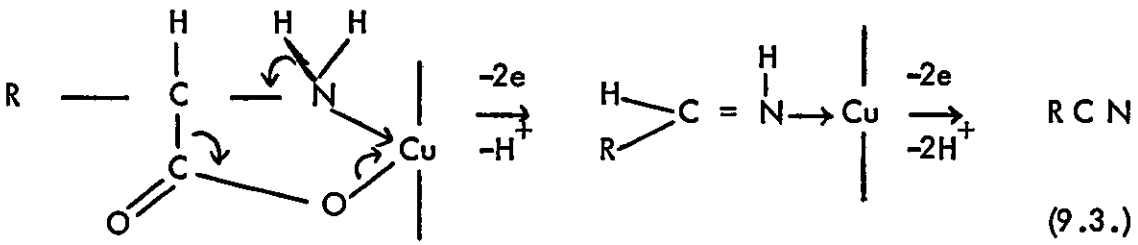

(9.3.)

Only in the case of the very bulky phenylglycine is a small amount of the imine released into the solution; the hydrolysis of which produces the trace of benzaldehyde

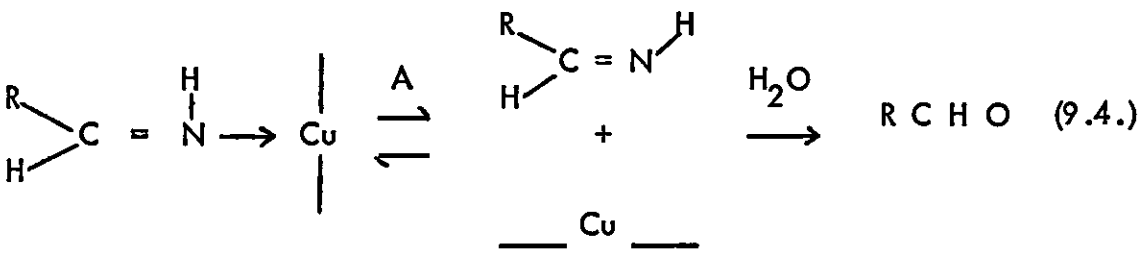

(9.4.)

Whether the removal of the imine intermediate from the electrode (A) is a slow

desorption process or a fast desorption/adsorption reaction, where the equilibrium lies very much towards the adsorbed state, is still not settled.

It is interesting to note that the presence of a thick oxide layer on the electrode markedly increases the rate of the oxidation. This possibly reflects the greater surface area available for the reaction, since the Cu(II) oxides of copper form needle-like crystals that grow from the electrode surface increasing the effective electrode area (compare Figure 46 with Figure 56).

9.3. (iv) Rotating electrode measurements A potentiodynamic/current curve, showing the reactions that occur for the system Cu|OH^-, α-amino acid at a rotating copper electrode, is shown in Figure 54. This trace shows three electrode reactions, the major reaction being the reaction at the Cu(II) oxide potential. This is in contrast to results obtained at stationary electrodes where four electrochemical reactions were observed, the major reaction being at the Cu(III) potential. The variation of these reaction peak heights with changes in the electrode rotation speed (see Figure 55) show that the Cu(I) and Cu(III) reaction peak heights remain constant with increasing rotation speed, whereas the Cu(II) reaction peak increased with a similar increase in the rotation speed of the electrode. These results indicate that whereas the Cu(I) and Cu(III) oxide/α-amino acid reactions appear to be controlled by solid phase processes, it is transport of reactants or products through the solution that is the rate controlling process for the Cu(II) oxide/α-amino acid reaction.

The products formed at the Cu(II) oxide peak potential of ~0.038 V

(n.h.e.) are most likely to be water soluble Cu(II)/α -amino acid complexes. This would explain the lack of oxidation products extracted after the preparative oxidations carried out at this potential; the complexes being more soluble in water than the ether used for the extraction of the organic products from the base electrolyte.

When the oxidative potential was increased to 0.75 V (n.h.e.) the products obtained from the oxidation of phenyl glycine were benzonitrile (98%) and benzaldehyde (2%). The ratio of these two products is the same as that found at stationary electrode. This is evidence that the mechanism for the release of the imine intermediate into the solution is a slow desorption process and not a fast desorption/adsorption process. If the latter had been true then a greater proportion of aldehyde in the oxidation product would have been expected when a rotating electrode was used; the imine being swept away into the solution before the readsorption had taken place.

CHAPTER 10

OXIDATION OF α-AMINO ACID AT OTHER ELECTRODES

10.1. Introduction

It has been shown in previous chapters (see Chapter 6 and 9) that, at both copper and silver electrodes, the electrode participates in the reaction mechanism and that α-amino acids are oxidised readily. In this present chapter a brief examination of other electrode materials, under similar experimental conditions, is considered to see to what extent this electrode participation affects the overall electrochemical oxidation. The electrodes considered are gold, platinum and PbO_2.

10.2. Previous work

Electrochemical oxidations of α-amino acids have been carried out under acidic conditions[108-114] at both Pt and PbO_2 electrodes. A summary of the relevant oxidations is shown in Table 12.

10.3. Experimental

The investigation was carried out using both linear sweep voltammetric and constant potential measurements. The experimental procedures for both of these techniques have been described in previous chapters.

TABLE 12

α -amino acid	Electrode	Medium	Products
Alanine	PbO_2	H_2SO_4	Acetaldehyde, HOAC, HCOOH CO_2 and NH_3
	PbO_2	HNO_3	HCHO and oxalic acid
Valine	PbO_2	H_2SO_4	Isobutyraldehyde and isobutyric acid
Leucine	Pt	H_2SO_4	Isovaleric acid, isovaleraldehyde isobutyric acid, acetone, HOAC HCO_2H, NH_3 and CO_2
	PbO_2	H_2SO_4	Isovaleraldehyde and isovaleric acid
	PbO_2	Na_2SO_4	Isovaleronitrile

10.4. Results

10.4. (i) Gold electrodes An anodic linear sweep trace for a gold electrode in NaOH electrolyte (1.0 mol l^{-1}) is shown in Figure 57 (a). There are three electrochemical processes, indicated by these curves, occurring in the potential range between the evolution reaction of hydrogen (~ -1.25 V (n.h.e.)) and that of oxygen (~ 1.35 V (n.h.e.)). The largest of these reactions occurred at ~ 0.85 V (n.h.e.), but even this reaction peak was extremely small (< 0.05 mA).

The effect of the addition of an α -amino acid to this electrode/elec-

FIG 57 L.S.V. curves for Au $|OH^-$, valine

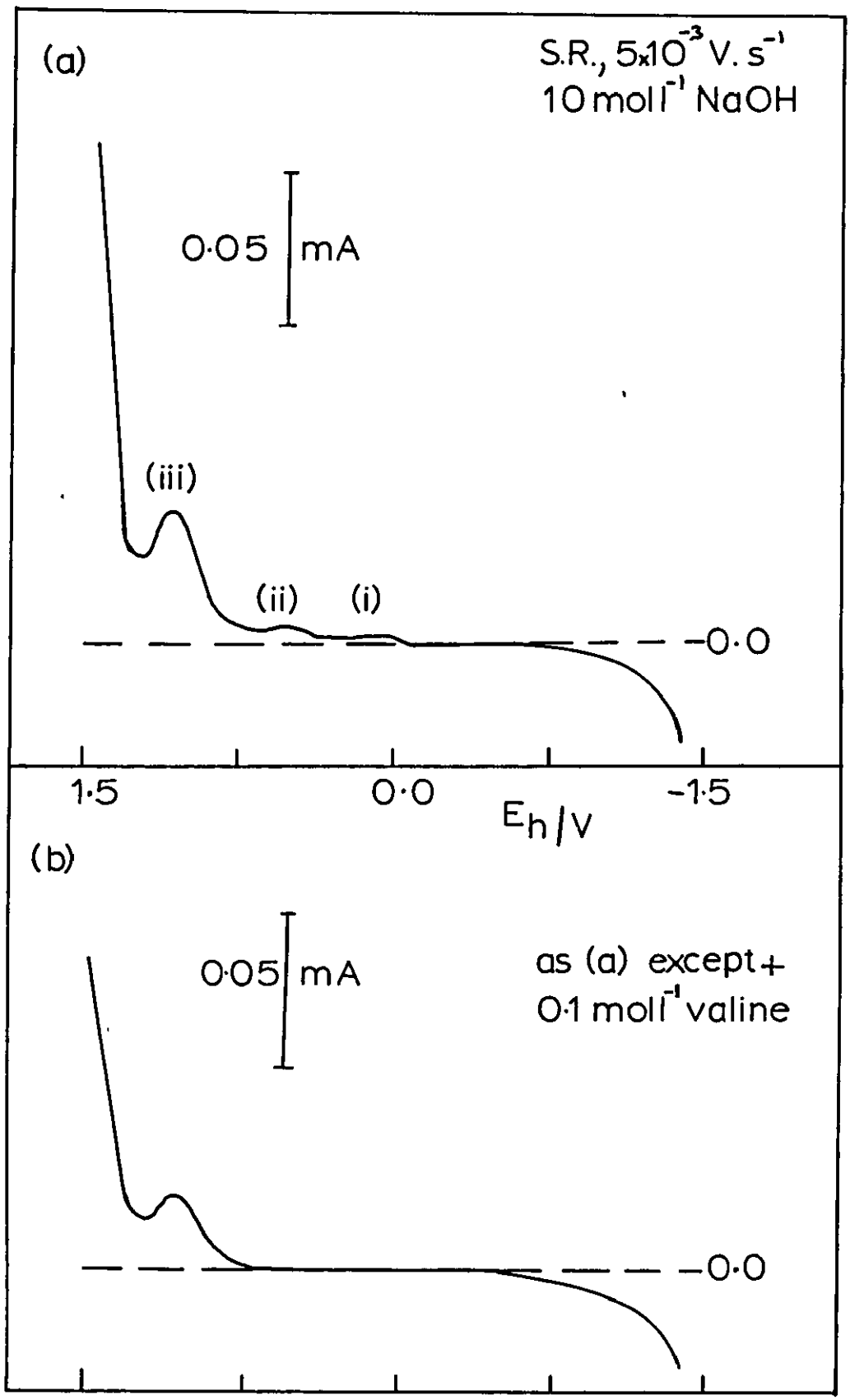

trolyte system is shown in Figure 57(b). The observed reduction of the peak/wave heights were found for all of the α-amino acids that were used in these experiments. This effect was also observed when n-butylamine was introduced into the system. The addition of n-butyric acid, however, caused an increase in the peak/wave heights. No products could be isolated from electrochemical oxidations of the α-amino acids at this peak potential (0.85 V (n.h.e.); even after 24 hours the quantaties of organic oxidation products were too small to be detected by g.l.c. analysis.

10.4. (ii) Platinum electrodes An anodic linear sweep trace for a platinum electrode in NaOH solutions (1.0 mol l^{-1}) is shown in Figure 58(a). No electrochemical processes were observed, between the potential of hydrogen evolution and that of oxygen, under the experimental conditions employed.

The addition of an α-amino acid produced a small current wave/peak at potentials slightly negative of the oxygen evolution reaction (see Figure 58 (b)). Preparative oxidations carried out at this potential yielded no products even though the potential was applied continuously for a period of 24 hours. Increasing the potential gave rise to higher cell currents (see Table 13) but even at the high positive potential of 1.25 V (n.h.e.) no oxidation products were obtained. Increasing the potential even further to 1.75 V (n.h.e.) gave rise to appreciable cell currents (~ 14.0 mA) and when an oxidation was carried out at this potential the oxidation productsiwere observed. Of these products the nor-aldehyde (50%) and the non nitrile (15%) were the two major constituents of the product mixture. The remaining

FIG 58 L.S.V. curves for Pt | OH^-, valine

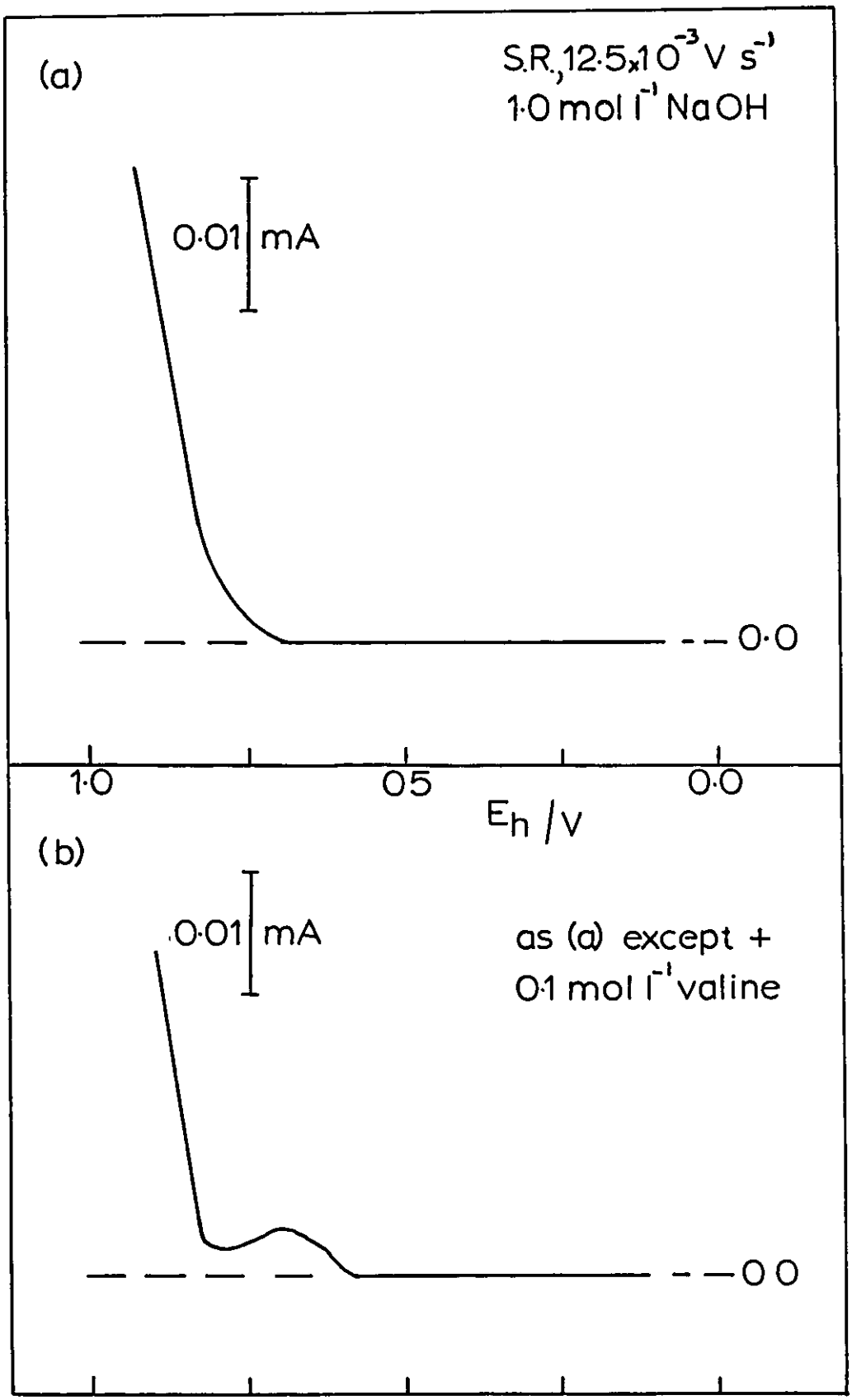

products were higher boiling compounds, possibly condensation products.

TABLE 13

Potential	Cell Current
0.75 V (n.h.e.)	< 0.001 mA
1.00 "	0.043 "
1.25 "	0.600 "
1.75 "	14.000 "

10.4. (iii) PbO_2 electrodes Preparative oxidations of α-amino acids carried out at potentials below that of the oxygen evolution reaction at PbO_2 electrodes in NaOH electrolyte (1.0 mol l^{-1}) yielded no oxidation products.

10.5. Discussion

Several investigations into the oxidation of gold electrodes in aqueous electrolytes have been made[115-123]. Considerable doubt over the identity of the various electrochemical reactions that occur is expressed by most of these workers. It seems likely that the final oxide layer produced, corresponding to reaction peak (iii), is Au_2O_3. The formation of the lower valent oxides Au_2O and AuO appear to be in doubt and reaction waves (i) and (ii) are more likely to be due to chemisorbed oxygen containing species than to the formation of these two oxides.

The addition of an α-amino acid to the Au|OH^- system has the effect of reducing the electrochemical processes corresponding to these reaction peak/waves, as shown by the decrease of the peak heights in the potential sweep trace (see Figure 57(b)). This effect is possibly due to the competition between the α-amino acid and oxygen containing species for adsorption at the electrode| electrolyte interphase. This effect was found for all the α-amino acids investigated and also for n-butylamine when it was introduced to the Au|OH^- system. It is significant that the reaction peak/wave heights increase when n-butyric acid is introduced into the same system. This may indicate that it is the formation of a Au-N bond that induces the preferential adsorption of the organic and hence the reduction of the peak heights, whereas ionic species such as $RCOO^-$ do not compete favourably with oxygen containing species for adsorption. The enhanced peak heights in the case of butyric acid is probably due to the oxidation of the n-butyrate in the solution.

The unsuccessful oxidations of α-amino acids carried out at Au, Pt and PbO_2 electrodes, at potentials below the corresponding oxygen evolution reactions, demonstrates the importance of the choice of electrode material in electrochemical oxidations of organic molecules. The oxidation of α-amino acids at a Pt electrode at 1.75 V (n.h.e.) produced at least ten reaction products, the nor aldehyde and nor nitrile being identified, but the remainder of the product mixture being of higher boiling compounds. This demonstrates the lack of specificity obtained at electrodes where the electrode material only acts a a source or

sink of electrons for an electro-organic reaction. The higher boiling reaction products from the Pt electrode oxidation may arise by free radical or "nascent" oxygen oxidations under these more severe conditions. The nascent oxygen oxidation seems to be the most likely of these alternatives since at platinum electrodes carboxylate ions are not oxidised at an appreciable rate at potentials below 2.0 V (n.h.e.).

CHAPTER 11

FINAL DISCUSSION

In the previous chapters it has been shown that the nature of the electrode material used for the oxidation of α-amino acids considerably influences the electro-organic reaction. At electrodes such as Pt, Au and PbO_2 no significant reaction, with α-amino acids, was observed at potentials below 1.0 V (n.h.e.), whereas coulombic yields of the nor-nitrile were obtained using copper and silver anodes.

A possible explanation of this behaviour is that inert electrodes such as Pt and Au do not take any specific part in the electrode reaction and this causes their apparent unreactivity. The role of such electrodes in electro-organic reactions is to act simply as a source or sink of electrons for the reaction involving the organic molecule. In the case of the silver and copper electrodes, where the electrode metal is directly involved in the reaction, oxidations of α-amino acids occur readily. An interesting comparison is the oxidation of organic compounds by metal ions such as Mn^{+3} and Co^{+3} where certain organic oxidations occur rapidly, providing that the metal ion acts in such a way that cyclic intermediates are formed.

It is interesting to note that the major electro-organic oxidations at silver and copper anodes occur at potentials at which the relevant oxides (e.g. AgO) are formed at the electrode. That is that the electro-organic oxid-

ations appear to occur most readily when oxide crystal sites are being formed on the electrode surface. A similar effect has been noted by Fleischmann et al[124] with the oxidation of organic compounds at nickel anodes. The oxidation of a range of organic compounds, at nickel anodes in aqueous alkaline solutions, have been studied and the conversion of primary amines, primary alcohols and secondary alcohols to the corresponding nitrile, carboxylic acid and ketone respectively have been reported. Most of the organic compounds oxidised by these workers were found to participate in the oxidation reaction at the same potential the potential at which the nickel anode was itself undergoing oxidation. The proposed mechanism for these oxidations was:

$$OH^- + Ni(OH)_2 \underset{}{\overset{-e}{\rightleftharpoons}} NiO(OH) + H_2O \qquad (11.1.)$$

$$NiO(OH) + \text{organic} \xrightarrow[\text{rate determining}]{\text{slow}} Ni(OH)_2 + \text{intermediate} \qquad (11.2.)$$

$$\text{Intermediate} \xrightarrow[\text{fast}]{-(n-1)e^-} \text{product} \qquad (11.3.)$$

Suitable electrode conditions for these specific electro-organic reactions appear to be a reactive electrode material at potentials at which oxide formation is occurring on the electrode surface. The formation of a higher valent oxide being necessary for a selective oxidation although complex formation does take place at potentials corresponding to the oxidation of the electrode to lower valent oxides (e.g. Cu_2O and Ag_2O).

The mechanism by which electrochemical oxide phase formation takes place have been much discussed. Mueller[125] seems to have been amongst the first to suggest that an initial film may be produced by a dissolution-precipitation process, the metal dissolving until a critical concentration, C^*, is reached in the vicinity of the anode, at which point precipitation takes place and the metal surface is blocked. The metal can dissolve as the metal cation or as a complexed species which means that homogeneous reactions may play a part. The metal dissolution may be totally irreversible, as in the case of most transition metals, or it may be reversible to some extent (e.g. Ag and Zn). It is assumed that mass transport of the metal cation within the electrode and of the anodic species X^{n-} to the electrode surface is unimportant. The concentration C* will generally be in excess of that thermodynamically in equilibrium with the precipitated material because of the need for super saturation before precipitation can occur. The precipitate is assumed to form at some plane close to the electrode surface causing the rate of the dissolution reaction to be lowered. It should be noted that the nuclei of the precipitated material will always be three-dimensional so that this mechanism cannot be expected to lead to mono-molecular films. It should also be noted that the precipitate will form near to the electrode surface but not on it. The ferm near should probably be taken to mean a distance that is considerably greater than the thickness of the electrode double layer.

An alternative mode of production of the oxide film at the electrode surface involves a solid state reaction. Anions from the electrolyte (e.g. O^{-2} or

OH^- in the above experiments) react with the metal directly without the metal cation entering the solution. This is analogous to the gas phase oxidation of metals. In this situation when a certain anodic potential is exceeded a film starts to form on the metal surface through the direct attack of the anion on the metal. At short times this film is non-uniform, consisting of discrete nuclei which may be two-dimensional or three-dimensional in nature. At longer times these nuclei coalesce to form a continuous film that may vary in thickness from one monolayer to several thousands of monolayers.

In the oxidation of silver and copper anodes in alkaline solutions the following reactions have been shown to be controlled by solid phase diffusion:

$$2Ag + 2OH^- \longrightarrow Ag_2O + H_2O + 2e \qquad (11.4.)$$

$$Ag_2O + 2OH^- \longrightarrow 2AgO + H_2O + 2e \qquad (11.5.)$$

$$2Cu + 2OH^- \longrightarrow Cu_2O + H_2O + 2e \qquad (11.6.)$$

$$Cu + 2OH^- \longrightarrow CuO + H_2O + 2e \qquad (11.7.)$$

These processes are most likely to have been controlled by electro crystallisation involving a solid state process of nucleation followed by the lateral growth of these nuclei. The other reaction that was investigated was:-

$$Cu + 2OH^- \longrightarrow Cu(OH)_2 + 2e \qquad (11.8.)$$

and it is concluded that the mechanism for the formation of a film of this oxide was by a dissolution-precipitation process.

The metal/metal oxide electrodes can participate in electro-organic reactions by two distinct modes of action. The first of these is the chemical oxidation of the organic molecule by electro chemically formed metal oxide. This type of electrochemical oxidation can be identified by an examination of the oxidation products of comparable electrochemical and chemical oxidations using those metal oxides. If the oxidation products are identical, or have occurred via a similar mechanism, it is most likely that the electrochemical oxidation is of this type. An example of this type of electrochemical oxidation is the oxidation of primary amines at an $Ag|AgO|OH^-$ electrode system at the AgO peak potential, where the oxidation products were found to be very similar to the products of the corresponding chemical oxidation using AgO as the oxidising agent (see Table 14). With this type of electrochemical oxidation it has been found that the ratio of the reaction products ~~are~~ very dependent upon the reaction conditions such as the concentration of the reactants and the base electrolyte ($[OH^-]$). A schematic reaction mechanism of this type of oxidation is as follows:

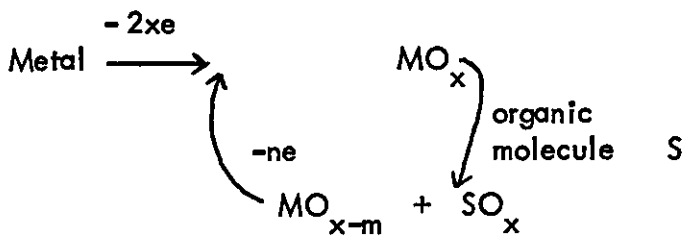

(11.9.)

TABLE 14 Comparison of electrochemical and chemical oxidations of amines

Amine	Electrochemical Product	Chemical Product
n-butylamine	n-butyronitrile n-butyraldehyde	n-butyronitrile n-butyraldehyde n-butyric acid
iso-butylamine	iso-butyronitrile iso-butyraldehyde	iso-butyronitrile iso-butyraldehyde iso-butyric acid
sec-butylamine	ethyl methyl ketone	ethyl methyl ketone
t-butylamine	t-butanol nitro-t-butane 2-methyl prop-1-ene	t-butanol nitro-t-butane 2-methyl prop-1-ene

The second type of electro-organic reaction involves the direct participation of the electrode metal oxide phase in the oxidation. In these oxidations the products from electrochemical oxidations will differ from those from chemical oxidations. An example of this behaviour is the oxidation of α -amino acids at an $Ag|AgO|OH^-$ electrode system (see Table 15).

It was found in these electro-organic oxidations that the reaction products were not very dependent on changes in the electrolyte or reactant concentrations. This is not unexpected since in these oxidations the reaction is taking place with the organic molecule bonded to the electrode surface; for strong adsorption when the surface is completely covered the reaction would be independent of the bulk concentrations. A schematic reaction mechanism for this type of electro-organic oxidation is:-

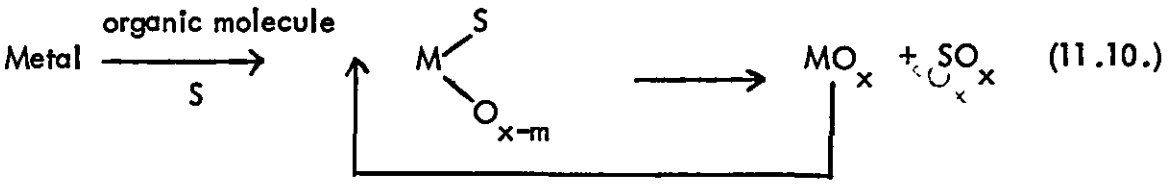

(11.10.)

TABLE 15 Comparison of electrochemical and chemical oxidations of α-amino acids.

α-amino acids	Electrochemical Products	Chemical Products
n-valine	butyronitrile	butyric acid
valine	iso-butyronitrile	iso-butyric acid
	iso-butyraldehyde	
n-leucine	valeronitrile	pentanoic acid
leucine	iso-valeronitrile	3-methyl butyric acid
	iso-valeraldehyde	
iso-leucine	2-me-butyronitrile	2-me-butyric acid
	2-me-butyraldehyde	

FURTHER WORK

1. A more detailed study, using experimental techniques other than L.S.V., should be undertaken to further investigate the reactions that occur at copper anodes in alkaline solutions, especially at potentials ~ 0.0 V (n.h.e.).

2. The investigation into the oxidation of organic compounds at copper and silver anodes should be extended to commercially more significant systems.

3. A wider range of electrode materials should be investigated for the oxidation of organic compounds so that a greater understanding of the variance of these reactions at different metal electrodes could be achieved.

REFERENCES

1. M.J. Allen, Organic Electrode Processes, Chapman and Hall London (1958)
2. P. Zuman, Progress in Physical Organic Chemistry, Vol.5, Interscience, New York, (1967)
3. W.E. Harris and W.H. Fadden, Analyt. Chem., 31 (1958) 114
4. T.G. Clarke, N.A. Hampson, J.B. Lee, J.R. Morley and B. Scanlon, J.Chem.Soc., (C) (1970) 815
5. N.A. Hampson, J.B. Lee and J.R. Morley, Electrochim.Acta., 16 (1971) 637
6. H. Helmholtz, Wied.Ann., 7 (1879) 377
7. A. Gouy, J.Phys., 9 (1910) 457
8. D.L. Chapman, Phil.Mag., 25 (1913) 475
9. O. Stern, Zeit.Electrochem., 30 (1924) 508
10. D.C. Grahame, Chem.Rev., 41 (1947) 441
11. A.N. Frumkin, Svensk.Kemisk.Tidskrift., 77 (1965) 300
12. A.N. Frumkin, J. Electrochem.Soc., 107 (1960) 461
13. W. Nernst, Z.Physik.Chem., 47 (1904) 52
14. T. Erdey-Gruz and M. Volmer, Zeit.Physik.Chem., 105A (1930)203
15. P. Delahay, Double Layer and Electrode Kinetics, Interscience, New York (1965)

16. J. Horiuti and M. Polanyi, Acta.Physicochim., U.S.S.R., 52 (1935) 505

17. J. Tafel, Zeit.Physik.Chem., 50 (1905) 641

18. K.J. Vetter, Zeit.Physik.Chem., 194 (1956) 284

19. G. Barker, Modern Electroanalytical Methods, Ed. G. Charlot, Elsevier, Amsterdam (1958)

20. S. Azim and A.C.Riddiford, Anal.Chem., 34 (1962) 1023

21. J.D. Newson and A.C. Riddiford, J. Electrochem.Soc., 108 (1961) 695

22. B. Hague, Alternating Current Bridge Methods, Pitman, London, (1962) Chapter 4

23. J.E.B. Randles, Trans.Faraday Soc., 50 (1954) 1246

24. P. Delahay, New Instrumental Methods in Electrochemistry, Interscience, New York (1954) Chapter 6

25. V.G. Levich, Physicochemical Hydrodynamics, Prentice Hall, New Jersey (1962)

26. A.C. Riddiford, Advances in Electrochemistry and Electrochemical Engineering, Ed. Delahay and Tobias, Interscience, New York, Vol. 4 (1965)

27. D.P. Gregory and A.C. Riddiford, J. Chem.Soc., (1956) 3756

28. D.P. Gregory and A.C. Riddiford, J.Electrochem.Soc., 107 (1960) 950

29. J. Jordan, R.A. Javick and W.E. Ranz, J.Am.Chem.Soc., 80 (1958) 3846

30. H. Gerischer and H. Krause, Z.Physik.Chem., 10 (1957) 264

31. D. Leikis, Dokl.Akad.Nauk., S.S.S.R., 112 (1957) 97

32. D. Leikis, E.S. Savastianov and I.G. Davaeva, J.Electrochem. Soc., 113 (1966) 1341

33. L. Ramaley and G.C. Enke, J. Electrochem.Soc., 114 (1967) 817

34. N.A. Hampson, D. Larkin and J.R. Morley, J. Electrochem.Soc., 114 (1967) 817

35. A.N. Frumkin, Svensk.Ken.Tidskr., 77 (1965) 300

36. N.A. Hampson, J.B. Lee, J.R. Morley and B. Scanlon, J. Electro anal.Chem., 24 (1970) 229

37. Y. Pleskov, Dokl.Akad. Nauk., S.S.R., 117 (1957) 645

38. W.S. Graff and H.H. Stadelmaier, J. Electrochem.Soc., 105 (1958) 446

39. R. Luther and F. Pokorny, Z. Anorg.Chem., 57 (1908) 290

40. A. Hickling and D. Taylor, Discuss Faraday.Soc., 1 (1947) 277

41. B.N. Kabanov and D.L. Leikis, Z. Electrochem., 62 (1958) 660

42. S. Yoshizawa and Z. Takehara, J. Electrochem.Soc., Japan, 31 (1963) 91

43. C.P. Wales and J. Burbank, J. Electrochem.Soc., 112 (1965) 13

44. G.W.D. Briggs, M. Fleischmann, D.J. Lax and H.R. Thirsk, Trans.Faraday.Soc., 64 (1968) 3124

45. T.P. Dirkse and D.B. De Vries, J.Phys.Chem., 63 (1959) 107

46. P. Stonehart, Electrochim.Acta., 13 (1968) 1789

47. T.G. Clarke, N.A. Hampson, J.B. Lee, J.R. Morley and B. Scanlon, Ber.Bunsenges.Phys.Chem., 73 (1969) 279

48. R.D. Giles and J.A. Harrison, J. Electroanal.Chem., 27 (1970) 161

49. R.D. Giles, J.A. Harrison and H.R. Thirsk, J. Electroanal.Chem., 22 (1969) 375

50. G. Croft, J. Electrochem.Soc., 106 (1959) 278

51. Z. Takenhara, Y.Namba and S. Yoshizawa, Electrochim.Acta., 13 (1958) 1395

52. F.I. Kukoz, N.Yu.Osipchuk and M.F. Shalozubov, Tr.Novo cherkassk. Politekh.Inst., 170 (1967) 84

53. M. Fleischmann, D.J. Lax and H.R. Thirsk, Trans.Faraday.Soc., 64 (1968) 3137

54. L.R. Subbaraman and L. Santappa, Proc.Ind.Acad.Sci., 64A (1966) 345

55. T.G. Clarke, N.A. Hampson, J.B. Lee, J.R. Morley and B. Scanlon, Canad.J.Chem., 47 (1969) 1649

56. T.G. Clarke, N.A. Hampson, J.B. Lee, J.R. Morley and B. Scanlon, J.Chem.Soc., C (1970) 815

57. T.G. Clarke, N.A. Hampson, J.B. Lee, J.R. Morley and B. Scanlon, Tetrahedron letters, 54 (1968) 5685

58. N.A. Hampson, J.B. Lee, J.R. Morley and B. Scanlon, Canad.J. Chem., 47 (1969) 3729

59. N.A. Hampson, J.B. Lee, K.I. MacDonald, J.R. Morley and B.Scanlon Tetrahedron, 26 (1970) 1109

60. N.A. Hampson, J.B. Lee and K.I. MacDonald, Electrochem. Acta., 17 (1972) 921

61. R.M. Herbst and H.T. Clarke, J. Biol.Chem., 104 (1934) 769

62. I.D. Spencer, Chem. and Ind., (1956) 796

63. R.G. Bacon and D. Stewart, J. Chem.Soc., C (1966) 1384

64. E. Muller, Z. Electrochem., 13 (1907) 133

65. W. Feitknecht and H. Lenel, Helv.Chim.Acta., 27 (1944) 775

66. A. Hickling and D. Taylor, Trans.Faraday.Soc., 44 (1948) 262

67. J.S. Halliday, Trans.Faraday Soc., 50 (1954) 171

68. A.L. L'Vov and A.V. Fortunatov, Nauch.Ezhegodnik., (1954) 29

69. F.F. Faizullice, E.D. Kochman and N.N. Muzurova, Materialy. Electrochim.Konferentsii. Kazansb., (1959) 63

70. R. Delhez, Bull.Soc.Roy.Sci.Liege., 30 (1961) 446

71. R.W. Ohse, Z. Phys.Chem. N.F., 21 (1959) 506

72. A.M. Shams, El. Din and F.M. Abd. El.Wahab, Electrochimica. Acta., 9 (1964) 113

73. B. Miller, J. Electrochem.Soc., 116 (1969) 1676

74. H.P. Leckie, J. Electrochem.Soc., 117 (1971) 1478

75. F. Boullon, J. Piron and J. Stevens, Bull.Soc.Chem. Belg., 67 (1958) 643

76. S.E.S. El.Wakkad and Sayeda.H.Emara, J.Chem.Soc., (1953) 3508

77. S.E.S. El.Wakkad and T.M. Salan, J.Chem.Soc. (1955) 1489

78. S.E.S. El.Wakkad and A.M. Shans.El.Din., J.Chem.Soc., (1954)3094

79. A. Allmand, J.Chem.Soc., (1914) 2151

80. Van.T. Marcovic and E. Atlic, Werkstoffe. und Korrosion. (1965) 958

81. A.M. Borshchevski, V.V. Skorcheletti and T.I. Mikhaleva, Zhur. Priklad.Khim., 39 (1966) 1427

82. V.A. Ploklov and V.N. Flerov, Zhur.Priklad.Khim., 40 (1967) 325

83. M.N. Ronzhia and A.L. Golubev, Korriziya.Melal.i.Splavov.s.b., (1965) 166

84. G. Rozovskis and A. Misevicius, Lietuvos.T.S.R. Mokslu.Akad. Darbai.Ser.B., (1965) 73

85. V.N. Flerov, Zhur.Fiz.Khim., 37 (1963) 1733

86. E.A. Ukshe and A. L. Levin, Dokl.Akad.Nauk., U.S.S.R., 105 (1955) 119

87. D.N. Staicopolus, J. Electrochem.Soc., 108 (1961) 900

88. B. Jakuszewski and Z. Kozlowski, Rocz.Chem., 36 (1962) 1873

89. B. Jakaszewski and Z. Kozlowski, Lodz.Tow.Nauk.Wydz. III Acta Chim., 9 (1964) 25

90. A.I. Levin, E.A.Ukshe and N.S. Brilina, Dokl.Acad.Nauk., S.S.S.R. 88 (1953) 697

91. M. Bonnemay, G. Bronocl., P.J. Jonville and C.R. Elevant, Acad. Sci. 260 (1965) 2565

92. M.A.V. Devanathan and B.V.K.S.R.A. Tilak, Chem.Rev., 65 (1965)635

93. V.L. Kheifet and B.S. Krasikov, Dokl.Acad.Nauk. S.S.S.R., 109 (1956) 586

94. V.L. Kheifets and B.S. Krasikov, Zh.Fiz.Khim., 31 (1958) 707

95. G.M. Deriaz, Ph.D Thesis, Birmingham University (1951)

96. D. Armstrong, N.A. Hampson and R.J. Latham, J. Electroanal. Chem., 23 (1969) 361

97. B.E. Conway, E. Gileadi and H. Angerstein-Kozlowska, J. Electrochem.Soc., 112 (1965) 341

98. R. de Levie, Electrochim.Acta., 9 (1964) 1231

99. R. de Levie, Advances in Electrochemistry and Electrochemical Engineering, Ed. P. Delahay, Interscience, New York, Vol.5. (1967)

100. P. Champoin, G. Crespy and J. Royon, C.R. Acad.Sci.Ser.C., 270 (1970) 1552

101. J. O'M. Bockris and H. Kita, J. Electrochem.Soc., 109 (1967) 928

102. J. O'M. Bockris and E. Mattsson, Trans.Faraday.Soc., 55 (1959) 1586

103. J. O'M. Bockris and M. Engo, Trans.Faraday Soc., 58 (1962) 1187

104. V. Markovac and B. Lovrecek, J. Electrochem.Soc., 113, (1966) 838

105. G.A. Wright, J.Electrochem.Soc., 114 (1967) 1263

106. O.R. Brown and H.R. Thirsk, Electrochimica.Acta., 10 (1965) 383

107. Stability constants, Chem.Soc., London, Spec.Publ. 17, (1964) 398

108. N.L. Weinberg and H.R. Weinberg, Chem.Rev., 68 (1968) 449

109. F. Fichter and F. Kuhn, Helv.Chim.Acta., 7 (1924) 167

110. Y. Takayama, T. Harada and S. Midano, Bull.Chem.Soc., Japan, 12, (1937) 342

111. Y. Takayama, Y. Tsubuku and T. Matsamoto, Bull.Chem.Soc., Japan, 17 (1942) 53

112. S. Miduno and Y. Takayama, Bull.Chem.Soc., Japan, 17 (1942) 136

113. Y. Takayama, Bull.Chem.Soc., Japan, 8 (1933) 213

114. Y. Takayama, Bull.Chem.Soc., Japan, 8 (1933) 173

115. A. Hickling, Trans.Faraday.Soc., 42 (1946) 518

116. H.A. Laitinen and M.S. Chao, J. Electrochem.Soc., 108 (1961) 726

117. K.J. Vetter and D. Bernat, Z. Electrochem., 62 (1958) 378

118. D. Clarke, T. Dickinson and W.M. Mair, Trans.Faraday.Soc., 55 (1959) 1937

119. S. Barnartt, J. Electrochem.Soc., 106 (1959) 722

120. S.B. Brummer and A.C. Makrides, J. Electrochem.Soc., 111 (1964) 1122

121. R.S. Sirohi and M.A. Genshaw, J. Electrochem.Soc., 116 (1969) 910

122. S.E.S. El.Wakkad and A.M. Shams El.Din., J.Chem.Soc., 9 (1954) 3098

123. K. Ogura, S. Haruyama and K. Nagasaki, J. Electrochem.Soc., 118 (1971) 531

124. M.Fleischmann, K.Korinek and D. Pletcher, J.Electroanal.Chem., 31 (1971) 39

125. W.J. Mueller, Z. Electrochem., 33 (1927) 401

APPENDIX

$$R \underset{k_-}{\overset{k_+}{\rightleftharpoons}} O + ne$$

$$I = nFA\,(k_+|R|_s - k_-|O|_s)$$

$$I = nFA\,\frac{D_R}{\delta_R}\,(|R| - |R|_s) = nFA\,\frac{D_O}{\delta_O}\,(|O|_s - |O|)$$

$$I_{L,R} = nFA\,\frac{D_R}{\delta_O}\,|R|$$

$$\therefore\ I = I_{L,R} - nFA\,\frac{D_R}{\delta_R}\,|R|_s = nFA\,\frac{D_O}{\delta_O}|O|_s - I_{L,O}$$

$$|R|_s = (I_{L,R} - I)\cdot\frac{\delta_R}{nFAD_R} \qquad |O|_s = (I + I_{L,O})\,\frac{\delta_O}{nFAD_O}$$

$$I = k_+\,\frac{\delta_R}{D_R}\,(I_{L,R} - I) - k_-\,\frac{\delta O}{D_R}\,(I + I_{L,O})$$

$$I\left\{1 + k_+\,\frac{\delta_R}{D_R} + k_-\,\frac{\delta_O}{D_O}\right\} = k_+\,\frac{\delta_R}{D_R}\cdot I_{L,R} - k_-\,\frac{\delta_O}{D_O}\cdot I_{L,O}$$

$$= nFA\{k_+|R| - k_-|O|\}$$

$$= I_\infty$$

$$\frac{1}{I_\infty} + \frac{1}{I_\infty}\left\{k_+\,\frac{\delta_R}{D_R} + k_-\,\frac{\delta_O}{D_O}\right\} = \frac{1}{I}$$

$$\text{or}\quad \frac{1}{I_\infty} + \frac{K}{\omega^{\frac{1}{2}}} = \frac{1}{I}$$

$$\text{Slope } K = \frac{\frac{k_+(\delta_R/\omega^{\frac{1}{2}})}{D_R} + \frac{k_-(\delta_O/\omega^{\frac{1}{2}})}{D_O}}{I_\infty}$$

$$= \frac{\frac{k_+(\delta_R/\omega^{\frac{1}{2}})}{D_R} + \frac{k_-(\delta_O/\omega^{\frac{1}{2}})}{D_O}}{nFA(k_+|R| - k_-|O|)}$$

$$= \frac{\frac{\delta_R/\omega^{\frac{1}{2}}}{D_R} + \frac{k_-}{k_+} \cdot \frac{(\delta_O/\omega^{\frac{1}{2}})}{D_O}}{nFA(|R| - \frac{k_-}{k_+}|O|)}$$

$$= \frac{\frac{\delta_R/\omega^{\frac{1}{2}}}{D_R} + k'e^{n\eta f}\frac{(\delta_O/\omega^{\frac{1}{2}})}{D_O}}{nFA(|R| - k'e^{n\eta f}|O|)}$$

valid irrespective of the velocity of reaction.

When R is solid $\frac{(\delta_R/\omega^{\frac{1}{2}})}{D_R} = 0.$

If $|R| >> k'e^{n\eta f}|O|$ because $|O|$ is very small.

Then $K = \frac{k'e^{n\eta f}}{nFA|R|}\frac{\delta_O/\omega^{\frac{1}{2}}}{D_O}$

i.e. $\log K \alpha\ n\eta f$